DEVELOPMENT OF PLANT-BASED MILKS THROUGH A POST pH-DRIVEN APPROACH

by

ANTHONY STEVANUS SURYAMIHARJA

(Under the Direction of Hualu Zhou)

ABSTRACT

The growing demand for plant-based milk underscores the need to enhance its nutritional value

through fortification and improved protein content. This study introduces the post pH-driven

method as a solution for curcumin fortification and oat protein solubility enhancement in plant-

based milk. The method was applied to extract curcumin from turmeric, achieving high

extraction efficiency (96.4 \pm 0.5%) and two-in-one efficiency (94.2 \pm 1.6%) in soymilk.

Additionally, it was used to treat oat protein, where a combination of heat treatment at 100°C and

citric acid acidification significantly improved protein solubility up to 70-75%. These findings

demonstrate the versatility of the post pH-driven method in developing functional plant-based

milk products. This study lays a strong foundation for improving plant-based milk formulations

through innovative extraction and solubilization techniques. Future research should focus on its

scalability, molecular interactions within food matrices, and sensory evaluation to optimize its

commercial applications.

INDEX WORDS: Plant-based milk, post pH-driven, curcumin, oat protein, heat treatment

DEVELOPMENT OF PLANT-BASED MILKS THROUGH A POST pH-DRIVEN APPROACH

by

ANTHONY STEVANUS SURYAMIHARJA

B.S., Oregon State University, 2023

A Thesis Submitted to the Graduate Faculty of The University of Georgia in Partial Fulfillment of the Requirements for the Degree

MASTER OF SCIENCE

ATHENS, GEORGIA

2025

© 2025

ANTHONY STEVANUS SURYAMIHARJA

All Rights Reserved

DEVELOPMENT OF PLANT-BASED MILKS THROUGH A POST pH-DRIVEN APPROACH

by

ANTHONY STEVANUS SURYAMIHARJA

Major Professor: Hualu Zhou Committee: Casimir C. Akoh Koushik Adhikari

Electronic Version Approved:

Ron Walcott Vice Provost for Graduate Education and Dean of the Graduate School The University of Georgia May 2025

DEDICATION

I dedicate my research to demonstrating that I deserve to complete this degree and ultimately, become a food scientist who can make an impact on food development.

ACKNOWLEDGEMENTS

I would like to express my deepest gratitude to God, whom I always follow, and through His guidance, I have been able to complete my graduate studies. I am also sincerely grateful to my family for giving me the opportunity to pursue my graduate studies at the University of Georgia, especially my mom and dad for trusting me to follow this path. Next, I would like to thank my girlfriend, Marianne, for always supporting me throughout my graduate journey. I have experienced many ups and downs, but she has always been there for me. I would like to extend my heartfelt appreciation to my principal investigator, Dr. Hualu Zhou, for being an outstanding mentor and professor. From you, I have truly learned the importance of work-life balance, and together, we have had many publications and accomplishments. Additionally, I am grateful to my committee members, Dr. Casimir Akoh and Dr. Koushik Adhikari, for their invaluable guidance. A special thank you to Dr. Casimir Akoh for assisting me and providing access to research facilities in Athens. Finally, I would like to thank my friends, Peter Chiarelli, Minghe Wang, Xiping Gong, Bobby Goss, Dylan limit, Cole Rogers, and peers at both the Athens and Griffin campuses. Without you, I would not have had the opportunity to experience so many new things, from the College Bowl competition to Phi Tau Sigma and many other fun and enriching experiences. From taking classes in my first year to completing my research in my second, I am deeply thankful to those who supported me both mentally and physically, so I could succeed and complete my graduate studies.

.

TABLE OF CONTENTS

	Page
ACKNOV	VLEDGEMENTSv
LIST OF	TABLESviii
LIST OF	FIGURESx
СНАРТЕ	R
1	INTRODUCTION AND LITERATURE REVIEW OF PLANT-BASED MILK1
	Introduction
	Production of plant-based milk alternatives4
	Nutritional and health of plant-based milk alternatives
	Gastrointestinal digestion of plant-based milk alternatives
	Environmental impacts
	Conclusions34
	References
2	ENHANCING THE EFFICIENCY AND SUSTAINABILITY OF PRODUCING
	CURCUMIN-INFUSED PLANT-BASED MILK ALTERNATIVES WITH A TWO-
	IN-ONE POST PH-DRIVEN PROCESSING STRATEGY48
	Abstract
	Introduction
	Materials and Methods
	Results and Discussion

	Conclusions.	72
	References	74
	Supporting Information	81
	References	89
3 HE	EATING AND ACIDIFICATION SIGNIFICANTLY IMPACT PH-SHIFTING	Г
TR	REATMENT: A CASE STUDY ON OAT PROTEIN ISOLATE	91
Ab	ostract	92
	Introduction	93
	Materials and Methods	96
	Results and Discussion	.102
	Conclusions	.123
	References	.124
Concluding st	atement/ Future directions	.131

LIST OF TABLES

Table 1.1: Nutrition facts of common commercial plant-based milk alternatives with different
brands. Data were collected from the label of each food product. Some milk products
with specific brands, for oats, soy, and coconut, are not available to obtain the data. The
low-fat milk is considered as a control group. The percentage values in the parentheses
are calculated based on three major components: fat, carbohydrate, and protein. The
symbol ('-') means that data is not available16
Table 1.2: The nutrition facts of plant materials collected from USDA FoodData Central
database (https://fdc.nal.usda.gov). The percentage values in the parentheses are
calculated based on three major components: fat, carbohydrate, and protein. The symbol
('-') means that data is not available
Table 1.3: Normalized fat profiles of different plant and animal sources. Raw data are collected
from the USDA FoodData Central database (https://fdc.nal.usda.gov). The symbol ('-')
means that data is not available19
Table 1.4: Normalized amino acid profiles of different plant and animal sources. Raw data for
plant sources are collected from the USDA FoodData Central database
(https://fdc.nal.usda.gov), while raw data for both "Milk" and "Human muscle" are
obtained from a previous study (Gorissen et al., 2018). Tryptophan, aspartic acid,
asparagine, and glutamine are not analyzed due to the unavailability of raw data for both
'Milk' and 'Human muscle'. The symbol ('-') means that data is not available20

Table S1: Nutrition fact of turmeric powder used in this study. The data was calculated based on
one serving size
Table S2: Nutrition facts and ingredients of Silk vanilla soy creamer
Table S3: Ingredients of Silk vanilla soy creamer
Table S4: The inventory of raw material inputs for producing curcumin-soymilk powder83
Table S5: The inventory of raw material inputs for producing turmeric-soymilk powder83
Table S6: Approximate energy consumption for producing both curcumin-soymilk and turmeric-
soymilk powders with approximately 1 kg of curcumin. The base-case for the production
rate is 1E4 kg soymilk solution fed to the process during each batch. The following data
is estimated by a techno-economic analysis of extraction of curcumin from turmeric87
Table S7: A snapshot of raw material inputs to produce the turmeric-soymilk powder with 10 kg
curcumin88
Table S8: A snapshot of raw material inputs to produce the curcumin-soymilk powder with 10 kg
curcumin 88

LIST OF FIGURES

n	_	_	_
Г	а	ջ	t

Figure	1.1: (A) The number of articles retrieved from the Web of Science Core Collection using
	the query: TS=("plant-based milk*") OR TS=("plant-based drink*") OR TS=("plant-
	based beverage*") OR TS=("milk alternative*") OR TS=("milk analog*"). "TS" stands
	for the topic keyword, and the search was conducted on 08/01/2024. The arrow indicates
	a significant increase in the number of articles published in 2020. (B) The percentage of
	research articles published with the keyword in the abstract within the past two years.
	The percentage was calculated by the ratio of the number of research articles published
	with an additional keyword, e.g., AB=("sensory*"), to the total number of research
	articles selected within the past two years
Figure	1.2: A need for a multi-dimensional strategy to accelerate the innovation of milk
	alternative products aims to not only meet but exceed customer expectations in terms of
	cost-effectiveness, nutritional and health value, taste and flavor, customer acceptance,
	and environmental friendliness. Picture was initially created with BioRender.com4
Figure	1.3: Particle size distributions of three commercial PBMA products. Data was collected
	from previous studies
Figure	1.4: Impact of food matrix on vitamin D bioaccessibility. "Tween emulsion" is the Tween
	20-stablized nanoemulsions as a control group. Insoluble calcium (CaCO ₃) was used in
	all samples. Data was collected from a previous study

Figure 1.5: Effects of polyphenol fortification on the visual appearance of plant-based milk
alternative and the bioaccessibility of polyphenols. "(CQR)M" represents a plant-based
milk alternative fortified with multiple polyphenols, specifically a blend of curcumin,
resveratrol, and quercetin, while the "Crystals" is a mixture of their crystalline forms.
Data was collected from a previous study
Figure 1.6: (A) Global warming potential (kg CO ₂ -eq/L milk) of different PBMAs compared to
dairy milk. The total value is contributed by four parts, including the "Crop production",
"Milk Processing", and "Packaging & End-of-Life", and "Co-Product Credit", and their
individual values are labeled on each bar plot, respectively. (B) Global warming potential
(kg CO ₂ -eq/kg protein) of different PBMAs compared to dairy milk. Data are obtained
from a life cycle assessment report
Figure 1.7: Water footprint results of different PBMAs and dairy milk. Water scarcity factor (SF)
applied for the calculations of water use. Data and calculations can be obtained from a
life cycle assessment report
Figure 2.1: A two-in-one PPD strategy for developing curcumin-infused PBMAs (e.g., soymilk).
The bioactive curcumin molecules can be directly extracted from raw turmeric and then
encapsulated into soymilk in one process69
Figure 2.2: The extraction efficiency, encapsulation efficiency, and two-in-one efficiency of both
turmeric-soymilk and curcumin-soymilk. The upper letter (A) represents the significant
differences between samples (p < 0.05). Their values from left to right are 96.4 ± 0.5 ,
$97.8 \pm 1.4, 94.2 \pm 1.6, 98.5 \pm 0.4, 100.1 \pm 1.1, 98.6 \pm 1.1\%$, respectively61
Figure 2.3: The UV-vis absorption spectrum of >97% curcumin and turmeric extract using 0.1 M
KOH. The absorbance values at the peak positions are labelled63

Figure 2.4: (A) Total embodied energy (MMBtu) and (B) carbon emissions (kg CO ₂ -eq) of raw
materials for producing both turmeric-soymilk and curcumin-soymilk powders with $\sim\!10$
kg curcumin. The "10x" (or "22x") value represents the ratio of the total embodied energy
(or carbon emissions) of curcumin-infused soy milk compared to that of turmeric-infused
soy milk. The listed ingredients (e.g., citric acid powder) contribute to the composition of
turmeric- or curcumin-infused soymilk product
Figure 2.5: (A) Appearance (Left: soymilk, Middle: curcumin-soymilk, and Right: turmeric-
soymilk) and (B) colors (L^* , a^* , b^* values) of three samples. Upper letters (A, B, and C)
represent the significant differences between samples (p < 0.05) for the individual L^* , a^* ,
or b^* . (C) Particle size distributions and (D) zeta potentials of raw soymilk, curcumin-
soymilk, and turmeric-soymilk. The mean particle diameters of soymilk, curcumin-
soymilk, and turmeric-soymilk are $0.854 \pm 0.009~\mu\text{m}, 0.856 \pm 0.009~\mu\text{m}, \text{and} 0.893 \pm$
$0.015~\mu m$, respectively. Upper letter (A) represents the significant differences between
samples (p < 0.05)
Figure 2.6: (A) Differential scanning calorimetry profiles of curcumin, turmeric, soymilk,
curcumin-soymilk, and turmeric-soymilk powders. The temperature corresponding to the
endothermic peak of each sample is labeled nearby. (B) The chemical stability of
curcumin in both curcumin-soymilk and turmeric-soymilk powders under a freezing
condition. The upper letter (A) represents the significant differences between all samples,
including both curcumin- and turmeric-soymilk with different storage days (p < 0.05)70
Figure S1: Standard curves for curcumin using the (A) UV-vis spectrophotometer and (B)
HPLC. Their linear equations and R^2 values are labeled, respectively81

rigure	52: (A) impact of different measurement methods (HPLC vs. 0 v-vis spectrophotometer)
	on the concentration of curcumin in either >97% curcumin or turmeric extract
	sample. (B) HPLC chromatograms of both >97% curcumin and turmeric samples. The
	upper letter (A) represents significant differences between samples (p < 0.05). The "97%
	Curcumin" was considered as a purified curcumin sample, while the "Turmeric-
	Extracted" sample refers to curcumin extracted from turmeric powder using the PPD
	method
Figure	S3: Mass balance flow charts for producing curcumin-soymilk (A) and turmeric-soymilk
	(B) powders with 10 kg of curcumin87
Figure	3.1: (A) Proximate composition of oat protein isolate, highlighting the protein content
	$(67.6 \pm 1.0\%)$ as the major component. (B) Differential scanning calorimetry thermogram
	of OPI, showing a denaturation peak at 113.9 °C
Figure	3.2: Schematic representation of the pH-shifting and heating treatment process for oat
	protein isolate. The process includes an initial pH adjustment to 12, heating at different
	temperatures (50 °C, and 100 °C) versus no-heat (25 °C), and subsequent acidification
	using either 3% citric acid or 0.1 M HCl. It highlights the structural changes induced by
	varying heating conditions and acid types during the treatment
Figure	3.3: Protein solubility (%) of oat protein isolate at varying pH levels and heating
	conditions. The treatments include (1) no heating (25 °C), (2) heating at 50 °C, and (3)
	heating at 100 °C, followed by pH adjustment using 3% citric acid. The inset
	fluorescence image shows protein aggregates formed under the no-heat condition with
	citric acid, as indicated by the arrow The scale bar is 100 µm106

Figure	3.4: (A) Remaining soluble proteins (%) of oat protein isolate under different heating
	conditions (S1: 25 °C, S2: 50 °C, S3: 100 °C) over storage periods of 0, 1, 3, and 7 days.
	(B) Visual observations of samples (S1, S2, S3) showing sedimentation behavior over
	time, with sediment heights indicated in red (Letter shows significance at $p \le 0.05$ among
	different days in each sample)
Figure	3.5: Protein solubility (%) of oat protein isolates at varying pH levels and heating
	conditions, with acidification using 0.1 M HCl. Treatments include (1) no heating (25
	°C), (2) heating at 50 °C, and (3) heating at 100 °C. The inset fluorescence image shows
	protein aggregates formed under the no-heat condition with HCl acidification, as
	indicated by the arrow. The scale bar is $100 \ \mu m$
Figure	3.6: (A) Visual observations of oat protein isolate samples at pH 12 and pH 7 after
	treatments with no heat (25 °C), heating at 50 °C, and heating at 100 °C, followed by
	acidification using citric acid. (B) Particle size distribution of the treated samples,
	measured after centrifugation at 10,000 rpm for 15 min, highlighting the impact of
	heating and pH adjustment
Figure	3.7: Zeta potential (mV) of oat protein isolate across varying pH levels and heat
	treatments. (A) Samples acidified with 3% citric acid after no heating (25 °C), heating at
	50 °C, or heating at 100 °C. (B) Samples acidified with 0.1M HCl after no heating (25
	°C), heating at 50 °C, or heating at 100 °C
Figure	3.8: (A) Z-average particle size (nm) of oat protein isolate samples (S2: 50 °C, S3: 100
	°C) over storage periods of 0, 1, 3, and 7 days. (B) Zeta potential (mV) of the same
	samples over the same storage periods, illustrating the effects of heating and storage on
	particle size and surface charge stability

Figure 3.9: SDS-PAGE analysis of OPI under different pH and heating conditions. Samples
include treatments at pH 7 and pH 12 with no heat (25 °C), heating at 50 °C, and heating
at 100 °C, alongside a protein ladder for molecular weight reference118
Figure 3.10: DSC thermograms of oat protein isolate under different pH and heating conditions.
Treatments include samples at pH 7 (heated at 100 °C or unheated at 25 °C) and samples
subjected to pH-shifting (7 to 12 to 7) with no heat (25 °C) or heating at 100 °C, followed
by acidification using either HCl or citric acid
Figure 3.11: Secondary structure content (%) of OPI under various pH and heating treatments, as
determined by FTIR spectroscopy. The samples include OPI powder and OPI treated at
pH 7 \rightarrow 12 with no heat (25 °C), heating at 100 °C, or after subsequent acidification to
pH 7 using citric acid or HCl. The contributions of β -sheet, α -helix, β -turns, and
random coil structures highlight the effects of pH-shifting, heating, and acidification on
protein secondary structure (The letters, A, B, C, show the significance at $p \le 0.05$
between samples for a specific secondary structure)

CHAPTER 1

INTRODUCTION AND LITERATURE REVIEW OF PLANT-BASED MILK¹

¹ Suryamiharja, A., Gong, X., and Zhou, H. 2024. Towards more sustainable, nutritious, and affordable plant-based milk alternatives: A critical review. *Sustainable Food Proteins*, 2:250-267. Reprinted here with permission of the publisher.

Introduction

The global rise in the adoption of plant-based foods, including plant-derived or processed, is a response to growing concerns over environmental sustainability, ethical considerations, and the pursuit of better health outcomes. Within the diverse array of plant-based foods, PBMAs carve out a unique niche. First, the variety of PBMAs options, including legume, nut, seed, cereal, and pseudo-cereal derived milks, offers consumers a broad spectrum of choices (Hidalgo-Fuentes et al., 2024). This diversity not only provides different taste preferences and nutritional needs but also underscores the adaptability of PBMAs to global dietary patterns. Second, PBMAs address the dietary restrictions of individuals with lactose intolerance, milk allergies, or hypercholesterolemia, and thus provide a safe and inclusive alternative (Silva et al., 2020a). Third, the production of PBMAs can be more efficient and scalable by using simple processing methods. This process can likely replicate the physicochemical properties of animalbased milks, unlike the complex procedures needed for the production of many other plant-based foods (such as meat alternatives) (McClements and Grossmann, 2021). Beyond catering to these needs, PBMAs stand out for their potential as vehicles for nutritional enhancement (McClements, 2020). They can be enriched with essential macronutrients or micronutrients, such as calcium, vitamins D and B₁₂, and plant-derived bioactive compounds, which benefits the development of nutritionally fortified PBMAs. Compared to animal-based milks, the increasing availability of PBMAs plays a vital role in enhancing global access to nutritionally rich, plantbased dietary options. This is largely due to the abundant availability of raw plant materials, which is especially beneficial for the countries that have a limited accessibility of dairy milks but a high availability of plant sources.

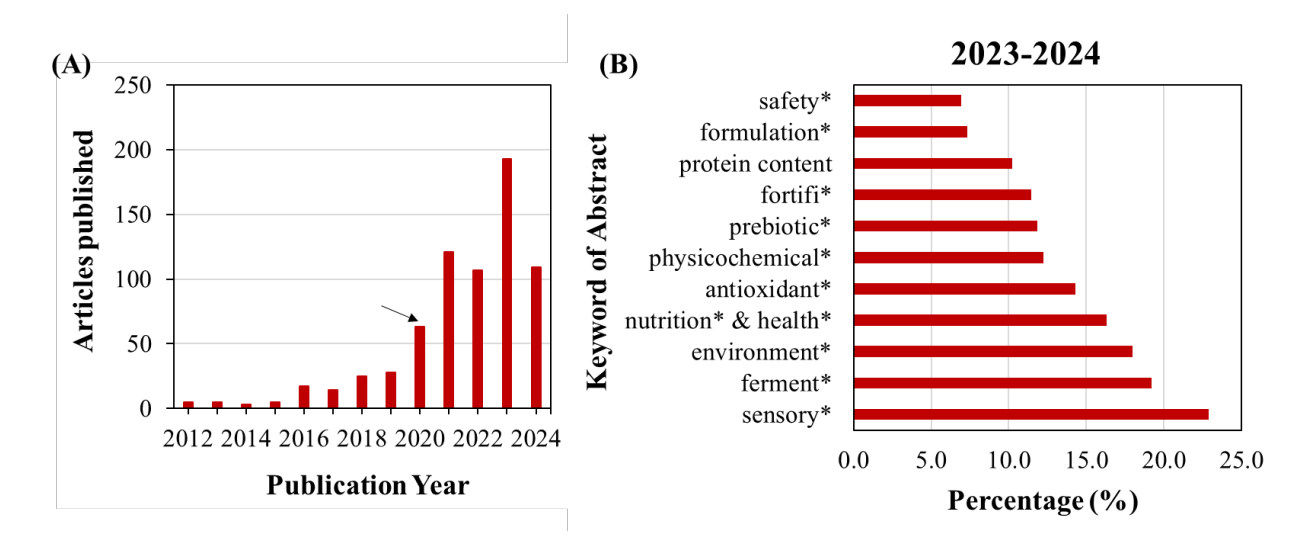


Figure 1.1. (A) The number of articles retrieved from the Web of Science Core Collection using the query: TS=("plant-based milk*") OR TS=("plant-based drink*") OR TS=("plant-based beverage*") OR TS=("milk alternative*") OR TS=("milk analog*"). "TS" stands for the topic keyword, and the search was conducted on 08/01/2024. The arrow indicates a significant increase in the number of articles published in 2020. (B) The percentage of research articles published with the keyword in the abstract within the past two years. The percentage was calculated by the ratio of the number of research articles published with an additional keyword, e.g., AB=("sensory*"), to the total number of research articles selected within the past two years.

The percentage of research articles with different keywords was calculated to reflect current research trends and scientific evolution (**Figure 1.1B**). It can be observed that keywords, such as sensory evaluation, fermentation-based production techniques, environmental impact, and nutrition and health, are frequently used in research articles (> 15%). To pave the way for the development of PBMAs, this review paper sets out to offer a comprehensive examination of the current landscape of PBMAs and provides an in-depth analysis covering various aspects. For example, understanding processing strategies is critical for achieving cost-effective production of

PBMAs. Delving into the nutritional profile and gastrointestinal digestion helps us understand the nutritional and health benefits of PBMAs. Additionally, careful consideration of the environmental impacts of PBMAs is necessary. It is noted that several review papers have been published to cover some critical aspects, including the flavor (Xie et al., 2023), sensory (Tireki et al., 2024), fermentation (Hidalgo-Fuentes et al., 2024; Zhao et al., 2024), and customer's perspectives (Sharma et al., 2024a). Combined with these review articles, important insights and recommendations can be provided to accelerate the innovation of milk alternative products that not only meet but exceed customer expectations in terms of cost-effectiveness, nutrition and health value, taste and flavor, customer acceptance, and environmental friendliness (**Figure 1.2**).



Figure 1.2. A need for a multi-dimensional strategy to accelerate the innovation of milk alternative products aims to not only meet but exceed customer expectations in terms of cost-effectiveness, nutritional and health value, taste and flavor, customer acceptance, and environmental friendliness. Picture was initially created with BioRender.com.

Production of plant-based milk alternatives

Many review papers have detailed the production of PBMAs from various plants (Aydar et al., 2020; McClements et al., 2019; Sharma et al., 2024b). However, they often lack a comprehensive discussion on how we can improve the stabilization and their fundamental principles. Therefore, this section will provide a brief introduction to processing strategies and focus on two key questions: how to measure or monitor PBMA stability and how to enhance stabilization through strategies such as homogenization, emulsification, and thickening.

Processing strategies

Two prevalent processing strategies are employed to create these dairy alternatives: first, the disruption and homogenization of plant materials such as nuts, seeds, or legumes; and second, the formation of oil-in-water emulsions through homogenizing oil, water, and emulsifiers (McClements et al., 2019). These methods are foundational in transforming solid plant materials into fluid systems that mimic the properties of traditional dairy milks.

The most common strategy for crafting PBMAs centers on utilizing raw plant materials like nuts, seeds, or legumes, which inherently contain oils and proteins as natural emulsifiers (Munekata et al., 2020). This method leverages the natural properties of plant sources by utilizing their oils for richness and flavor and using plant proteins to stabilize the emulsion. This approach eliminates the need for added emulsifiers and is also cost-effective due to the utilization of raw materials. However, a tranditional processing strategy potentially encompasses various complex processes, including roasting, soaking, blanching, milling, filtration, ingredient addition, sterilization, and homogenization. Each of these steps could significantly impact the quality of PBMAs. For instance, roasting can enhance flavor but may also lead to some nutritional loss (Özdemir et al., 2001). Soaking and blanching can reduce anti-nutritional factors

but might also affect the texture and nutrient content (Khandelwal et al., 2010). Milling and filtration determine the particle size and nutrition loss, as well as influence both the mouthfeel and stability of the final product. Significantly, various processing technologies can be further applied to enhance a product's stability, flavor, and nutritional profile by creating a uniform mixture. Fermentation involves using beneficial microorganisms to improve the taste, texture, and nutritional content of the product while also enhancing its shelf life and stability (Tangyu et al., 2019). Enzyme treatments are used to break down complex molecules, improving digestibility and nutrient availability, and can also modify the texture and flavor profile (Mehany et al., 2024). Homogenization, which involves breaking down fat molecules to create a uniform and stable mixture, is essential for preventing separation and improving mouthfeel (Mehany et al., 2024). Together, these technologies work synergistically to produce high-quality, stable, and nutritious products that meet consumer expectations. All these processes must be carefully optimized to balance the nutritional profile, taste, flavor, and overall cost, while also considering environmental impacts like CO₂ emissions and energy consumption.

Another strategy involves formulating oil-in-water emulsions by adding specific oils and emulsifiers to achieve a milk-like consistency and nutritional profile (McClements et al., 2019). Common oils used include almond, soy, and seed oils, known for their healthful fats and ability to blend smoothly into water with the help of emulsifiers such as plant proteins derived from plant materials, lecithin derived from soy or sunflowers, and carrageenan extracted from seaweed. These emulsifiers are crucial for stabilizing the emulsion, ensuring the oil droplets remain dispersed within the water rather than separating (McClements et al., 2019). One significant advantage of this strategy is the customized ingredients, for example, a high protein content can be effectively formulated into product development. To achieve a homogenous

mixture that closely mimics the texture and appearance of dairy milk, a homogenizer is employed. This device applies intense mechanical shear to the mixture, breaking down oil droplets to microscopic sizes and evenly distributing them throughout the liquid. Thus, the principles of PBMA production are a blend of traditional food processing techniques and modern technological advancements aimed at delivering a product that meets consumer expectations for nutrition, taste, and sustainability.

Stabilization of plant-based milk alternatives

The stabilization of PBMAs is contributed by two main factors which are the behavior of dispersed food components inside the system (*e.g.*, oil bodies, fat droplets, or plant fragments) and the nature of the aqueous solution (*e.g.*, pH, mineral composition, sugar content, viscosity, and density) (McClements, 2020). These two factors are subject to change and control, especially when the PBMA is induced with mechanical energy from homogenization and temperature change. In terms of destabilization, PBMA destabilization can be divided into physical destabilization, chemical destabilization, and microbial deterioration. For example, physical destabilization consists of common emulsion destabilization such as flocculation, coalescence, particle coalescence, oiling off, creaming, and sedimentation (Akoh, 2017). It is therefore critical to understand the fundamentals of stabilization, which can enable us to develop high-quality PBMAs. Thus, four critical aspects will be discussed, including the homogenization, emulsification, thickening, and measurement of stabilizing capability.

Homogenization

Homogenization is a critical step to improve the stability of PBMAs (Sherman et al., 2024). This process involves the application of mechanical forces to create a uniform system of the water and substrate phases for preventing potential separation and sedimentation.

Homogenization effectively reduces the size of fat globules through the application of large mechanical forces. This process allows emulsifiers, such as plant proteins, to adsorb onto the surface of oil droplets, preventing rapid coalescence and reducing the average size of oil droplets. A variety of mechanical devices can be employed to achieve this, including high-shear mixer, high pressure valve homogenizer, microfluidizer, ultrasonic homogenizer, colloid mill, etc. (McClements et al., 2019). High-shear mixers generate intense shear forces to create fine particles to enhance the creaminess and consistency. High-pressure valve homogenizers pass the mixture under extreme pressure through a narrow valve, which breaks down large particles to a microscopic level for improved stability (He and Xu, 2024). Microfluidizer can also be applied to formulate a homogeneous system by channeling the milk through microchannels at high velocities. Ultrasonic homogenizers apply high-frequency sound waves to create cavitation, which reduces particle size and improves uniformity (Sarangapany et al., 2022). Lastly, colloid mills use rotating discs to finely grind the plant material, which can be used to facilitate smoother textures. Both PBMAs and dairy milks will undergo homogenization. For dairy milks, a key focus of homogenization is on the oil droplets, as other components, such as casein proteins, have high water solubility. In contrast, for PBMAs, homogenization is crucial for the plant components as well, many of which, like plant proteins and fibers, have low water solubility. Effective filtration and homogenization are therefore essential for the production of stable PBMAs. Importantly, some other non-thermal innovative techniques have been used for PBMAs, such as fermentation and pulsed electric fields (PEF) (Sharma et al., 2024b; Silva et al., 2020a). For example, through the metabolic activities of microorganisms, fermentation can increase the viscosity and homogeneity of PBMAs due to the exopolysaccharides formation, reducing phase separation and settling of insoluble particles (Harper et al., 2022). Additionally,

PEF treatment improves the stability of PBMAs by reducing particle size and enhancing the content of bioactive compounds (Morales-de la Peña et al., 2023). However, it is critical to consider other potential impacts, including nutrition loss, taste and flavor, manufacturing expenses and environmental factors (*e.g.*, CO₂ emissions and energy use). To develop high-quality PBMAs, it is essential to consider multiple factors to identify the optimal solution.

Emulsification

Although various homogenizers can create more uniform and smaller particles, the absence of sufficient emulsifiers will result in aggregation. This is because plant-derived proteins and carbohydrates tend to aggregate due to strong attractive hydrophobic interactions and weak repulsive electrostatic interactions (McClements et al., 2019). Emulsifiers are normally used to reduce the interfacial free energies of hydrophobic components (*e.g.*, oils) in PBMAs. Therefore, effective stabilization of PBMAs critically depends on the careful selection and functionality of emulsifiers, which are tasked with forming a robust barrier around oil droplets to prevent their aggregation. This barrier is crucial for withstanding environmental stresses encountered during storage and use, such as fluctuations in pH, the presence of salts, interactions with other ingredients, and variations in temperature (McClements et al., 2019). Optimizing emulsifier properties is therefore crucial to ensure the stability of PBMAs. Commonly used emulsifiers include the plant proteins (*e.g.*, pea, lentil, and soy) (Vogelsang-O'Dwyer et al., 2021), polysaccharides (*e.g.*, gum arabic), and surfactants (*e.g.*, lecithin) (McClements, 2015).

Plant proteins are considered natural emulsifiers with varied amino acid compositions that can bind both the hydrophilic and hydrophobic sites of the emulsion system (Kim et al., 2020). However, plant proteins are very sensitive to the pH environment (Li and Xiong, 2021). As an example, plant-based proteins, such as pea, lentil, and faba bean, form emulsions that are

highly unstable near their isoelectric point (pH 5), high ionic strengths (>50 mM), and high temperatures (>70°C) (Gumus et al., 2017). There are also plant-based emulsifiers that can be used or combined with protein to provide better emulsion stability such as plant-based saponins and polysaccharides (McClements, 2020). Plant-based saponins and polysaccharides are stable over most of these conditions (McClements et al., 2019). Phospholipids, such as lecithin naturally occurring in plants such as soy and sunflowers, can also be incorporated into PBMAs to further improve the overall stability. Additionally, some extra steps can be used to improve the performance of plant-based emulsifiers, including the formation of covalent conjugation such as using the Maillard reaction, physical complexes using electrostatic attraction, and simple mixing (McClements, 2020; Lima et al., 2023).

Thickening

Texture modifiers, such as thickening agents, may be added to increase the viscosity of the aqueous phase. Stoke's law illustrates the velocity (v) of rigid spherical particles or the creaming velocity traveling upwards in an ideal liquid because of gravity.

$$v = -\frac{2gD^{2}(\rho_{2} - \rho_{1})}{18\eta_{1}},$$
(1)

where D and η_1 are the diameter of particles and the viscosity of solvent respectively, which plays a critical role in determining the creaming velocity. A wide range of natural biopolymers can be used as thickening agents, including those from land plants (such as starch, pectin, locust bean gum, or guar gum), seaweed (carrageenan or alginate), and microbial fermentation (xanthan gum) (McClements, 2015). For example, additives such as gums and thickeners are added to increase the viscosity of the PBMAs (Mackley et al., 2013). This will also impact the organoleptic property of PBMAs, especially if the milk is made for a specific type of product

such as plant-based creamers (Theocharidou et al., 2021). Chemically speaking, thickening agents are also able to improve the particle stability by retarding gravitational separation like creaming and protein sedimentation. When plant-based emulsifiers or plant proteins do not function effectively, charged polymers can further form a protective coating around the oil bodies. For example, charged carrageenan can adsorb the surface of the protein that is going to be positively charged in an acidic environment, thus it prevents aggregation and maintains the stability (Guzey and McClements, 2006).

Quantitative measurement of stabilization

To quantify the stabilization of PBMAs, it is key to understand how to measure their stabilizing capabilities. Various characterizations can be used to measure the stabilization capacities of PBMAs (Guzey and McClements, 2006). For example, particle size distribution and zeta potential are critical parameters for assessing the stability of PBMAs. Monitoring changes in particle size distribution over time can indicate the presence of aggregates or destabilization phenomena. Additionally, zeta potential measures the electrostatic repulsion or attraction between particles in a colloidal system. A high zeta potential value indicates strong repulsive forces between particles, which helps prevent aggregation and promotes stability. Conversely, a low or near-zero zeta potential may lead to particle flocculation or coalescence, resulting in milk instability. We analyzed the particle size distributions of three commercial PBMAs, as shown in Figure 1.3. It can be observed that the stability of PBMAs could still be significantly different from that of homogenized dairy milks (Mäkinen et al., 2015). The results reveal that particle sizes predominantly range from 0.1 to 1000 µm. Notably, significant variations were observed among almond milk samples from different brands, which indicates that stabilization issues in PBMAs have not been effectively addressed in production.

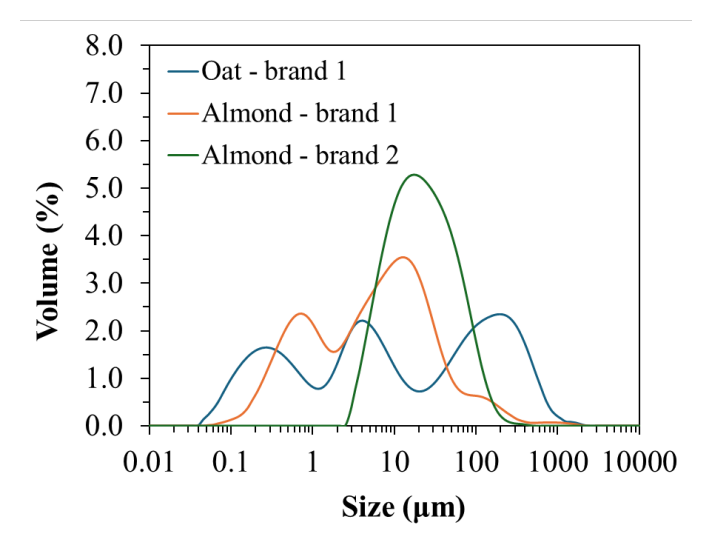


Figure 1.3. Particle size distributions of three commercial PBMA products. Data was collected from previous studies (Zhou et al., 2021b; Zhou et al., 2021a).

The rheological properties (*e.g.*, viscosity) play a crucial role in assessing the stability of PBMAs (Silva et al., 2019). Viscosity refers to the resistance of a fluid to flow and is influenced by factors such as particle size, concentration, and composition. In PBMAs, viscosity can affect stability by influencing the dispersion and movement of particles within the liquid. Higher viscosity may impede particle settling and phase separation, leading to improved stability. Conversely, low viscosity may result in rapid sedimentation or creaming, compromising the uniformity and shelf life of the milk. By measuring viscosity, researchers and manufacturers can quantify the flow behavior of PBMAs under various conditions and optimize formulation parameters to achieve desired stability characteristics. Additionally, viscosity measurements can guide the selection of stabilizers and thickeners to enhance the viscosity profile and stability of PBMAs, ensuring consistent quality and consumer satisfaction. Milk products with different viscosities can exhibit similar stability. For example, dairy milk has a low mean particle size ($d_{32} = 0.36 \ \mu m$) and low viscosity (3.15 mPa·s), while one of the almond milks has a high mean

particle size ($d_{32} = 1.10 \mu m$) and high viscosity (19.08 mPa·s) (Jeske et al., 2017). This suggests that stability can be resulted from a combination of multiple properties.

It should be mentioned that measuring the creaming rate and gravitational separation of PBMAs can reflect the stabilization parameters. Gravitational separation is another common way to cause the instability of PBMAs and occurs when the dispersed particles within the milk begin to separate under the influence of gravity (McClements, 2015). This phenomenon primarily is reflected by the inhomogeneity of density,

$$F_{g} = -\frac{4}{3}\pi r^{3} (\rho_{2} - \rho_{1})g,$$
(2)

where r is the radius of the particle, g is the acceleration of gravity, and ρ_1 and ρ_2 refer to the density of continuous and dispersed phases, respectively. This suggests that heavier components tend to migrate towards the bottom of the container (e.g., sedimentation), while lighter components rise to the top (e.g., creaming). The rate of gravitational separation is influenced by several factors including the size and density of the dispersed particles, the viscosity of the continuous phase, and the overall uniformity. Gravitational-induced separation in PBMAs comes from the fact that it has different ingredients dispersed in it and each of them has a different density. This different density will lead to gravitational separation when the ingredient is no longer dispersed into the solution which can either go down or go up depending on the density. For example, the gravitational separation of PBMA will tend to 'cream' due to the presence of a large amount of oils on the top, which have a lower density than water. However, plant-based fragments, protein aggregates, and calcium carbonate particles tend to 'sediment' since they have higher molecular weight leading to higher density. To counteract gravitational separation, manufacturers often add stabilizers or thickening agents to increase the viscosity or refine homogenization techniques to decrease particle size. These strategies enhance the colloidal

stability of PBMAs, to prevent the separation of layers and ensure a uniform product throughout its shelf life.

Challenges and future directions

Unlike dairy milks, stabilizing PBMAs remains a challenge due to the lower watersolubility of many plant-derived components, such as proteins and carbohydrates. This challenge is further exacerbated by the demand for clean-label products, which precludes the addition of extra food ingredients like emulsifiers and thickening agents. Apparently, addressing this challenge requires a deeper understanding of fundamental science and the introduction of innovative processing techniques. Several key questions need to be addressed to achieve this. First, we need to understand how different plant components (e.g., proteins, carbohydrates, and small compounds) affect stabilization. Unlike a simple oil-in-water emulsion, PBMAs are complex colloidal systems due to the diverse plant-derived components required to meet nutritional needs. This necessitates a deeper understanding of their structure-property-function relationships. For example, increasing the water solubility of plant proteins requires an understanding of how structural information determines interactions and influences overall stability. Second, we still need to investigate the impact of different innovative processing techniques on the stabilization. At present, many food techniques can be used to alter the physicochemical properties and structures of plant-derived components. For example, we need to know how advanced mechanical techniques (e.g., ultra high-pressure homogenization) can alter the native structure of plant components, which suggests that the operating conditions often need to be optimized. In addition, several advanced non-mechanical techniques (e.g., enzymatic processing and microbial fermentation) can be used to transform their large structures into smaller ones (Xie et al., 2023). These treatments can likely significantly increase the watersolubility of plant-derived components (Hidalgo-Fuentes et al., 2024). However, we still need to know how they change their structures and enhance the stabilization of PBMAs. Importantly, current processing strategies often produce insoluble by-products, so it is also critical to develop innovative strategies to minimize the food waste.

Nutrition and health of plant-based milk alternatives

Nutrition facts of plant-based milk alternatives and their raw materials

It is desirable for PBMAs to provide a nutritious alternative to traditional dairy milk. We therefore selected the four most popular PBMAs, such as almond, oat, soy, and coconut, to compare their nutrition facts (Table 1.1). A key distinction between PBMAs and traditional daily milk lies in their protein content, which follows this trend: low-fat milk \approx soy >> oat > almond > coconut, which is highly associated with the low water-solubility and emulsifying capability of plant proteins. An additional emulsifier, sunflower lecithin, is often added to stabilize the coconut and almond milks. For the fat content, sunflower oil is often added to enhance the properties (e.g., creaminess) of oat milk. Compared to the low-fat milks, most of them have a higher amount of total fat derived from intrinsic nut oils and added sunflower oil. For the carbohydrates, the oat milks have the highest content for three selected samples, but they are not due to the presence of a large amount of sugar, instead due to the larger starches or polysaccharides derived from oats. The presence of carbohydrates can increase the viscosity of milk systems, so oat milks can be free of the addition of thickening agents. This is different from other PBMAs, in which several thickening agents (e.g., cane sugar, locust bean gum, gellan gum) are normally added. In addition, both vitamins (e.g., vitamin A, B, E, and D) and minerals (e.g., calcium, potassium, and iron) are often included in these milk systems, to increase their nutrition value.

Table 1.1. Nutrition facts of common commercial plant-based milk alternatives with different brands. Data were collected from the label of each food product. Some milk products with specific brands, for oats, soy, and coconut, are not available to obtain the data. The low-fat milk is considered as a control group. The percentage values in the parentheses are calculated based on three major components: fat, carbohydrate, and protein. The symbol ('-') means that data is not available.

	Almond				Oat			Soy		Coconu	t	Low-fat milk
Name Serving size	Brand 1	Brand 2	Brand 3	Brand 4	Brand 2	Brand 3	Brand 4	Brand 1	Brand 4	Brand 3	Brand 4	Brand 4
(mL) Calories	240	240	240	240	240	240	240	240	240	240	240	240
(kcal)	60	130	40 3.5	40	100	130	120	80 4.5	100	80	50	110 2.5
Total fat (g) Saturated fat	2.5 (22%)	11 (58%)	(54%)	3 (50%)	3 (13%)	7 (32%)	5 (21%)	(27%)	4 (21%)	5 (33%)	5 (71%)	(11%)
(g)	0	1	0	0	0	0.5	0.5	0.5	0.5	4.5	5	1.5
Trans Fat (g) Polyunsatura		0	0	0	0	0	0	0	0	0	0	0
ted fat (g)	0.5	-	-	-	-	-	-	2.5	-	-	-	-
Monounsatur ated fat (g) Cholesterol	1.5	-	-	-	-	-	-	1	-	-	-	-
(mg) Total	0	0	0	0	0	0	0	0	0	0	0	15
carbohydrate s (g)	8 (70%)	3 (16%)	<1 (<15%)	2 (33%)	17 (74%)	14 (64%)	16 (67%)	4 (24%)	8 (42%)	9 (60%)	<1 (14%)) 12 (53%)
Dietary fiber (g) Total sugars	0	1	0	1	3	2	2	2	1	0	0	0
(g) Added sugar	7	1	0	<1	1	3	7	<1	6	7	<1	12
(g)	7	0	0	0	0	3	7	0	6	5	0	0
Proteins (g) vitamin A	1 (9%)	5 (26%)	2 (31%)	1 (17%)	3 (13%)	1 (5%)	3 (13%)	8 (48%)	7 (37%)	1 (7%)	<1 (14%)	8 (36%)
(mcg) Vitamin E	140	-	-	90	-	-	160	150	90	-	90	170
(mg) Vitamin D	4	-	-	7.5	-	-	-	0	-	-	-	-
(mcg) Vitamin B ₂	2	0	0	5	-	0	3.6	3	5	-	5	2.5
(Riboflavin) (mg) Vitamin B ₁₂	-	-	-	-	-	-	0.6	0.5	0.4	-	-	-
(mcg)	-	-	-	0.6	-	-	1.2	3	1.2	-	1.2	-
Sodium (mg)	150	5	140	150	120	110	140	75	85	110	30	125
Calcium (mg)) 470	60	440	50	22	240	350	300	300	280	140	300

Potass (mg)	sium	0	160	60	0	110	380	390	320	280	170	0	360
Iron (mg)	0.5	1	0.2	0	1	0.2	0	1.1	1	0.4	0	0
Additi		Sunflower Lecithin	-	Sunflower Lecithin	e Sunflower Lecithin	-	-	-	-	-	Sunflower r Lecithin		-
Additi Oils	ional	-	-	-	-	-	Sunflowe r Oil	Sunflower Oil	-	- Cane sugar,	-	-	-
Thick	U	Cane sugar, Locust bean gum,		Locust bean gum, Gellan	Locust bean gum, Gellan			Gellan	Gellan	Locust bean gum, Gellan	gum,	Gellan	
agents	8	Gellan gum	-	gum	gum	-	-	gum	gum	gum	Pectin	Gum	-

It is noted that insoluble plant residues are typically filtered out during the production of PBMAs. These residues contain many valuable insoluble plant components. For example, in almond milk production, residues known as 'almond pulp' are rich in insoluble fibers, proteins, and other nutrients. Thus, it is necessary to discuss the nutrition facts of raw plant materials, to provide a clear picture of potential nutrition loss due to the use of processing strategies. Table 1.2 compares the nutritional content of almond, oat, soybean, and coconut materials. Almonds are rich in fats (49.9%), contributing to their creamy texture and flavor, while coconuts have high water (47%) and saturated fat content (33.5%), offering unique consistency and flavor. Both almonds and coconuts have higher fat content compared to oats and soybeans, but the types of fats differ (Table 1.3). For example, almond fats are primarily monounsaturated (66.2%) and polyunsaturated (25.8%), whereas coconut fats are predominantly saturated (94.3%), mainly medium-chain fatty acids like SFA 12:0 (47.3%). In contrast, whole dairy milk fats consist mostly of long-chain saturated fatty acids (43.9%), including SFA 16:0 (32.3%) and SFA 18:0 (11.6%). It has been reported that plant-derived medium-chain saturated and unsaturated fats can provide various health benefits (Daryani et al., 2024). For example, these include improved lipid profiles and enhanced energy metabolism. Medium-chain fats, such as those found in coconuts,

are rapidly metabolized and can be used as a quick energy source, potentially aiding in weight loss (Daryani et al., 2024). Additionally, unsaturated fats, like those found in almonds, can support cardiovascular health by reducing bad cholesterol levels and increasing good cholesterol levels (Kalita et al., 2018).

In addition, oats are high in carbohydrates (66.3%), which provides natural sweetness and energy (Table 1.2). This is also consistent with the observation in the oat milks, in which the total carbohydrates contribute $68.3 \pm 2.4\%$ of major components (proteins, fats and carbohydrates). One potential reason is the presence of soluble carbohydrates. For example, most oats contain the soluble fiber, β -glucan, which forms a viscous solution in the digestive tract. It lowers postprandial glucose and insulin levels, and potentially enhances insulin sensitivity in diabetic and nondiabetic patients (Behall et al., 2006). The FDA recognizes that 3 g of β-glucan daily reduces coronary heart disease risk (Jenkins et al., 2002). Thus, the addition of oats can provide natural and health-promoting texturing agents for the development of high-quality PBMAs. Soybeans are notable for their high protein content (36.5%) (**Table 1.2**), which is also reflected in PBMAs (Table 1.1). Table 1.4 provides the amino acid profiles of various plant and animal sources. The dispensable/indispensable amino acid profile of soybeans (41.7/58.3%) closely resembles that of daily milk (44.0/56.0%) and human muscle (52.3/47.7%). However, these plant proteins still contain lower amounts of indispensable amino acids, such as lysine and leucine (Table 1.4). Overall, the total amount of indispensable amino acids in plant materials is generally lower compared to dairy milk (**Table 1.4**). Additionally, plant proteins typically have much lower water-solubility than animal-based proteins (Grossmann and McClements, 2023). This indicates that a greater amount of PBMAs must be consumed to achieve a balanced intake of essential amino acids, compared to dairy milks.

Table 1.2. The nutrition facts of plant materials collected from USDA FoodData Central database (https://fdc.nal.usda.gov). The percentage values in the parentheses are calculated based on three major components: fat, carbohydrate, and protein. The symbol ('-') means that data is not available.

	Almond	Oat	Soybean	Coconut
Total mass (g)	100	100	100	100
Energy (kcal)	579	389	446	354
Water (g)	4.41	8.22	8.54	47
Fat (g)	49.9 (53.8%)	6.9 (7.7%)	19.9 (23.0%)	33.5 (64.4%)
Fatty acids, total saturated (g)	3.8	1.22	2.88	29.7
Fatty acids, total	31.6	2.18	4.4	1.42
monounsaturated (g)				
Fatty acids, total	12.3	2.54	11.3	0.366
polyunsaturated (g)				
Ash (g)	2.97	1.72	4.87	0.97
Calcium (mg)	269	54	277	14
Potassium (mg)	733	429	1800	356
Sodium (mg)	1	2	2	20
Carbohydrate (g)	21.6 (23.3%)	66.3 (73.6%)	30.2 (34.9%)	15.2 (29.2%)
Fiber, total dietary (g)	12.5	10.6	9.3	9
Total sugars (g)	4.35	-	7.33	6.23
Protein (g)	21.2 (22.9%)	16.9 (18.8%)	36.5 (42.1%)	3.33 (6.4%)

Table 1.3. Normalized fat profiles of different plant and animal sources. Raw data are collected from the USDA FoodData Central database (https://fdc.nal.usda.gov). The symbol ('-') means that data is not available

	Almond	Oat	Soybean	Coconut	Whole milk
Fatty acids, total saturated	8.0	20.5	15.5	94.3	70.0
SFA 4:0 (Butyric acid)	0.0	-	-	-	2.5
SFA 6:0 (Caproic acid)	0.0	-	-	0.6	2.0
SFA 8:0 (Caprylic acid)	0.0	-	-	7.5	1.3
SFA 10:0 (Capric Acid)	0.0	-	-	5.9	3.2
SFA 12:0 (Lauric Acid)	0.0	-	-	47.3	3.7
SFA 14:0 (Myristic Acid)	0.0	-	0.3	18.6	11.4
SFA 16:0 (Palmitic Acid)	6.5	17.3	11.4	9.0	32.3
SFA 18:0 (Stearic Acid)	1.5	0.0	3.8	5.5	11.6

Fatty acids, total monounsaturated	66.2	36.7	23.7	4.5	25.9
MUFA 18:1 (Oleic Acid)	65.6	36.4	23.4	4.5	26.1
Fatty acids, total polyunsaturated	25.8	42.8	60.8	1.2	4.1
PUFA 18:2 (Linoleic Acid)	25.8	40.7	53.4	1.2	4.3
Σ SFA + MUFA + PUFA	100.0	100.0	100.0	100.0	100.0

Table 1.4. Normalized amino acid profiles of different plant and animal sources. Raw data for plant sources are collected from the USDA FoodData Central database (https://fdc.nal.usda.gov), while raw data for both "Milk" and "Human muscle" are obtained from a previous study (Gorissen et al., 2018). Tryptophan, aspartic acid, asparagine, and glutamine are not analyzed due to the unavailability of raw data for both 'Milk' and 'Human muscle'. The symbol ('-') means that data is not available.

	Almond	Oat	Soybean	Coconut	Milk	Human muscle
Indispensable Amino Acids						
Threonine	3.0	3.8	4.7	3.7	5.1	4.8
Methionine	0.8	2.1	1.5	1.9	3.0	2.8
Phenylalanine	5.7	5.9	5.7	5.2	5.1	6.3
Histidine	2.7	2.7	2.9	2.4	2.7	4.6
Lysine	2.9	4.6	7.3	4.5	8.5	10.9
Valine	4.3	6.2	5.4	6.2	5.2	7.1
Isoleucine	3.8	4.6	5.3	4.0	4.2	5.6
Leucine	7.5	8.5	8.9	7.6	10.1	10.4
Tryptophan	-	-	-	-	-	-
Σ Essential	30.8	38.4	41.7	35.3	44.0	52.3
Dispensable Amino Acids						
Serine	4.6	5.0	6.3	5.3	5.8	3.8
Glycine	7.3	5.6	5.0	4.8	2.2	5.1
Glutamic acid	31.5	24.6	21.1	23.3	24.2	21.5
Proline	4.9	6.2	6.4	4.2	10.6	0.0
Cysteine	1.1	2.7	1.8	2.0	0.3	0.0
Alanine	5.1	5.8	5.1	5.2	3.8	6.7
Tyrosine	2.3	3.8	4.1	3.1	5.5	3.3
Arginine	12.5	7.9	8.4	16.7	3.8	7.2
Aspartic acid	-	-	-	-	-	-
Asparagine	-	-	-	-	-	-
Glutamine	-	-	-	-	-	-

Σ Nonessential	69.2	61.5	58.3	64.6	56.0	47.7
Σ Essential + Nonessential	100.0	100.0	100.1	100.0	100.0	100.0

Micronutrients and health benefits

In addition to macronutrients, plant materials are often rich in micronutrients, particularly bioactive compounds like polyphenols, which are usually absent in dairy milks. This makes PBMAs more competitive in terms of their health benefits. PBMAs offer an ideal medium for the presence of various components, including vitamins, minerals, and nutraceuticals (McClements, 2020). While hydrophilic compounds can be directly incorporated into aqueous phase of PBMA systems, hydrophobic compounds pose a challenge due to their poor solubility. However, the diverse composition of PBMAs, featuring oil bodies stabilized by plant-based emulsifiers or proteins, facilitates the encapsulation of hydrophobic compounds, like oil-soluble vitamins. For instance, many PBMAs are fortified with vitamins A, E, and D (Table 1.1). Understanding the properties of milk systems and oil phase enables further fortification with essential fatty acids like DHA and EPA (McClements and McClements, 2023). Additionally, PBMAs are frequently fortified with essential minerals, notably calcium and potassium, to support bone health, muscle function, and nerve transmission (Aksoylu Özbek et al., 2023). Calcium fortification typically involves incorporating calcium carbonate or tricalcium phosphate into the formulations, to ensure adequate mineral levels and meet diverse dietary needs. This fortification strategy underscores the roles of PBMAs as viable alternatives to traditional dairy milks, to provide a broad spectrum of consumer preferences and nutritional requirements (Aksoylu Özbek et al., 2023).

The bioactive compounds from original plant materials can offer health benefits (Daryani et al., 2024). For example, isoflavones in soymilk can reduce memory dysfunction in

Alzheimer's patients, increase bone mineral density post-menopause, and lower blood pressure and insulin levels (Akhlaghi et al., 2020; Sathyapalan et al., 2018). Avenanthramides in oat milk show promising chemo-preventive and anticancer effects (Turrini et al., 2019). Sesamin and sesamolin in sesame milk provide neuroprotection against cerebral ischemia (Cheng et al., 2006). Almond milk, with 6.33 mg of vitamin E per 100 g, offers significant antioxidant benefits (Chalupa-Krebzdak et al., 2018). The antioxidant activity in PBMAs, due to the presence of polyphenols, plays a crucial role in preventing oxidative damage to nucleic acids, proteins, lipids, and DNA (Balsano and Alisi, 2009).

Fortifying PBMAs with nutraceuticals like polyphenols, curcuminoids, and carotenoids from other plant materials has garnered significant research attention, due to their potential health benefits (McClements, 2020). These compounds, sourced from various natural origins, contribute to the functional and nutritional profile of PBMAs. Studies have demonstrated the efficacy of incorporating hydrophobic compounds like curcumin, which can be seamlessly encapsulated within the oil bodies of PBMAs (Zheng et al., 2021). Innovative post pH-based methods have been developed to successfully integrate polyphenols into different PBMA matrices, to ensure their stability and bioaccessibility (Csuti et al., 2023). Encapsulation within oil bodies provides protection against auto-oxidation and chemical degradations, and thus safeguard the bioactivity of the incorporated compounds (Sani et al., 2022). It is noted that the bioavailability and functionality of fortified compounds is intricately linked to the structural attributes of milk systems. For example, the choice of oil type profoundly impacts the delivery efficiency of carotenoids in emulsions, with evidence suggesting a preference for long-chain fatty acids like corn oil (Qian et al., 2012). Other factors could also play an important role in

their gastrointestinal stability and absorptions, including oil droplet size, oil phase composition, and emulsifier type (Tan et al., 2022).

It is crucial to know how the nutritional profiles of PBMAs can align with dietary guidelines and recommendations for various populations, including vegetarians, vegans, athletes, and individuals with dietary restrictions (Tso and Forde, 2021). Given that current PBMAs often lack protein content, it becomes more important to balance the protein intakes, in particular for the athletes who need higher protein content and the presence of amino acids, to support muscle repair and recovery. It is noted that many plant materials lack some essential amnio acids, so it is important to include more plant sources (Day, 2013). However, plant materials provide other essential nutrients, like diverse types of fats, fibers, minerals, vitamin D, and vitamin B12. For individuals with dietary restrictions, such as lactose intolerance or milk allergies, PBMAs offer a safe and nutritious alternative that avoids common allergens, but they could have other nutderived allergens. Importantly, incorporating other plant materials can be a better choice for the development of healthier plant diets, which is an effective strategy to increase the diversity of nutrients. Moreover, PBMAs can be tailored to enhance specific nutritional needs, such as adding omega-3 fatty acids for heart health, including higher levels of iron and zinc for those at risk of deficiencies, or fortifying bioactive compounds from different plants. Overall, the versatility and fortification potential of PBMAs make them a suitable option to meet the diverse dietary needs and recommendations of various population groups.

Gastrointestinal digestion of plant-based milk alternatives

Even if PBMAs have comparable nutritional profiles to dairy milks, their components may have a different gastrointestinal fate. It has been widely acknowledged that the digestion process differs between PBMAs and dairy milks, and potentially impacts macronutrient

absorption rates in the gastrointestinal tract (Sridhar et al., 2023). These differences may stem from variations in composition, processing conditions, and structural properties. The gastric environment could significantly affect the gastrointestinal fate of PBMAs by influencing their structural changes and nutrient release kinetics. Understanding these dynamics is crucial for optimizing the nutritional benefits of PBMAs and tailoring products to meet consumer needs.

Proteins, lipids, and carbohydrates

Protein gastrointestinal digestion has a similar pathway to the other macronutrients which primarily starts from the stomach with the presence of pepsin, followed up by more digestion in the small intestine by proteases such as trypsin and chymotrypsin (Shaghaghian et al., 2022). To evaluate the gastrointestinal digestion of plant proteins in the PBMAs, an *in vitro* and *in vivo* model of gastrointestinal digestion can be made. Recent studies have investigated the digestion behavior of PBMAs, including almond, oat and soy milks (Wang et al., 2020; Wang et al., 2021, 2022). Results revealed distinct behaviors among PBMAs made from almonds, soybeans, and oats under gastric conditions. Almond milk exhibited flocculation and rapid layering of oil bodies, while soymilk formed sedimented particles and oat milk showed minimal structural changes (Wang et al., 2020; Wang et al., 2021, 2022). Another study used the INFOGEST method to evaluate the protein quality of milk-, plant-, and insect-based protein materials. Milk-based protein materials had the highest protein digestibility (86.1–90.8%), followed by soy (85.1%) and wheat (82.3%). These materials had significantly higher protein digestibility compared with zein (65.1%), cricket (63.6%), and mealworm (69.5%) (Komatsu et al., 2023).

The gastrointestinal digestion of fat starts in the stomach which induces a temporary digestion or breakdown of by preduodenal lipases and emulsification by peristalsis (Wang et al., 2013). The primary breakdown occurs in the pancreas by pancreatic lipase and phospholipase A2

for phospholipids producing free fatty acids. PBMAs inherit the benefit of plant sources which have more unsaturated fat than saturated fat. A recent study has investigated the nutritional value of four commercial PBMAs (almond, hemp, oat, and soy), in particular for fatty acid profiles (Martínez-Padilla et al., 2020). The fatty acid analysis results showed that most of the products predominantly contained oleic acid (C18:1 ω -9) and linoleic acid (C18:2 ω -6). These essential fatty acids were reported to bring several health benefits such as anti-inflammatory benefits, modulate gene transcription, cell membrane structure, and cytokines precursors (Glick and Fischer, 2013).

Unlike traditional dairy milks, which primarily contains lactose, the carbohydrate composition of PBMAs varies widely depending on the source. For instance, almond milk contains primarily carbohydrates from almonds, such as simple sugars (glucose and fructose) and fiber, while soy milk contains complex carbohydrates like oligosaccharides and soluble fiber from soybeans, and oat milks have the highest content of carbohydrates. During digestion, enzymes in the gastrointestinal tract break down these carbohydrates into smaller molecules for absorption. However, the presence of fiber and other compounds in PBMAs may affect the rate and extent of carbohydrate digestion, impacting blood sugar levels and overall nutrient absorption. For example, carbohydrates such as dietary fiber and resistant starches may not be absorbed in the small intestine which make them pass over to the large intestine (Grabitske and Slavin, 2009). The remaining dietary fibers and resistance starches are going to be broken down by gut bacteria by fermentation producing gases and short-chain fatty acids. These short chain fatty acids are useful to be used as the fuel for this bacteria which impacts the activities and versatility of this bacteria for human health and wellbeing (Carlson and Slavin, 2016). Since dietary fiber is less digested in the gastrointestinal tract, they do not increase the glucose blood

level as high as simple sugar which can be beneficial for human health to reduce the risk of diabetes type II and cardiovascular disease (Hodge et al., 2004).

Vitamins, nutraceuticals, minerals, and anti-nutrients

Fat-soluble vitamins like A, D, and E in PBMAs undergo distinct digestion kinetics influenced by the milk matrix and compounds such as carbohydrates (Tan and McClements, 2021). Understanding vitamin digestion in PBMAs is crucial for nutritional assessment and formulation optimization to enhance bioavailability. Vitamin D is often used to fortify both animal-based or PBMAs, in order to enhance the absorption of calcium and phosphorus. Recent studies have examined the effect of additives like TiO₂, carbohydrate-based nanocellulose, or calcium on vitamin D bioaccessibility. It was observed that a low bioaccessibility of vitamin D was observed in fortified PBMAs and the presence of calcium could further reduce this effect (Figure 1.4) (Zhou et al., 2021a; Zhou et al., 2021b). In addition, fortification with calcium, particularly using different calcium forms (CaCl₂ versus CaCO₃), may further decrease vitamin D bioaccessibility due to insoluble calcium soap formation in the small intestine (Zhou et al., 2021b; Dima and Dima, 2020). This underscores the importance of considering calcium forms in PBMA fortification to maintain optimal vitamin absorption.

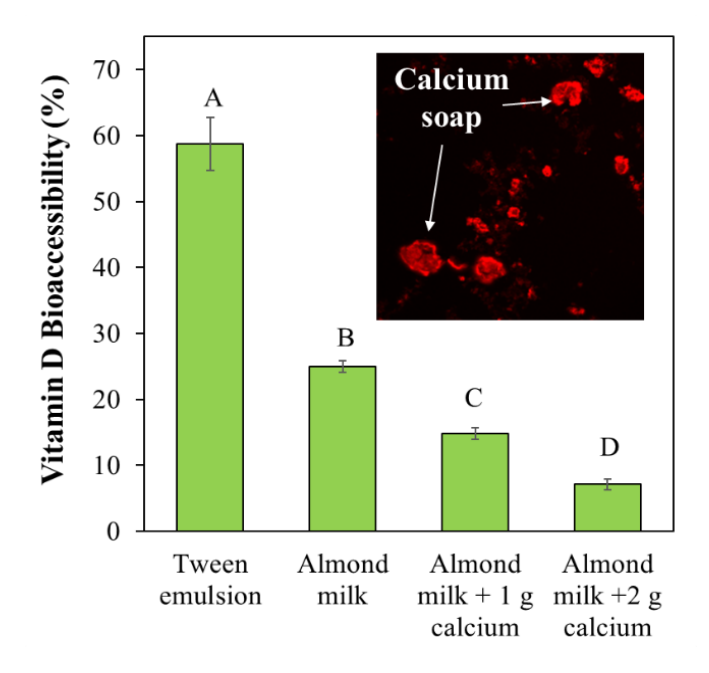


Figure 1.4. Impact of food matrix on vitamin D bioaccessibility. "Tween emulsion" is the Tween 20-stablized nanoemulsions as a control group. Insoluble calcium (CaCO₃) was used in all samples. Data was collected from a previous study (Zhou et al., 2021b).

Furthermore, PBMAs have been recognized as ideal vehicles for fortifying nutraceuticals from other plants, as evidenced by a study on curcumin-fortified PBMAs. Curcumin, for instance, was effectively incorporated into almond, cashew, coconut, and oat milk analogs (Zheng et al., 2021). Lipid digestion and curcumin bioaccessibility were consistent across all PBMAs and using a post pH-driven method significantly increase the curcumin bioaccessibility observed in milk analogs (>60%) compared to its free form (5%). This highlights the potential of PBMAs as effective carriers for enhancing the bioavailability of nutraceutical compounds like curcumin. Besides, a previous study showed that the fortification of multiple polyphenols can be used to not only change the appearance of PBMAs, but also enhance the bioaccessibility of hydrophobic polyphenols (**Figure 1.5**).

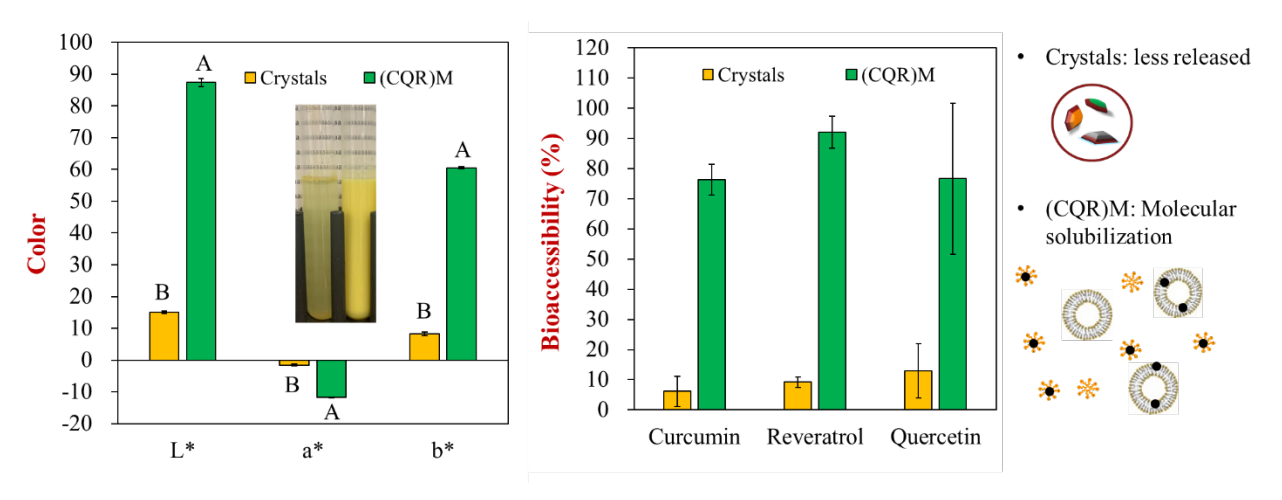


Figure 1.5. Effects of polyphenol fortification on the visual appearance of plant-based milk alternative and the bioaccessibility of polyphenols. "(CQR)M" represents a plant-based milk alternative fortified with multiple polyphenols, specifically a blend of curcumin, resveratrol, and quercetin, while the "Crystals" is a mixture of their crystalline forms. Data was collected from a previous study (Zheng et al., 2023).

It is a common practice to fortify PBMAs with various minerals, to enhance their nutritional value. A comparative elemental analysis of milk from mammals (cow, goat, and donkey) and various PBMAs (such as soy, rice, oat, spelt, almond, coconut, hazelnut, walnut, cashew, hemp, and quinoa) revealed notable differences in mineral composition (Astolfi et al., 2020). For example, PBMAs, compared to goat and cow milks, showed variations in the sources of major minerals, like calcium, potassium, magnesium, sodium, and phosphorus. For other minerals, soy milk contained notable amounts of copper and iron, coconut milk had chromium and selenium, and hemp milk contained molybdenum. Importantly, toxic trace elements such as arsenic, cadmium, mercury, and lead were found to be negligible in all samples. Additionally, a separate study examined mineral content in various plant-based beverages (rice, cashew nut, almond, peanut, coconut, oat, soy milks), and revealed wide-ranging mineral concentrations (Silva et al., 2020b). For instance, calcium content ranged from 10 to 1697.33 mg/L for rice and

coconut milk, respectively, while magnesium content varied from 6.29 to 268.43 mg/L for rice and cashew nut beverages. Iron content ranged from 0.76 mg/L to 12.89 mg/L in rice samples, while zinc content varied from 0.57 mg/L to 8.13 mg/L in oat and soya milk samples, respectively.

The presence of antinutrients such as protease inhibitors, phytates, lectins, and trypsin inhibitors in PBMAs poses significant challenges to nutritional digestion and absorptions (Sharma et al., 2024b). These antinutrients are known to inhibit nutrient absorption and digestion but can be denatured and inactivated through heat. Phytates, which serve as storage forms of phosphorus and inositol in cereals, pulses, nuts, and seeds, can form soluble complexes with divalent cations like zinc, iron, and calcium in the acidic pH of the stomach, thus reducing the bioavailability of these essential nutrients (López-Moreno et al., 2022; Kumar et al., 2010). The effectiveness of reducing phytates can be enhanced with the use of phytase enzymes. Common antinutrients include lectins in cereals and nuts, trypsin inhibitors in legumes, tannins in legumes, and saponins in legumes (Daryani et al., 2024). Effective elimination methods include microwave treatment for lipoxygenase, and high hydrostatic pressure treatment for trypsin inhibitors (Kubo et al., 2021).

Challenges and future directions

At present, concerns have been raised regarding substituting dairy milk with PBMAs. For example, the labeling of PBMAs as "milk" has been a contentious issue. It seems like the term "milk" should either refer to products as currently defined by the FDA or to those providing comparable nutritional value to standard dairy milk, from a pediatric medical and nutritional standpoint (Laudon and Diamantas, 2022). It is desirable for PBMAs to have a competitive or even superior nutritional profile compared to dairy milks. Achieving this goal requires further

research. For example, we need to understand the nutrient flow from raw plant materials, PBMA products, to digestion and absorption. Plant materials used in PBMAs offer valuable ingredients, such as medium-chain saturated and unsaturated fats, fiber-rich carbohydrates, and bioactive compounds. However, a significant challenge is how to maximize their utilization from raw materials in the development of PBMAs. Many valuable plant components (e.g., proteins, fibers, and bioactive compounds) can be often discarded, due to their low water-solubility. We therefore need more data evidence to highlight the potential waste or new processing strategies for better food development. Another challenge is how to increase the protein content, in particular essential amnio acids. Blended PBMAs can be a promising direction for constructing a more balanced protein profile (Lee et al., 2024). The presence of anti-nutritional factors could hinder nutrient absorption. Future efforts can therefore focus on their impacts on the nutritional profile of PBMAs or introducing new techniques, such as enzymatic treatments and fermentation, to break down anti-nutritional factors and improve protein solubility. Particularly, fermentation technology has been used to improve the flavor and quality of PBMAs as well as their nutritional properties {Terefe, 2022 #1554}. Additionally, exploring novel plant sources to develop hybrid products could provide balanced nutrition and improved health benefits. Currently, there is a relatively poor understanding of how different PBMAs affect the human gut microbiome and the implications for long-term human health. Ensuring that PBMAs offer comprehensive nutritional support while maintaining their appeal as sustainable and health-conscious alternatives is crucial for their future success.

Environmental impacts

Life cycle assessments (LCAs)

The growing concern over environmental degradation and the ever-increasing threat of global warming have put immense pressure on communities worldwide to adopt more sustainable practices. One significant contributor to environmental stress is the dairy industry, known for its high greenhouse gas emissions and substantial water usage (Guzmán-Luna et al., 2022). In response to these challenges, there has been a notable rise in the popularity of PBMAs. These alternatives, such as almond, soy, oat, and coconut milk, are expected to offer potential solutions to mitigate environmental impacts. Currently, many research articles claim that producing PBMAs generally results in lower CO₂ emissions and requires less water compared to conventional dairy milk (Khanpit et al., 2024; Aydar et al., 2020). Generally, the global warming potential (GWP) values of PBMAs are often lower than 1 kg CO₂-eq per liter of milk, whereas dairy milks exceed 1 kg CO₂-eq per liter (Khanpit et al., 2024). For instance, a life cycle assessment report indicates that almond, oat, and coconut milks have lower CO₂ emissions compared to dairy milk (Milk > Coconut > Oat > Almond) (Buchan et al., 2022). This report categorizes the environmental impact into four contributions: "Crop Production," "Milk Processing," "Packaging & End-of-Life (EOL)," and "Co-Product Credit." Notably, the "Packaging & EOL" contribution has the largest impact due to the use of recyclable polyethylene terephthalate (PET) in the packaging materials, surpassing the contributions from "Crop Production" and "Milk Processing" (Figure 1.6A). It is important to note that most PBMAs have lower protein content, which can significantly alter the trend when evaluated on a protein basis, showing a different order of Coconut > Milk \approx Almond > Oat for their GWP values (**Figure 1.6B**). This is largely due to the lower protein levels in PBMAs, particularly in coconut milk.

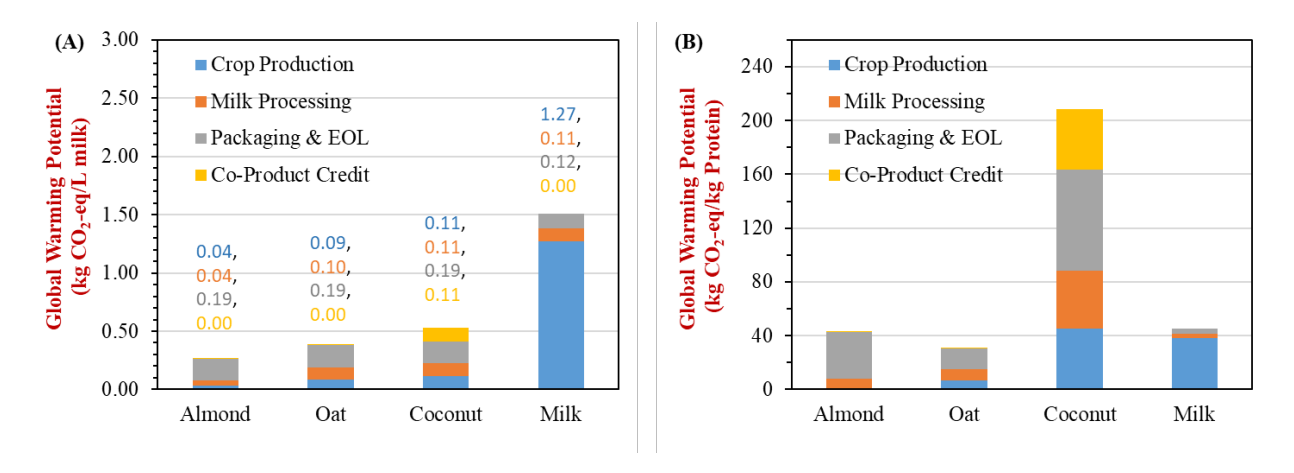


Figure 1.6. (A) Global warming potential (kg CO₂-eq/L milk) of different PBMAs compared to dairy milk. The total value is contributed by four parts, including the "Crop production", "Milk Processing", and "Packaging & End-of-Life", and "Co-Product Credit", and their individual values are labeled on each bar plot, respectively. (B) Global warming potential (kg CO₂-eq/kg protein) of different PBMAs compared to dairy milk. Data are obtained from a life cycle assessment report (Buchan et al., 2022).

The water footprint of PBMAs is another critical factor in assessing their environmental sustainability. This life cycle assessment report, which adjusted water use in PBMAs with different water scarcity factors, also provided insights into this aspect (Buchan et al., 2022). Compared to conventional dairy milk, which requires approximately 41,700 liters of water per liter of milk produced after adjustment, PBMAs generally have a lower water footprint, though the exact amount varies among different types (**Figure 1.7**). However, almond milk is an exception, with a relatively higher water footprint among PBMAs, needing about 45,600 liters of water per liter due to the irrigation demands of almond trees. This observation, highlighted in previous studies as well, is mainly due to the significant water required to grow almonds (Khanpit et al., 2024; McClements et al., 2019). As expected, the dominant water use for both

PBMAs and dairy milk comes from crop or dairy raw milk production, which far exceeds the water used in milk processing or ingredient handling.

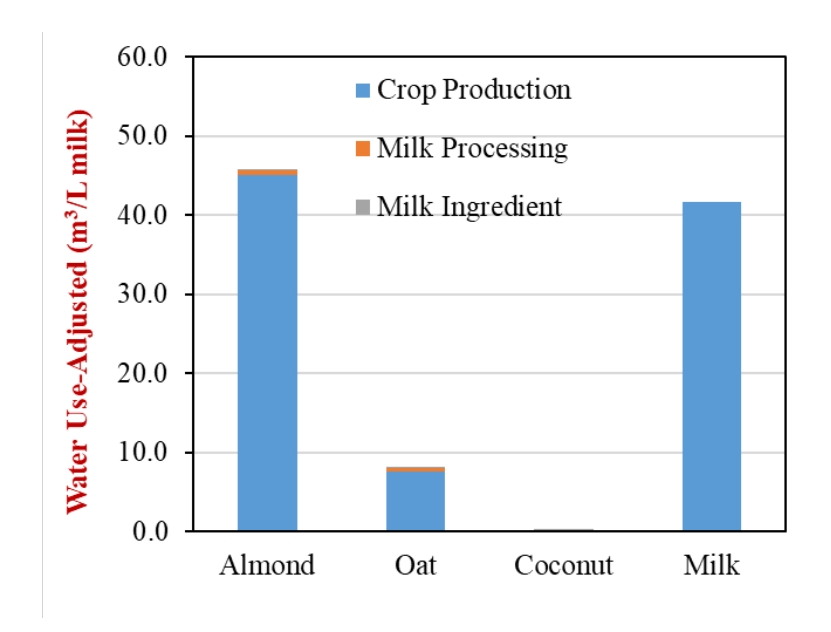


Figure 1.7. Water footprint results of different PBMAs and dairy milk. Water scarcity factor (SF) applied for the calculations of water use. Data and calculations can be obtained from a life cycle assessment report (Buchan et al., 2022).

Challenges and future directions

It is crucial to have quantitative models to provide data evidence regarding the environmental impacts of PBMAs. However, it should be noted that data obtained from LCAs can vary significantly, highlighting the importance of considering data variance (Khanpit et al., 2024). Although many programs have been developed to conduct LCAs, the calculations rely on numerous assumptions, and various factors can influence the results. These factors include the origin of raw materials, processing conditions, packaging types, and transportation methods. Therefore, a reliable and unified model is needed to provide accurate quantitative measurements. To address these challenges, developing a standardized and comprehensive LCA model is essential. Such a model should integrate consistent methodologies and account for all relevant

variables to ensure comparability and reliability of the data. This could be achieved through the use of advanced digital simulation platforms, such as those based on artificial intelligence (AI)(De Silva and Alahakoon, 2022). An AI-based digital platform could streamline the data collection process, enhance the accuracy of predictions, and allow for real-time adjustments and comparisons based on varying conditions. By employing a unified digital simulation platform, researchers and industry stakeholders could obtain comparable data, which will facilitate better decision-making and policy development. This approach would not only improve the reliability of environmental impact assessments but also promote transparency and consistency across studies, ultimately contributing to more sustainable practices in the production and consumption of PBMAs.

Conclusions

This review has provided a comprehensive overview of current status and challenges of PBMAs. We began by exploring the production processes and underlying principles of PBMAs, focusing on two key formulation strategies. We then examined the stabilization of PBMAs through three fundamental aspects: homogenization, emulsification, and thickening, along with quantitative measurements to assess stabilization capabilities. Next, we explored the nutritional profiles and health aspects of PBMAs and their raw materials, discussing the gastrointestinal digestion of macronutrients and micronutrients in PBMAs. Lastly, the environmental impacts of PBMAs are discussed. Importantly, we also provided detailed discussions on their challenges and future directions in every aspect. Overall, this review highlights the multifaceted considerations involved in the production, stabilization, nutrition, digestion, and environmental impacts of PBMAs. It underscores the need for a multi-dimensional optimization strategy to design and produce more sustainable, nutritious, tasty, and affordable PBMAs. We particularly

need a comprehensive understanding of the structure-property-function relationships of plant components. It is essential to understand the flow of nutrients, energy, and carbon emissions from raw plant materials to PBMA products, as well as their digestion and absorption, especially the impacts of processing technologies. These tasks require collaboration among experts from various fields to accelerate the innovation of milk alternatives. Additionally, PBMAs can serve as a versatile base for creating various other popular food products, such as cream, ice cream, yogurt, cheese, and butter. Therefore, it is crucial to develop various PBMA-derived food products to meet different customers' needs.

References

- Abrieux A, Avilla M, Bagla A, Chang G, Haskins L, Keys V, et al. The evolving market of plant-based milk: Alfalfa and other potential sources. 2022.
- Akhlaghi, M, Ghasemi Nasab, M, Riasatian, M, Sadeghi, F. Soy isoflavones prevent bone resorption and loss, a systematic review and meta-analysis of randomized controlled trials. Crit Rev Food Sci Nutr. 2020;60:2327-41.

 https://doi.org/10.1080/10408398.2019.1635078
- Akoh, CC. Food lipids: chemistry, nutrition, and biotechnology. Boca Raton: CRC Press; 2017
- Aksoylu Özbek, Z, Taşkın, B, & Sözeri Atik, D. Fortification of plant-based food analogs. In:

 Aydar AY, editor. Plant-based foods: ingredients, technology, and health aspects. Cham:

 Springer International Publishing; 2023. p. 35-72
- Astolfi, M. L, Marconi, E, Protano, C, Canepari, S. Comparative elemental analysis of dairy milk and plant-based milk alternatives. Food Control. 2020;116:107327. https://doi.org/10.1016/j.foodcont.2020.107327
- Aydar, EF, Tutuncu, S, Ozcelik, B. Plant-based milk substitutes: bioactive compounds, conventional and novel processes, bioavailability studies, and health effects. J Funct. Foods. 2020;70:103975. https://doi.org/10.1016/j.jff.2020.103975
- Balsano, C, Alisi, A. Antioxidant effects of natural bioactive compounds. Curr Pharm Design. 2009;15:3063-73.
- Behall, KM, Scholfield, DJ, Hallfrisch, JG, Liljeberg-Elmståhl, HGM. Consumption of both resistant starch and β-glucan improves postprandial plasma glucose and insulin in women. Diabetes Care. 2006;29:976-81. https://doi.org/10.2337/dc05-2012

- Buchan, L, Henderson, A, Unnasch, S. Ripple milk life cycle assessment. 2022.
- Carlson, J, Slavin, J. Health benefits of fibre, prebiotics and probiotics: a review of intestinal health and related health claims. Quality assurance and Safety of Crops & Foods. 2016;8:539-54. https://doi.org/10.3920/QAS2015.0791
- Chalupa-Krebzdak, S, Long, CJ, Bohrer, BM. Nutrient density and nutritional value of milk and plant-based milk alternatives. Int Dairy J, 2018;87:94-92. https://doi.org/10.1016/j.idairyj.2018.07.018
- Cheng, F-C, Jinn, T-R, Hou, RC, Tzen, JT. Neuroprotective effects of sesamin and sesamolin on gerbil brain in cerebral ischemia. Int J Biomed Scie IJBS. 2006;2:284-8.
- Csuti, A, Zheng, B, & Zhou, H. Post pH-driven encapsulation of polyphenols in next-generation foods: principles, formation and applications. Crit Rev Food Sci Nutr. 2023; 1-15. https://doi.org/10.1080/10408398.2023.2258214
- Daryani, D, Pegua, K, & Aryaa, SS. Review of plant-based milk analogue: its preparation, nutritional, physicochemical, and organoleptic properties. Food Sci Biotechnol. 2024;33:1059-73. https://doi.org/10.1007/s10068-023-01482-z
- Day, L. Proteins from land plants potential resources for human nutrition and food security.

 Trends in Food Sci Technol. 2013;32:25-42. https://doi.org/10.1016/j.tifs.2013.05.005
- De Silva, D, Alahakoon, D. An artificial intelligence life cycle: from conception to production.

 Patterns, 3
- Dima, C, Dima, S. Bioaccessibility study of calcium and vitamin D3 co-microencapsulated in water-in-oil-in-water double emulsions. Food Chem. 2020;303:125416. https://doi.org/10.1016/j.foodchem.2019.125416
- FAO. Dairy market review: emerging trends and outlook 2023. Italy: FAO Rome; 2023.

- GFI. Plant-based meat, seafood, eggs, and dairy. 2023 State of the Industry Report. 2023.
- Glick, NR, Fischer, MH. The role of essential fatty acids in human health. J. Evid Based Complementary Altern Med. 2013;18:268-89. https://doi.org/10.1177/215658721488788.
- Gorissen, SHM, Crombag, JJR, Senden, JMG, Waterval, WAH, Bierau, J, Verdijk, LB, et al.

 Protein content and amino acid composition of commercially available plant-based protein isolates. Amino Acids. 2018;50:1685-95. https://doi.org/10.1007/s00726-018-2640-5
- Grabitske, HA, Slavin, JL. Gastrointestinal effects of low-digestible carbohydrates. Crit Rev Food Sci Nutr. 2009;49:327-60. https://doi.org/10.1080/10408390802067126
- Grossmann, L, McClements, DJ. Current insights into protein solubility: a review of its importance for alternative proteins. Food Hydrocoll. 2023;137:108416.

 https://doi.org/10.1016/j.foodhyd.2022.108416
- Gumus, CE, Decker, EA, McClements, DJ. Gastrointestinal fate of emulsion-based ω-3 oil delivery systems stabilized by plant proteins: lentil, pea, and faba bean proteins. J. Food Eng. 2017;207:90-8. https://doi.org/10.1016/j.jfoodeng.2017.03.019
- Guzey, D, McClements, DJ. Formation, stability and properties of multilayer emulsions for application in the food industry. Adv Colloid Interface Sci. 2006;128-130:227-48. https://doi.org/10.1016/j.cis.2006.11.021
- Guzmán-Luna, P, Mauricio-Iglesias, M, Flysjö, A, Hospido, A. Analysing the interaction between the dairy sector and climate change from a life cycle perspective: a review.

 Trends in Food Sci Technol. 2020;126:168-179.

 https://doi.org/10.1016/j.tifs.2021.09.001

- Harper, AR, Dobson, RCJ, Morris, VK, Moggré, G-J. Fermentation of plant-based dairy alternatives by lactic acid bacteria. J. Microbial Biotechnol. 2020;15:1404-21. https://doi.org/10.1111/1751-7915.14008
- He, A, Xu, B. High-pressure homogenisation improves food quality of plant-based milk alternatives. Int J Food Sci Technol. 2024;59:399-407. https://doi.org/10.1111/ijfs.16822
- Hidalgo-Fuentes, B, de Jesús-José, E, Cabrera-Hidalgo, A d J., Sandoval-Castilla, O, Espinosa-Solares, T, González-Reza, RM, et al. Plant-based fermented beverages: nutritional composition, sensory properties, and health benefits. Foods. 2024;13:844.
- Hodge, AM, English, DR, O'Dea, K, Giles, GG. Glycemic index and dietary fiber and the risk of type 2 diabetes. Diabetes Care. 2004;27:2701-6. https://doi.org/10.2337/diacare.27.11.2701
- Jenkins, DJA, Kendall, CWC, Vuksan, V, Vidgen, E, Parker, T, Faulkner, D, et al. Soluble fiber intake at a dose approved by the US Food and Drug Administration for a claim of health benefits: serum lipid risk factors for cardiovascular disease assessed in a randomized controlled crossover trial123. Am J Clin Nutr. 2022;75, 834-9. https://doi.org/10.1093/ajcn/75.5.834
- Jeske, S, Zannini, E, Arendt, EK. Evaluation of physicochemical and glycaemic properties of commercial plant-based milk substitutes. Plant Foods Hum Nutr. 2017;72:26-33. https://doi.org/10.1007/s11130-016-0583-0
- Kalita, S, Khandelwal, S, Madan, J, Pandya, H, Sesikeran, B, Krishnaswamy, K. Almonds and cardiovascular health: a review. Nutrients. 2018;10:468.

- Khandelwal, S, Udipi, SA, Ghugre, P. Polyphenols and tannins in Indian pulses: effect of soaking, germination and pressure cooking. Food Res Int. 2010;43:526-530. https://doi.org/10.1016/j.foodres.2009.09.036
- Khanpit, V, Viswanathan, S, Hinrichsen, O. Environmental impact of animal milk vs plant-based milk: critical review. J Clean Prod. 2024;449:141703. https://doi.org/10.1016/j.jclepro.2024.141703
- Kim, W, Wang, Y, Selomulya, C. Dairy and plant proteins as natural food emulsifiers. Trends in Food Sci Technol. 2020;105:261-72. https://doi.org/10.1016/j.tifs.2020.09.012
- Komatsu, Y, Tsuda, M, Wada, Y, Shibasaki, T, Nakamura, H, Miyaji, K. Nutritional evaluation of milk-, plant-, and insect-based protein materials by protein digestibility using the INFOGEST digestion method. J Agric Food Chem. 2023;71:2503-13. https://doi.org/10.1021/acs.jafc.2c07273.
- Kubo, MTK, dos Reis, BHG, Sato, LNI, Gut, JAW. Microwave and conventional thermal processing of soymilk: inactivation kinetics of lipoxygenase and trypsin inhibitors activity. LWT. 2021;145:11275. https://doi.org/10.1016/j.lwt.2021.111275
- Kumar, V, Sinha, AK, Makkar, HPS, Becker, K. Dietary roles of phytate and phytase in human nutrition: A review. Food Chem, 2010;120:945-59. https://doi.org/10.1016/j.foodchem.2009.11.052
- Laudon, KG, Diamantas, K. What's in a name? updates on plant-based product labeling Regulations. FDLI Update. 2020;30.
- Lee, PY, Leong, SY, Oey, I. The role of protein blends in plant-based milk alternative: a review through the consumer lens. Trends Food Sci Technol. 2024;143:104268. https://doi.org/10.1016/j.tifs.2023.104268

- Li, R, Xiong, YL. Sensitivity of oat protein solubility to changing ionic strength and pH. J Food Sci. 2021;86:78-85. https://doi.org/10.1111/1750-3841.15544
- Lima, RR, Stephani, R, Perrone, ÍT, and de Carvalho, AF. Plant-based proteins: a review of factors modifying the protein structure and affecting emulsifying properties. Food Chemistry Adv. 2023;3:100397. https://doi.org/10.1016/j.focha.2023.100397
- López-Moreno, M, Garcés-Rimón, M, Miguel, M. Antinutrients: lectins, goitrogens, phytates and oxalates, friends or foe? J Functional Foods. 2022;89:104938. https://doi.org/10.1016/j.jff.2022.104938
- Mackley, MR, Tock, C, Anthony, R, Butler, SA., Chapman, G, Vadillo, DC.The rheology and processing behavior of starch and gum-based dysphagia thickeners. J Rheol. 2013;57:1533-53. https://doi.org/10.11221/1.4820494
- Mäkinen, OE, Uniacke-Lowe, T, O'Mahony, JA, Arendt, EK. Physicochemical and acid gelation properties of commercial UHT-treated plant-based milk substitutes and lactose free bovine milk. Food Chem. 2015;168:630-38.

 https://doi.org/10.1016/j.foodchem.2014.07.036
- Martínez-Padilla, E, Li, K, Blok Frandsen, H, Skejovic Joehnke, M, Vargas-Bello-Pérez, E, Lykke Petersen, I. In Vitro Protein Digestibility and Fatty Acid Profile of Commercial Plant-Based Milk Alternatives. Foods. 2020;9:1784. https://doi.org/10.3390/foods9121784
- McClements, DJ. Food emulsions: principles, practices, and techniques. Boca Raton, FL:CRC press;2015.

- McClements, DJ. Development of next-generation nutritionally fortified plant-based milk substitutes: structural design principles. Foods. 2020;9:421. https://doi.org/10.3390/foods9040421
- McClements, DJ, Grossmann, L. The science of plant-based foods: constructing next-generation meat, fish, milk, and egg analogs. Compr Rev Food Sci Food Saf. 2021;20:4049-100. https://doi.org/10.1111/1541-4337.12771
- McClements, DJ, Newman, E, McClements, IF. Plant-based milks: a review of the science underpinning their design, fabrication, and performance. Compr Rev Food Sci Food Saf. 2019;18:2047-67. https://doi.org/10.1111/1541-4337.12505
- McClements, IF, McClements, DJ. Designing healthier plant-based foods: fortification, digestion, and bioavailability. Food Res Int. 2023;169:112853. https://doi.org/10.1016/j.foodres.2023.112853
- Mehany, T, Siddiqui, SA, Olawoye, B, Olabisi Popoola, O, Hassoun, A, Manzoor, MF, et al.

 Recent innovations and emerging technological advances used to improve quality and process of plant-based milk analogs. Crit Rev Food Sci and Nut. 2024;64:7237-67.

 https://doi.org./10.1080/10408398.2023.2183381
- Morales-de la Peña, M, Arredondo-Ochoa, T, Welti-Chanes, J, Martín-Belloso, O. Application of moderate intensity pulsed electric fields in red prickly pears and soymilk to develop a plant-based beverage with potential health-related benefits. Innov Food Sci Emerg Technol. 2023188:10342. https://doi.org/10.1016/j.ifset.2023.103421
- Munekata, PES, Domínguez, R, Budaraju, S, Roselló-Soto, E, Barba, FJ, Mallikarjunan, K, Lorenzo, JM. Effect of innovative food processing technologies on the physicochemical

- and nutritional properties and quality of non-dairy plant-based beverages. Foods. 2020;9,:288
- Özdemir, M, Açkurt, F, Yildiz, M, Biringen, G, Gürcan, T, Löker, M. Effect of roasting on some nutrients of hazelnuts (Corylus Avellena L.). Food Chem. 2001;73:185-90. https://doi.org/10.1016/S0308-8146(00)00260-0
- Qian, C, Decker, EA, Xiao, H, and McClements, DJ. Nanoemulsion delivery systems: influence of carrier oil on β-carotene bioaccessibility. Food Chem. 2012;135L1440-1447. https://doi.org/10.1016/j.foodchem.2012.06.047
- Sani, MA, Tavassoli, M, Azizi-Lalabadi, M, Mohammadi, K, McClements, DJ. Nano-enabled plant-based colloidal delivery systems for bioactive agents in foods: design, formulation, and application. Adv Colloid Interface Sci. 2022;305:102709.

 https://doi.org/10.1016/j.cis.2022.102709
- Sarangapany, AK, Murugesan, A, Annamalai, AS, Balasubramanian, A, Shanmugam, A. An overview on ultrasonically treated plant-based milk and its properties A Review. Appl Food Res. 2022;2:100130. https://doi.org/10.1016/j.afres.2022.100130
- Sathyapalan, T, Aye, M, Rigby, AS, Thatcher, NJ, Dargham, SR, Kilpatrick, ES. et al. Soy isoflavones improve cardiovascular disease risk markers in women during the early menopause. Nutr Metab Cardiovasc Dis. 2018;28:691-97. https://doi.org/10.1016/j.numecd.2018.03.007
- Shaghaghian, S, McClements, DJ, Khalesi, M, Garcia-Vaquero, M, Mirzapour-Kouhdasht, A.

 Digestibility and bioavailability of plant-based proteins intended for use in meat
 analogues: a review. Trends in Food Sci Tech. 2022;129:646-56.

 https://doi.org/10.1016/j.tifs.2022.11.016

- Sharma, N, Yeasmen, N, Dube, L, Orsat, V. Rise of plant-based beverages: a consumer-driven perspective. Food Rev Int. 2024a;1-27. https://doi.org/10.1080/87559129.2024.2351920
- Sharma, N, Yeasmen, N, Dubé, L, and Orsat, V. A review on current scenario and key challenges of plant-based functional beverages. Food Biosci. 2024b;60:104320. https://doi.org/10.1016/j.fbio.2024.104320
- Sherman, IM, Mounika, A, Srikanth, D, Shanmugam, A, Ashokkumar, M. Leveraging new opportunities and advances in high-pressure homogenization to design non-dairy foods.

 Comp Rev Food Sci Food Saf. 2024;23:13282. https://doi.org/10.1111/1541-4337.13282
- Silva, ARA, Silva, MMN, Ribeiro, BD. Health issues and technological aspects of plant-based alternative milk. Food Res Int. 2020a;131:108972.

 https://doi.org/10.1016/j.foodres.2019.108972
- Silva, JGS, Rebellato, AP, Caramês, ETdS., Greiner, R, Pallone, JAL. In vitro digestion effect on mineral bioaccessibility and antioxidant bioactive compounds of plant-based beverages.

 Food Res Int. 2020;130:108993. https://doi.org/10.1016/j.foodres.2020.108993
- Silva, K, Machado, A, Cardoso, C, Silva, F, Freitas, F. Rheological behavior of plant-based beverages. Food Sci Tech. 2019;40:258-63.
- Sridhar, K, Bouhallab, S, Croguennec, T, Renard, D, Lechevalier, V. Recent trends in design of healthier plant-based alternatives: nutritional profile, gastrointestinal digestion, and consumer perception. Crit Rev Food Sci Nutr. 2023;63:10483-98. https://dor.org/10.1080/10408398.2022.2081666
- Tan, Y, McClements, DJ. Improving the bioavailability of oil-soluble vitamins by optimizing food matrix effects: A review. Food Chem. 2021;348:129148.
 https://doi.org/10.1016/j.foodchem.2021.129148

- Tan, Y, Zhou, H, McClements, DJ. Application of static in vitro digestion models for assessing the bioaccessibility of hydrophobic bioactives: A review. Trends Food Sci Technol. 2022;122:314-27. https://doi.org/10.1016/j.tifs.2022.02.028
- Tangyu, M, Muller, J, Bolten, CJ, Wittmann, C. Fermentation of plant-based milk alternatives for improved flavour and nutritional value. Appl Microbiol Biotechnol. 2019;103:9263-75. https://doi.org.10.1007/s00253-019-10175-9
- Theocharidou, A, Ahmad, M, Petridis, D, Vasiliadou, C, Chen, J, Ritzoulis, C. Sensory perception of guar gum-induced thickening: correlations with rheological analysis. Food Hydrocoll. 2021;111:106246. https://doi.org/10.1016/j.foodhyd.2020.106246
- Tireki, S, Balkaya, M, Erdem, DE, Coskun, G, Gunay, E, Cekirge, M. A review on sensory parameters and evaluation methods of plant-based protein foods. Food Rev Int. 2024;1-20. https://doi.org/10.1080/87559129.2024.2370944
- Tso, R, Forde, CG. Unintended consequences: nutritional impact and potential pitfalls of switching from animal- to plant-based foods. Nutrients. 2021;13:2527.
- Turrini, E, Maffei, F, Milelli, A, Calcabrini, C, and Fimognari, C. Overview of the anticancer profile of avenanthramides from oat. Int J Mol Sci. 2019;20:4536.
- Vogelsang-O'Dwyer, M, Zannini, E, Arendt, EK. Production of pulse protein ingredients and their application in plant-based milk alternatives. Trends Food Sci Technol. 2021;110:364-74. https://doi.org/10.1016/j.tifs.2021.01.090
- Wang, TY, Liu, M, Portincasa, P, and Wang, DQH. New insights into the molecular mechanism of intestinal fatty acid absorption. Eur J Clin Invest. 2013;43:1203-23.

- Wang, X, Ye, A, Dave, A, Singh, H. In vitro digestion of soymilk using a human gastric simulator: impact of structural changes on kinetics of release of proteins and lipids. Food Hydrocoll. 2021;111:106235. https://doi.org/10.1016/j.foodhyd.2020.106235
- Wang, X, Ye, A, Dave, A, Singh, H. Structural changes in oat milk and an oat milk-bovine skim milk blend during dynamic in vitro gastric digestion. Food Hydrocoll. 2022;124: 107311. https://doi.org/10.1016/j.foodhyd.2021.107311
- Wang, X, Ye, A, Singh, H. Structural and physicochemical changes in almond milk during in vitro gastric digestion: impact on the delivery of protein and lipids. Food Funct, 2020;11:4314-26. https://doi.org/10.1039/C9FO02465D
- Xie, A, Dong, Y, Liu, Z, Li, Z, Shao, J, Li, M, Yue, X. A review of plant-based drinks addressing nutrients, flavor, and processing technologies. Foods. 2023;12:3952.
- Yu, Y, Li, X, Zhang, J, Li, X, Wang, J, Sun, B. Oat milk analogue versus traditional milk: comprehensive evaluation of scientific evidence for processing techniques and health effects. Food Chem X. 2023;19:100859. https://doi.org/10.1016/j.fochx.2023.100859
- Zhao, J, Zeng, X, Xi, Y, Li, J. Recent advances in the applications of lactobacillus helveticus in the fermentation of plant-based beverages: a review. Trends Food Sci Technol. 2024;147:104427. https://doi.org/10.1016/j.tifs.2024.104427
- Zheng, B, Zhou, H, McClements, DJ. Nutraceutical-fortified plant-based milk analogs: bioaccessibility of curcumin-loaded almond, cashew, coconut, and oat milks. LWT Food Sci Technol. 2021;147. https://doi.org./10.1016/j.lwt.2021.111517
- Zheng, B, Zhou, H, McClements, DJ. Co-encapsulation of multiple polyphenols in plant-based milks: formulation, gastrointestinal stability, and bioaccessibility. Foods. 2023;12:3432. https://doi.org/10.3390/foods12183432

- Zhou, H, Liu, J, Dai, T, Muriel Mundo, JL, Tan, Y, Bai, L, McClements, DJ. The gastrointestinal fate of inorganic and organic nanoparticles in vitamin D-fortified plant-based milks. Food Hydrocoll. 2021a;112:106310. https://doi.org/10.1016/j.foodhyd.2020.106310
- Zhou, H, Zheng, B, Zhang, Z, Zhang, R, He, L, McClements, DJ. Fortification of plant-based milk with calcium may reduce vitamin D bioaccessibility: an in vitro digestion study. J. Agric Food Chem. 2021b;69:4223-4233. https://doi.org/10.1021/acs.jafc.1c01525

CHAPTER 2

ENHANCING THE EFFICIENCY AND SUSTAINABILITY OF PRODUCING CURCUMININFUSED PLANT-BASED MILK ALTERNATIVES WITH TWO-IN-ONE POST PHDRIVEN PROCESSING STRATEGY 2

² Suryamiharja, A., Gong, X., Akoh, C.C., and Zhou, H. 2025. Enhancing the efficiency and sustainability of producing curcumin-infused plant-based milk alternatives with a two-in-one post pH-driven processing strategy. *Food Frontiers*, 6:716-726. Reprinted here with permission of the publisher.

Abstract

Increasing food sustainability and health benefits is essential to meet the demands of a growing global population while minimizing environmental impact. This study used a green two-in-one post pH-driven processing strategy to develop a sustainable and healthy plant-based milk alternative. It achieved both extraction and encapsulation in one step by directly incorporating the health-promoting curcumin from turmeric into soymilk. A high processing efficiency was observed, $94.2 \pm 1.6\%$, with a high extraction efficiency of $96.4 \pm 0.5\%$. Using raw turmeric instead of a purified curcumin significantly enhanced the sustainability in the use of raw materials, e.g., reducing the CO₂-eq emissions by 22 times and energy use by 10 times, even with a very small percentage of curcumin (~0.03 wt%) in the formulation. This strategy underscores the importance of using raw materials and minimizing processing steps to develop more sustainable foods. Additionally, the incorporation of curcumin was found to impart a yellow color to soymilk. No significant changes were observed in other physicochemical properties like particle size, zeta potential, and melting behavior, as most curcumin molecules were encapsulated within the lipid phase of soymilk. The curcumin-infused soymilk also maintained excellent storage stability for one month under freezing temperature.

Keywords: Food sustainability, health-promoting, plant-based milk, soymilk, turmeric, curcumin, carbon emissions

Introduction

Numerous plant-derived bioactive compounds, such as polyphenols, have applications in health and wellness, including their use as antioxidants, anti-inflammatory agents, and anticancer agents (Cuevas-Cianca et al., 2023; Salehi et al., 2020). One example is curcumin derived from *Curcuma longa L.* (Turmeric). Curcumin has been employed in managing chronic diseases (Aggarwal & Sung, 2009), enhancing immune function (Peng et al., 2021), and promoting mental health (Sathyabhama et al., 2022). Additionally, it is increasingly being incorporated into functional foods, nutraceuticals, and pharmaceuticals to leverage their therapeutic properties for improved health outcomes (Rafiee et al., 2019). However, curcumin has very low water solubility and chemical stability, resulting in poor oral bioavailability (Liu et al., 2020). This limitation significantly reduces its therapeutic efficacy, as only a small fraction of the ingested curcumin reaches the systemic circulation. Consequently, various delivery systems, such as the use of nanoparticles, have been developed to enhance the bioavailability and stability of curcumin, thereby maximizing its health benefits (Pan-On et al., 2022).

Plant-based milk alternatives (PBMAs), such as almond, oat, and soy milks, serve as an excellent delivery system for enhancing the bioavailability of curcumin (McClements, 2020). PBMA can provide a lipid-rich environment that aids in the solubilization and stabilization of hydrophobic curcumin, thereby facilitating its absorption in the digestive tract (Zhou et al., 2021a, 2021b). Incorporating curcumin into PBMAs is considered a promising functional food innovation, which not only harnesses the health benefits of curcumin but also leverages the sustainability of plant-based ingredients in PBMAs (Zheng et al., 2021a). Recently, research has successfully demonstrated the potential of PBMAs as effective delivery systems for bioactive compounds like curcumin (Zheng et al., 2021a, 2023). These studies observed that PBMAs can

significantly enhance the solubility and stability of curcumin, leading to greater utilization and improved bioavailability. Incorporating curcumin into PBMAs not only enhances their health benefits but also provides a convenient way to consume this compound daily. Consequently, curcumin-infused PBMAs are gaining attention as functional foods with the potential to greatly support overall human health and well-being.

However, incorporating curcumin into PBMAs can be challenging due to its poor solubility and chemical instability (Manasa et al., 2023). Various formulation techniques have been proposed, including mechanical methods (Gökdemir et al., 2020; Shirsath et al., 2021), heat treatments (Jiang et al., 2020), and the use of organic solvents (Dhivya & Rajalakshmi, 2018). However, many of these incorporation methods face practical challenges, including high production costs, complex manufacturing processes, and potential negative environmental impacts. The pH-driven method is an emerging technique to increase the solubility and stability of polyphenols (e.g., curcumin) in PBMAs (Zheng et al., 2023). By using an alkaline solution, curcumin can be transformed into its deprotonated form, which enhances its water-solubility in aqueous solution. This curcumin-dissolved solution can then be directly added to PBMA, followed by an acidification process (e.g., adding citric acid) to neutralize the curcumin molecules. This simple process ensures the effective encapsulation of curcumin within PBMAs, offering a promising solution to the challenges of incorporating curcumin by reducing production costs and simplifying the manufacturing process. For example, this method has been used to encapsulate curcumin into different PBMAs such as almond, cashew, coconut, and oat milk (Zheng et al., 2021a). A recent study showed that this method produced a high encapsulation efficiency (>86%) and improved the bioaccessibility of curcumin (>60%) compared to its crystalline form (~5%) (Zheng, Zhang, et al., 2019). This finding is supported by various studies,

which indicate that curcumin can be incorporated into milk products with relatively high encapsulation efficiency (Du et al., 2022; Gao et al., 2022; Zheng, Lin, et al., 2019; Zhou et al., 2024).

Although the pH-driven method is effective for delivering polyphenols like curcumin, it faces negative environmental impacts due to the raw materials used. For instance, many studies depend on purified curcumin powders extracted with organic solvents, which are costly and unsustainable (Jiang et al., 2021). To address this challenge, we propose a two-in-one post pH-driven (PPD) processing strategy (Csuti et al., 2023). This strategy has two key aims: first, to use raw plants directly for developing more sustainable and cost-effective foods, and second, to attain high processing efficiency by carefully controlling and optimizing the processing conditions. In this study, we demonstrated the feasibility of integrating both extraction and encapsulation in one step. Through this strategy, curcumin can be directly incorporated from raw turmeric into soymilk. We hypothesize that this two-in-one PPD processing strategy will be more sustainable compared to conventional processing strategy, while also demonstrating high efficiency in both extraction and encapsulation. This work aims to provide critical insights for developing health-promoting PBMAs and serves as a representative example of plant-based food innovation by integrating different raw plants to enhance food sustainability and health.

Materials and Methods

Materials

Turmeric powder (Georgia Gold Turmeric Powder) was obtained from American Turmeric Company (Bainbridge, Georgia), and the curcumin standard (purity > 97.0%) was purchased from TCI America (Portland, Oregon). Vanilla silk soy creamer (~10 wt% fat), as an example of soymilk, was sourced from Earth Fare in Athens, Georgia. Potassium hydroxide

(CAS 1310-58-3) was acquired from Mallinckrodt Chemicals (St. Louis, Missouri), while citric acid (CAS 77-92-9) and sodium citrate dihydrate (CAS 6132-04-3) were obtained from Sigma Aldrich (St. Louis, Missouri). The sodium phosphate monobasic monohydrate (CAS 10049-21-5), sodium phosphate dibasic heptahydrate (CAS 7782-85-6), acetic acid glacial J.T. Baker™ (CAS 64-19-7), Koptec's pure 200 proof pure ethanol (CAS 64-17-5), and acetonitrile (HPLC grade, CAS 75-05-8) were purchased from Fisher Scientific (Waltham, Massachusetts).

Formulation of curcumin-infused soymilk using two-in-one PPD method

To incorporate curcumin from turmeric powder into soymilk (turmeric-soymilk), 0.5 g turmeric powder was dissolved in 10 mL 0.1 M KOH solution. This solution was vortexed at the highest speed for 1-min and then centrifuged for 10-min at 2,000 rpm in a closed centrifuge tube (15 mL), to minimize oxygen exposure under the alkaline condition. 2.5 mL of supernatant was then mixed into 50 mL soymilk, to achieve a loading capacity of 1 mg of curcumin per gram of fat in the soy milk, as validated in a previous study (Zheng, Zhang, et al., 2019). Sequentially, the solution was adjusted to pH 7 using a pH 3 citrate buffer. For comparison, curcumin powder was also used to formulate curcumin-infused soymilk (curcumin-soymilk). In this process, 10 mL of 0.1 M KOH solution was used to fully dissolve 20 mg of curcumin crystals, following the same formulation process as the curcumin-soymilk.

Making curcumin-infused soymilk powder

To obtain both curcumin- and turmeric-soymilk powders, freeze drying (EPIC Freeze Dryer, Millrock Technology, Inc, Kingston, New York) was conducted within a total of 33.5 h, which has two freezing steps with ramping rates of 0 and 0.5 °C/min and hold time of 0.5 h and 4 h subsequently. Primary drying was applied for 18 h to fully sublimate the ice into gas at a shelf temperature from -33 to 10 °C. The secondary drying was applied at a shelf temperature of

40 °C with a total time of 6 h. The storage temperature was maintained at 20 °C and the vacuum at 0 mTorr for 4 h. An extra freeze treatment was applied to reach the temperature of -51 °C and a hold time of 1 h. The sample was then ground using pastel and mortar immediately to avoid moisture from the air. The sample was stored in an Amber container in a freezer (-14 °C) for stability study.

Concentration of curcumin

A UV-vis spectrophotometer (Agilent Cary 60) was used to measure the concentration of curcumin. The standard curve obtained was y = 6.2891x - 0.1427 ($R_2 = 0.998$), where x is the absorbance value, and y is the concentration of curcumin in ppm (**Figure S1A**). Pure curcumin was dissolved in acidified ethanol (1 wt% acetic acid, v/v), and the absorbance peak was at a wavelength of 430 nm. The quantification of curcumin was also compared to the analysis of HPLC-DAD/RID (Shimadzu Nexera XS inert series) with a C18 column (ZORBAX Stable Bond C18, 4.6 x 250 mm, 5 μ m, 80 Å, 400 bar). Pure curcumin crystal was first dissolved in the KOH solution (pH 13), and then acidified ethanol. The mobile phase was a mixture of acidified ethanol and acetonitrile (55:45, v/v). The HPLC analysis was performed at a flow rate of 1 mL/min, ambient temperature (25 °C), injection volume of 20 μ L, with a total run time of 8 min. The absorbance peak was at a wavelength of 422 nm. The standard curve for HPLC was y = 5.4977x - 0.0002 ($R_2 = 0.999$), where x is the area (a.u.) × 1.E-6, and y is the concentration of curcumin in ppm (**Figure S1B**).

Determination of processing efficiency

The two-in-one processing strategy integrates both extraction and encapsulation processes in one step, and its efficiency is defined as follows,

Two-in-one efficiency = $\frac{c_1}{c_0} \times 100\%$, (1)

where C_0 refers to the ideal concentration of curcumin in curcumin-infused milk, assuming no curcumin loss during processing. This ideal concentration is based on the initial curcumin concentration in turmeric powder, measured using an ethanol-based method as a reference. In this method, 20 mg of turmeric powder was dissolved in 100 mL of ethanol and stirred for 1 h at 800 rpm. The resulting solution was centrifuged for 5 min at 2,000 rpm to obtain a clear solution, which was then used for UV-vis measurement. C_1 refers to the measured concentration of curcumin in curcumin-infused milk formulated by the two-in-one PPD method. To measure the concentration of curcumin in curcumin-infused milk, the samples were centrifuged for 5 min at 2,000 rpm, diluted with acidified ethanol, vortexed for 30 s, and filtered using Whatman paper (11 μ m, 9 cm). Both extraction efficiency and encapsulation efficiency were determined as follows:

Extraction efficiency =
$$\frac{C_{ex}}{C_o}$$
 × 100%, and

Encapsulation efficiency
$$=\frac{c_1}{c_{ex}} \times 100\%$$
, (2)

where $C_{\rm ex}$ refers to the concentration of curcumin extracted from turmeric or curcumin powder by the PPD method.

Determination of processing sustainability

The energy consumption and carbon emissions were estimated using the Technoeconomic, Energy & Carbon Heuristic Tool for Early-Stage Technologists (TECHTEST) provided by the U.S. Department of Energy (IEDO, 2024). We compared two different processing strategies to produce curcumin-infused soymilk powders. The first strategy was a conventional two-step process that began with extracting purified curcumin, which was then

55

used as the raw material to formulate curcumin-infused soymilk powder. The second strategy was the two-in-one PPD processing, which used turmeric as the raw material to directly formulate turmeric-infused soymilk powder. The functional unit for comparison is the production of curcumin-infused powders with approximately 10 kg of curcumin. More details, including the processing flow chart and the parameters used for raw material inputs and manufacturing, can be found in the supporting information.

Appearance Instrumental Color

The colorimetric analysis was conducted using an instrumental colorimeter (ColorFlex EZ 45/0 LAV, Hunter Colorimeter, Reston, Virginia). The L^* , a^* , and b^* values were measured by pouring 10 mL of the sample into a transparent petri dish. The black and white standardized plates were used as the blanks with the standardized light source (D65) and detection angle (10 degrees). The photos were taken using an iPhone 13 camera with a black background and white light.

Particle size and zeta potential

The particle size was analyzed using a Mastersizer 3000 particle analyzer (Malvern Panalytical, Westborough, MA). Approximately 2 mL of the sample was introduced into the instrument to achieve 24% obscuration, using a refractive index of 1.47. A 60 s equilibration period was then applied prior to the actual measurement (Abdo et al., 2023). The zeta potential measurement was analyzed using Zetasizer Pro (Malvern Panalytical, Westborough, MA). A 0.02 mL sample was diluted with 9.98 mL of phosphate buffer (pH 7) and then transferred into the specified cuvettes for analysis. The sample was equilibrated for 30 s, and the mean zeta potential (mV) was measured.

Differential scanning calorimetry (DSC)

Differential scanning calorimetry (DSC 204 F1 Phoenix, NETZSCH Instruments North America LLC, Burlington, MA) was used to obtain DSC profiles of all samples, including pure curcumin, turmeric powder, soymilk powder, curcumin-soymilk powder, and turmeric-soymilk powder. Approximately 10 mg of the sample was placed in a crucible (with an empty crucible as a blank). The temperature range was set from 30 to 240 °C, with an increasing rate of 10 °C per min. The measurement was conducted under a nitrogen atmosphere, and the results were analyzed using built-in software.

Storage stability

Different time intervals (0, 1, 7, 14, and 30 days) were used for the stability test of curcumin in both curcumin-soymilk and turmeric-soymilk samples. These samples were put in a container and were stored under freezing conditions at -14°C, to assess their stability over time. In brief, 0.1 g of the sample was dissolved in 10 mL of acidified ethanol (1 wt% acetic acid) and stirred for 20-min, with a saran wrap placed over the top of the beaker. The sample was then centrifuged for 10-min at 2,000 rpm and evaluated using a UV spectrophotometer at 430 nm wavelength.

Remaining (%) =
$$\frac{D_x}{D_0} \times 100\%$$
, (3)

where D_0 and D_x is the concentration of curcumin at 0-day and x-day, respectively.

Statistical analysis

At least three measurements were carried out for all experiments, followed with the calculations of mean and standard error. One-way ANOVA, followed by a post hoc Tukey HSD test (p < 0.05), was used to determine statistical significance (Vasavada, 2016).

Results and Discussion

Two-in-one PPD processing strategy for developing health-promoting PBMAs

A schematic of the two-in-one PPD processing strategy is shown in **Figure 2.1**. This processing strategy is designed for the development of polyphenol-powered PBMAs. It leverages two key principles. First, it can be sustainably used to incorporate a diverse range of plantderived polyphenols into various PBMAs, maximizing their health benefits. Adding healthpromoting polyphenols from various plants can significantly enhance the nutritional and health profile of PBMAs (Cosme et al., 2020). For instance, integrating turmeric, known for its curcumin content, can create a healthier product and contribute to better public health outcomes (Kocaadam & Şanlier, 2017). Second, this strategy shows promise for addressing the challenge of processing efficiency by minimizing the chemical degradation of polyphenols in alkaline solutions. We focused on controlled operating conditions to enhance processing efficiency. For example, minimizing oxygen exposure can significantly reduce chemical degradation, and rapid processing can be achieved as polyphenols can be quickly extracted due to their high solubility when negatively charged in an alkaline solution (Csuti et al., 2023). Meanwhile, an acidic buffer can be readily added to neutralize the alkaline solution when incorporated into the PBMA system. Using curcumin-infused soymilk as an example, this study aims to demonstrate the practical feasibility of this processing strategy.

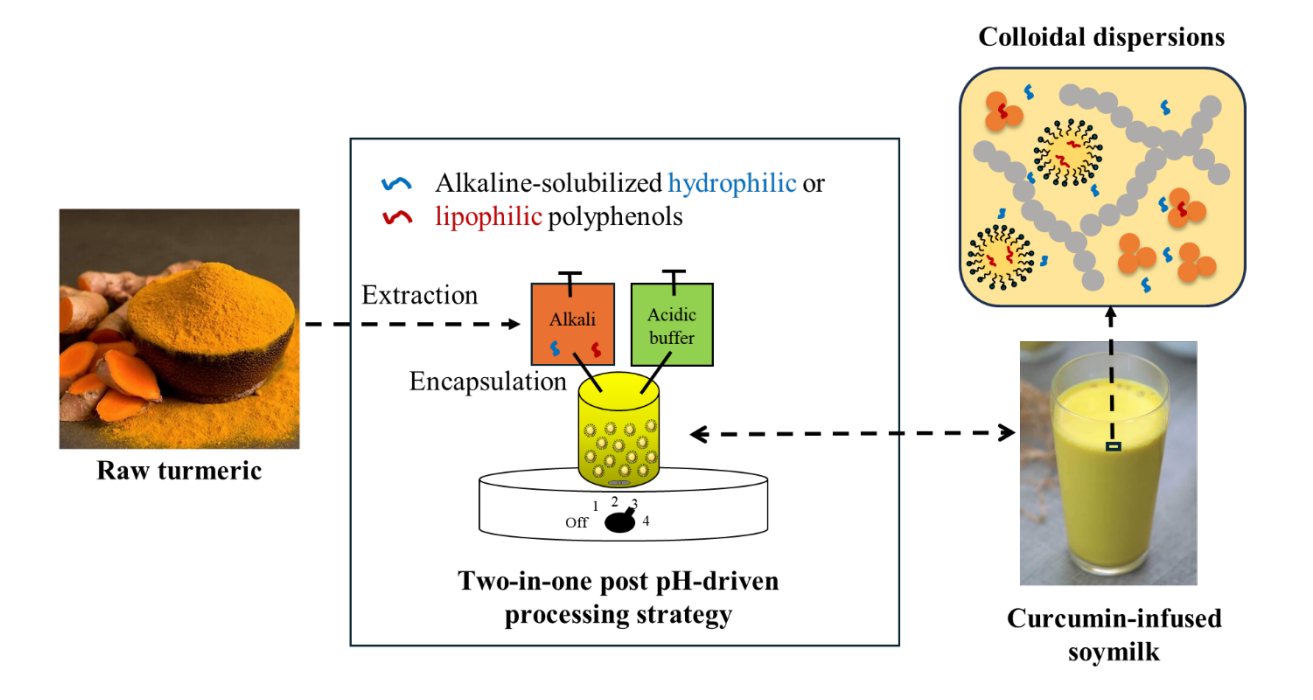


Figure 2.1. A two-in-one PPD strategy for developing curcumin-infused PBMAs (e.g., soymilk). The bioactive curcumin molecules can be directly extracted from raw turmeric and then encapsulated into soymilk in one process.

Increased efficiency of PPD processing strategy

One of our research focuses is to determine whether this PPD method maintains high operational efficiency when incorporating curcumin from turmeric into soymilk. Results show that the two-in-one efficiency is $94.2 \pm 1.6\%$, indicating that the PPD method is highly effective in incorporating curcumin from either curcumin or turmeric powder into soymilk (**Figure 2.2**). Regarding the efficacy of the pH-driven method for producing curcumin-enhanced soymilk, a previous study demonstrated that the pH-driven method is effective in solubilizing curcumin into soymilk, achieving a high processing efficiency of $91.3 \pm 2.7\%$ (Zheng, Zhang, et al., 2019). To provide a comparable study, this study used the same brand of soymilk product and the initial amount of curcumin concentration (1 mg/g fat). A slightly higher processing efficiency (98.6 \pm

1.1%) was observed in producing the curcumin-soymilk samples (**Figure 2.2**). This study reduced both the operating time and the exposure level to oxygen, which reduces the potential chemical degradation of curcumin in alkaline solution and thus result in higher operating efficiency.

Importantly, one critical point is that the curcumin is less sensitive to the alkaline solutions, compared to other polyphenols (e.g., quercetin and resveratrol) (Peng et al., 2019). For example, only about 10% of curcumin undergoes chemical degradation within 1 h, while the operation of this work can be completed within a few minutes. Consequently, a high extraction efficiency (96.4 \pm 0.5 %) is also observed in **Figure 2.2**, which suggests that the curcumin can be fully extracted from raw turmeric by using the alkaline solution. Overall, when producing curcumin-infused soymilk, the production of turmeric-soymilk yielded similar results to that of curcumin-soymilk, demonstrating the effectiveness of the PPD method in both applications. Additionally, the PPD method not only successfully replicates the findings of the previous study, but also demonstrates slightly higher effectiveness in solubilizing curcumin into soymilk. This improvement is attributed to the controlled operating conditions, such as reduced operating time and minimized oxygen exposure.

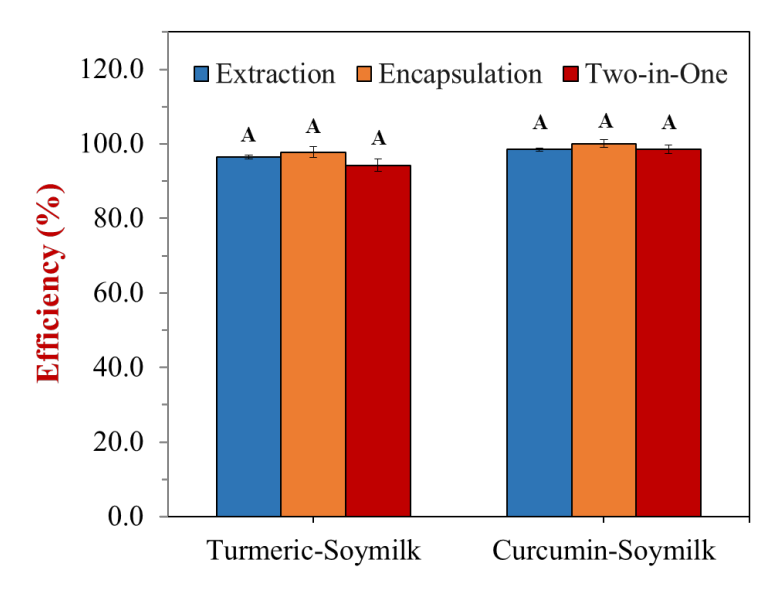


Figure 2.2. The extraction efficiency, encapsulation efficiency, and two-in-one efficiency of both turmeric-soymilk and curcumin-soymilk. The upper letter (A) represents the significant differences between samples (p < 0.05). Their values from left to right are 96.4 ± 0.5 , 97.8 ± 1.4 , 94.2 ± 1.6 , 98.5 ± 0.4 , 100.1 ± 1.1 , $98.6 \pm 1.1\%$, respectively.

Given the complex system of turmeric powder, which not only includes 2.1 ± 0.1% of curcumin, but also other plant components (*e.g.*, proteins and polysaccharides), it raises a question whether other components can be co-extracted under the alkaline solutions or not. According to the nutrition facts of turmeric powder, it has approximately 1 g protein, 3 g fat, and 4 g carbohydrates with 1 g fiber included (see **Table S1**). Some of them can be dissolved in an alkaline solution with a high pH value, for example, the protein has the alkaline solubilized amino acids (*e.g.*, tyrosine and lysine). Thus, we compared the UV-vis absorption spectra of both >97% curcumin and turmeric extract (**Figure 2.3**). A blue shift (from 430 to 420 nm) can be observed in the absorption spectrum of turmeric extract. This could be caused by the presence of other plant components, such as proteins or polysaccharides that might interact with curcumin. Although identifying the specific component(s) responsible was not the primary focus of this

study, it is important to explore whether other plant components can also be effectively extracted and contribute to the blue shift. Future studies are therefore needed to investigate this further and understand the broader applications and implications of our findings. To exclude the impact of other turmeric components on measuring the concentration of curcumin, HPLC was also used to determine the curcumin concentration in the turmeric extract (Figure S2). The results indicated no significant differences in determining the concentration of curcumin using either a UV-vis spectrophotometer or HPLC for both purified curcumin and curcumin extracted from turmeric (Figure S2A). This suggests that the UV-vis spectrophotometer can accurately measure the curcumin concentration in turmeric powder. Additionally, the chromatograms for both pure curcumin and curcumin extracted from turmeric powder show the same retention time at approximately 2.6 minutes (Figure S2B). It suggested that the curcumin was effectively extracted from turmeric powder and encapsulated into the soymilk. Combined with the high processing efficiency, it can be concluded that the two-in-one PPD processing strategy is highly effective in developing curcumin-infused PBMAs from the turmeric powder.

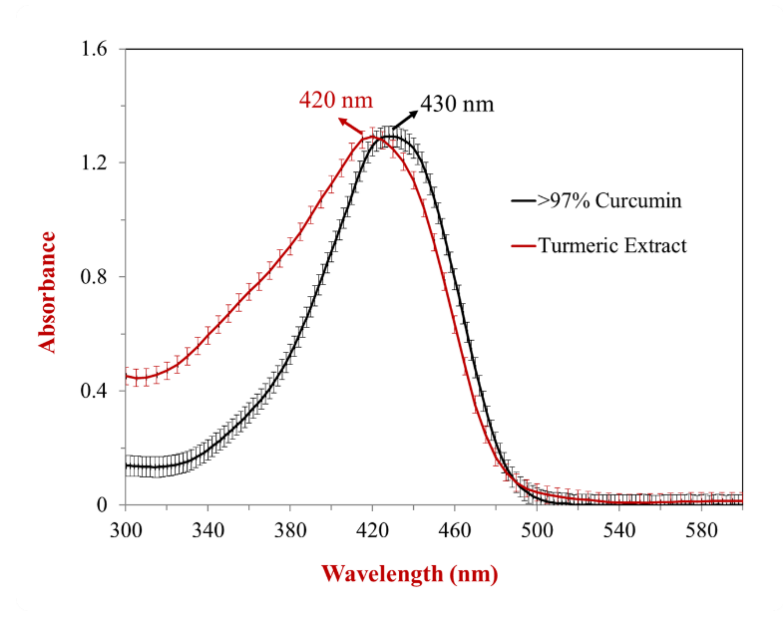


Figure 2.3. The UV-vis absorption spectrum of >97% curcumin and turmeric extract using 0.1 M KOH. The absorbance values at the peak positions are labelled.

Enhanced sustainability of two-in-one PPD processing strategy

The two-in-one PPD processing strategy is expected to enhance sustainability by using raw turmeric powder as the material input and combining both extraction and encapsulation steps. However, the extent of this improvement has not been clearly quantified. This study provides a quantitative assessment of the processing sustainability of this new strategy by comparing the embodied energy and carbon emissions of raw materials used for producing curcumin- or turmeric-soymilk powders with approximately 10 kg of curcumin (Figure 2.4). The results clearly showed that both the total embodied energy and carbon emissions of raw materials were significantly reduced with the new strategy, particularly in carbon emissions. This significant difference can be attributed to the use of different raw materials (curcumin versus turmeric). It was reported that 7.55 MMBtu is needed to produce 1 kg of turmeric powder with 0.7627 kg CO₂-eq emissions, while 2,175.59 MMBtu is needed to produce 1 kg of curcumin powder with 104,000 kg CO₂-eq emissions (Kurniawati et al., 2023; Zerazion et al., 2016). As a result, the total embodied energy of raw materials for producing curcumin-soymilk is ten times larger than that for producing turmeric-soymilk, with an even more significant difference in total embodied carbon emissions, which are 22 times larger. It should be noted that our calculations did not include potential manufacturing energy consumption and carbon emissions, as this labscale experiment cannot be directly applied to industrial-scale production and some parameters may not fully represent actual conditions. Instead, we provided a rough estimation of manufacturing energy consumption based on ideal processing conditions (see Figure S3 and **Table S6**). It was found that the drying process could dominate manufacturing energy

consumption, but its total energy use and carbon emissions could be within a negligible range. Even so, future work is needed to conduct a more accurate assessment for producing curcumininfused soymilk powders. Overall, these results clearly demonstrated the enhanced sustainability of the two-in-one PPD processing strategy, suggesting that it can be an effective method to improve the sustainability of our food systems by using raw materials and minimizing processing steps.

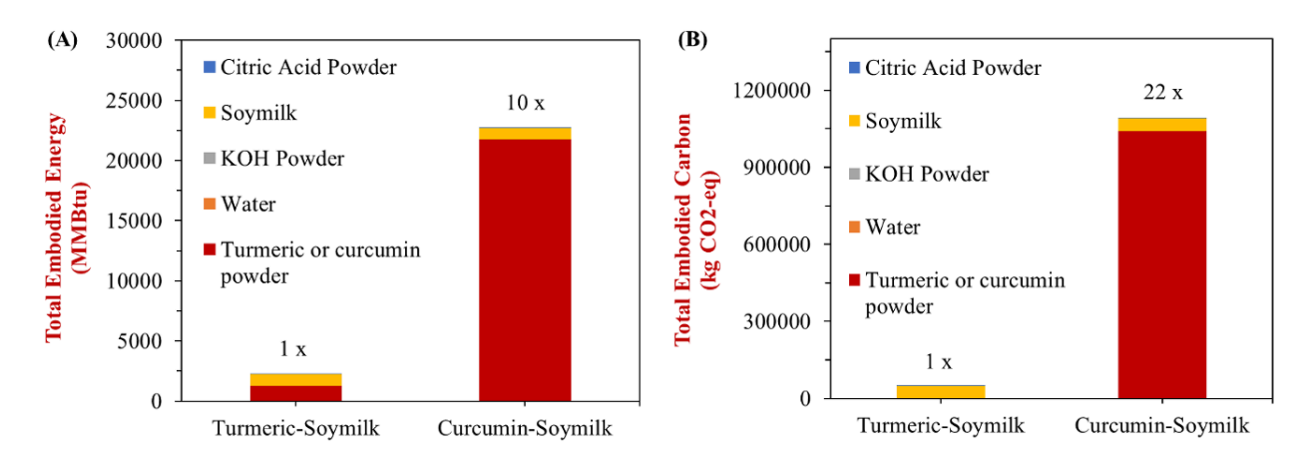


Figure 2.4. (A) Total embodied energy (MMBtu) and (B) carbon emissions (kg CO₂-eq) of raw materials for producing both turmeric-soymilk and curcumin-soymilk powders with ~10 kg curcumin. The "10x" (or "22x") value represents the ratio of the total embodied energy (or carbon emissions) of curcumin-infused soy milk compared to that of turmeric-infused soy milk. The listed ingredients (e.g., citric acid powder) contribute to the composition of turmeric- or curcumin-infused soymilk product. Their specific data and calculations can be found in the supporting information (see **Table S7 and S8**).

Impact of adding curcumin on the physicochemical properties of soymilk

Appearance instrumental color

The colors $(L^*, a^*, and b^* values)$ of liquid soymilk, curcumin-soymilk, and turmericsoymilk were measured using a colorimeter, and pictures of their liquid or powdered samples can be found in Figure 2.5A and 2.5B. Curcumin is a widely used yellow pigment in foods, contributing to a higher yellowness (b^* value) in curcumin-soymilk or turmeric-soymilk compared to regular soymilk. This yellowness can be retained in both powders after a freezing drying process. This suggests that the curcumin has been effectively encapsulated in the soymilk. However, the b* value of turmeric-soymilk was lower than that of curcumin-soymilk, despite having the same concentration of encapsulated curcumin in both samples. This difference is observable in the pictures of both liquids, although it appears negligible in the powdered forms of curcumin-infused soymilk. This could be attributed to the presence of additional turmeric components, which reduces the yellowness of curcumin in solution. Besides, the a^* values of both curcumin-included samples were more negative than that of soymilk, due to the addition of curcumin, but its overall strength is much weaker than those of b^* values. Obviously, the L^* values (darkness/lightness) of the samples were contributed by the presence of soymilk, because considerable small oil-droplets can contribute to the lightness of soymilk (Zhou et al., 2021b). Overall, the addition of curcumin significantly altered the appearance of soymilk, imparting a distinctive yellow hue. This color change could affect customer acceptance, as visual appeal plays a crucial role in consumers' perception of food quality and attractiveness (Downham & Collins, 2000). A noticeable color shift might lead to preconceived notions about taste and overall quality, potentially influencing purchasing decisions and consumer satisfaction.

Understanding these visual impacts is essential for product development and marketing strategies to ensure positive consumer response in future studies.

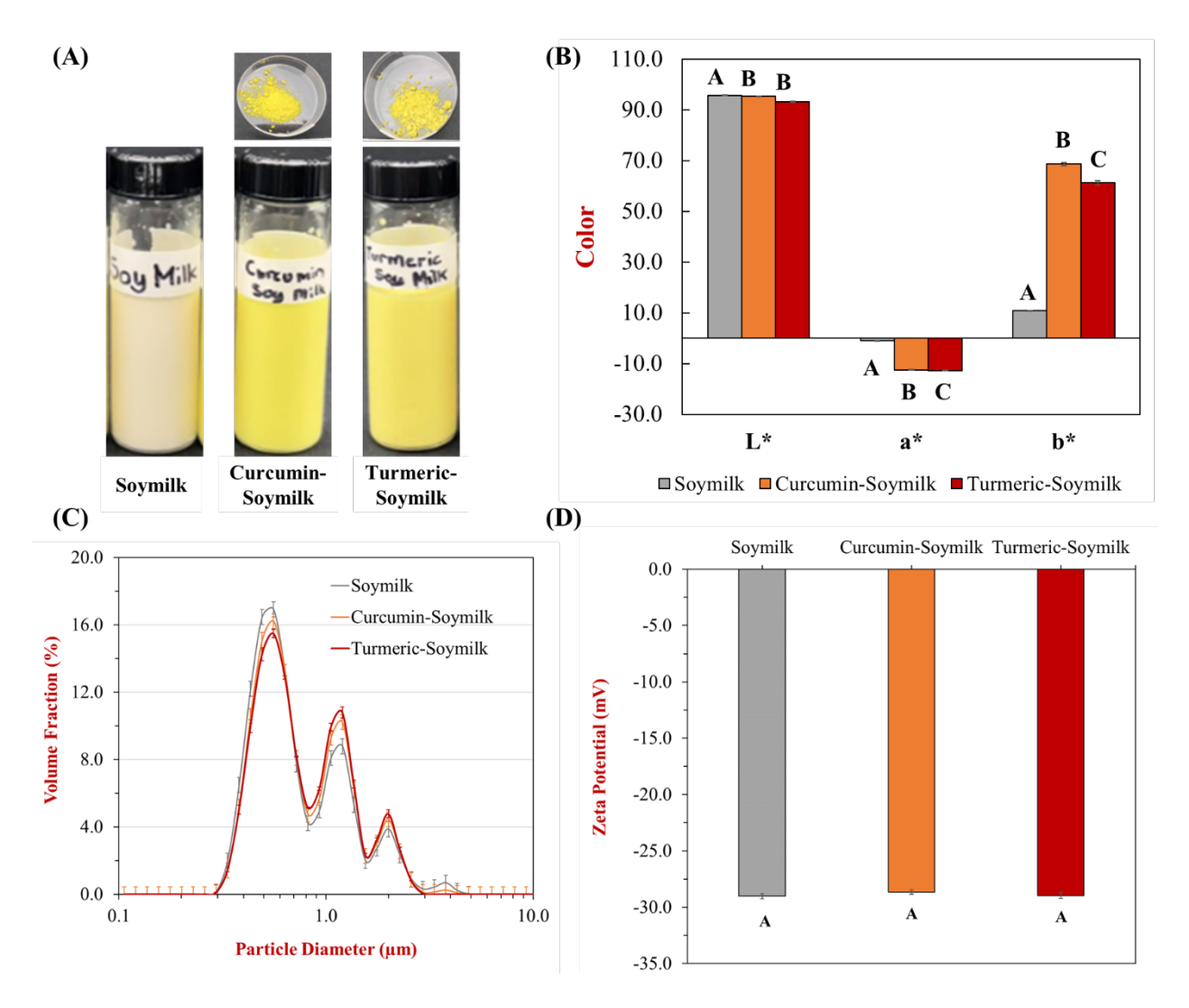


Figure 2.5. (A) Appearance (Left: soymilk, Middle: curcumin-soymilk, and Right: turmeric-soymilk) and (B) colors (L^* , a^* , b^* values) of three samples. Upper letters (A, B, and C) represent the significant differences between samples (p < 0.05) for the individual L^* , a^* , or b^* . (C) Particle size distributions and (D) zeta potentials of raw soymilk, curcumin-soymilk, and turmeric-soymilk. The mean particle diameters of soymilk, curcumin-soymilk, and turmeric-soymilk are 0.854 ± 0.009 μm, 0.856 ± 0.009 μm, and 0.893 ± 0.015 μm, respectively. Upper letter (A) represents the significant differences between samples (p < 0.05).

Particle size and zeta potential

Particle size and zeta potential measurements are critical indicators for evaluating the stability of colloidal systems. The particle size distribution provides important insights into the uniformity and potential aggregation of particles within the system. A significant increase in particle size may indicate aggregation, leading to decreased stability. Figure 2.5C shows the particle size distributions of three types of samples. It clearly shows that the soymilk sample had three different peaks, located near 0.5, 1.2, and 2.0 µm, and its mean particle diameter was approximately 0.854 ± 0.009 µm. After adding either curcumin or turmeric extract, the particle size distribution was slightly altered, but the peak positions were not. It is noted that curcumin has a low water solubility, so the curcumin molecules must be mostly encapsulated inside the oil droplets in the soymilk, rather than in the aqueous phase. For example, the curcumin molecules can be hydrophobically driven into the lipid phase of soymilk (Zhou et al., 2021a). It was also found that the amount of larger particles was slightly increased, in particular after incorporating turmeric extract. This is also consistent with the observation of a slightly higher mean particle size of turmeric-soymilk (0.893 \pm 0.015 μ m) compared to curcumin-soymilk (0.856 \pm 0.009 μm). This is likely due to the presence of large turmeric components.

Similarly, zeta potential measures the surface charge of particles, which influences the electrostatic repulsion between them. The measurements of all three samples showed negative charges, ranging from -28.665 to -29.025 mV (Figure 2.5D). These surface charges could be due to the presence of highly negatively charged emulsifiers in soymilk, such as maltodextrin and lecithin (see Table S3). These values, being close to -30 mV, indicate that the samples were sufficiently stable against aggregation. High absolute zeta potential values suggested strong electrostatic repulsion between particles, which prevented them from coming together and

aggregating, thus maintaining the stability of the colloidal system. It also suggested that the addition of curcumin did not alter the interfacial properties of soymilk. Overall, the inclusion of curcumin or turmeric extract did not result in a significant change of mean particle size and zeta potential, which indicates that their inclusion could not lead to a significant change of particle stability.

It is also essential to investigate the impact of curcumin addition on other physicochemical properties of PBMAs, particularly their rheological characteristics. Several studies have examined the effects of curcumin on the apparent shear viscosity of various PBMAs, noting that these PBMA products generally exhibit shear-thinning behavior—that is, their apparent viscosity decreases as shear rate increases. It should be mentioned that our previous study introduced curcumin into various PBMAs using the pH-driven method led to noticeable changes in flow properties, particularly in more viscous options like oat and cashew nut milks (Zheng et al., 2021b). Specifically, these samples exhibited a marked decrease in their consistency coefficient, indicating a reduction in thickness or resistance to flow, and an increase in their flow behavior index, suggesting a shift toward a more Newtonian flow profile (Zheng et al., 2021b). Furthermore, recent research has shown that the addition of turmeric juice, which is rich in total solids, increases the viscosity of PBMAs (Basha et al., 2024). This implies that not only curcumin but also other solid components in turmeric may influence the overall texture and mouthfeel of the final product. These findings underscore the need for a more comprehensive analysis of rheological properties to optimize curcumin-fortified PBMAs for the consumer acceptance.

Differential scanning calorimetry

The DSC measurement can be used to determine various thermal properties of a material. It provides valuable information on phase transitions such as melting points. Representative DSC measurements were conducted to evaluate the melting behavior of curcumin, turmeric, soymilk, curcumin-soymilk, and turmeric-soymilk powders (Figure 2.6A). The DSC analysis of curcumin powder showed a sharp peak at 187.4 °C, indicating the presence of its crystalline form. A previous study indicated the crystalline form of curcumin has an endothermic melting peak due to the interactions of curcumin molecules via O-H...O hydrogen bonds along with C-H...O bonds (Sanphui et al., 2011). Interestingly, the turmeric powder did not include an endothermic peak of curcumin. Instead, it showed a clear endothermic peak at 126.1 °C, which is much lower than that of the curcumin crystal. The soymilk showed a clear endothermic peak at approximately 216.1°C, which could be attributed to the presence of the maltodextrin as one of the major ingredients listed in the soymilk (Elnaggar et al., 2010). Similarly, both curcuminsoymilk and turmeric-soymilk exhibited a peak similar to that of soymilk, without a distinct peak from either the curcumin or turmeric powder. This suggests that the inclusion of curcumin or turmeric extract has little impact on the DSC profile of soymilk. Overall, the entire DSC profiles of both curcumin-soymilk and turmeric-soymilk were quite similar, indicating that adding turmeric extract produces results comparable to those seen with the addition of curcumin.

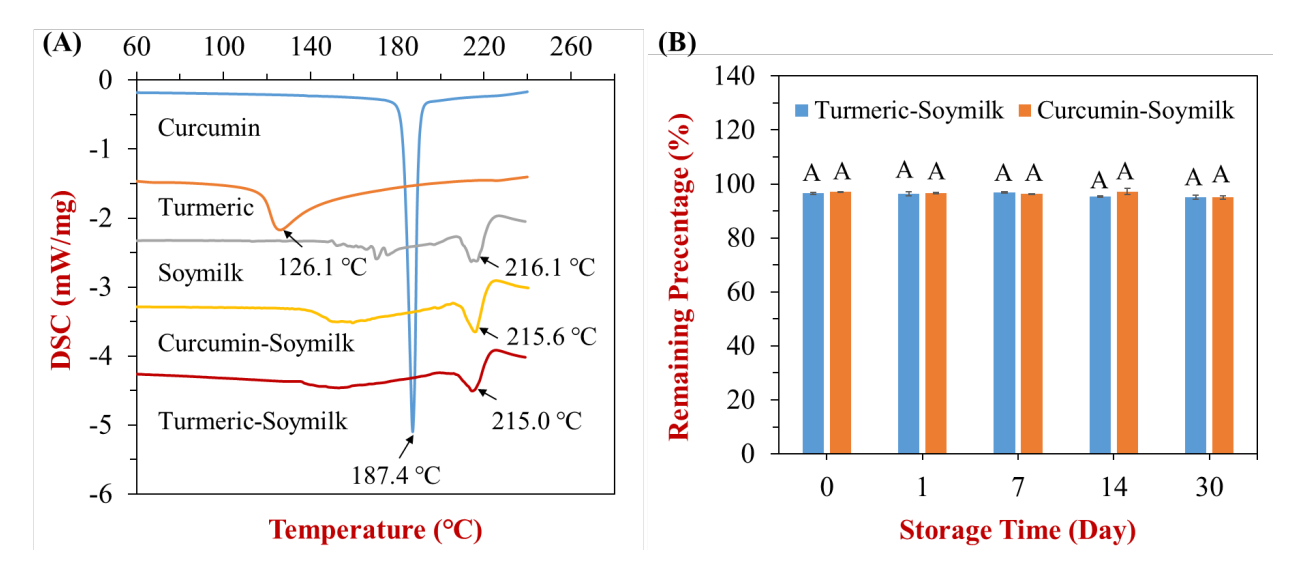


Figure 2.6. (A) Differential scanning calorimetry profiles of curcumin, turmeric, soymilk, curcumin-soymilk, and turmeric-soymilk powders. The temperature corresponding to the endothermic peak of each sample is labeled nearby. (B) The chemical stability of curcumin in both curcumin-soymilk and turmeric-soymilk powders under a freezing condition. The upper letter (A) represents the significant differences between all samples, including both curcuminand turmeric-soymilk with different storage days (p < 0.05).

Storage stability of curcumin in both curcumin- and turmeric-soymilk

It is a challenge to maintain the storage stability of curcumin, because the stability of curcumin is highly sensitive to environmental stress, including factors such as light exposure, temperature fluctuations, and pH levels. These factors can significantly impact the shelf-life and effectiveness of curcumin, necessitating careful consideration of storage and formulation strategies to maintain its stability (Zheng & McClements, 2020). Storing curcumin powder in freezing conditions has been considered as a highly effective strategy to maintain its stability, due to reduced light and oxygen exposure, as well as the low temperature. In this study, we further investigated whether this storage condition is effective for maintaining the stability of

curcumin in both curcumin-soymilk and turmeric-soymilk powders. We also examined whether the two different formulations have varying impacts on the storage stability of curcumin. The results indicated an insignificant change in curcumin concentration over one month. It was noted that a slight decrease in curcumin concentration occurred on the first day, which can be attributed to the loss during the freeze-drying process (**Figure 2.6B**). Both curcumin-soymilk and turmeric-soymilk samples showed that the curcumin content remained stable throughout the 30-day period (**Figure 2.6B**). This stability verifies that storing these powders under a freezing condition is an effective strategy for preserving curcumin, preventing its degradation, and extending its shelf-life. Additionally, no significant difference was observed in the two different formulations. The encapsulation of curcumin in soymilk likely extended its shelf life, protecting it from oxidation and chemical degradation. A similar chemical stability test using a different encapsulation material showed the same trend, confirming that encapsulated curcumin has improved stability during storage (Kharat et al., 2017; Yuan et al., 2022).

Proposed mechanism for enhancing curcumin solubility, stability, and bioavailability for curcumin-infused PBMAs

Soymilk can serve as an effective delivery system to enhance curcumin's bioavailability, providing a lipid-rich environment that aids in the solubilization and stabilization of this hydrophobic curcumin compound, thereby facilitating its absorption in the digestive tract. Initially, curcumin molecules become highly soluble in an alkaline solution due to the deprotonation of phenolic OH groups. Upon acidification, the negatively charged curcumin molecules are neutralized, allowing them to be driven into the lipid phase of soy milk through hydrophobic interactions. This solubilization within the lipid phase helps stabilize curcumin over extended periods; for instance, previous studies have shown that curcumin's stability is

maintained for up to a month when stored at 4°C (Zheng, Lin, et al., 2019; Zheng et al., 2017). As curcumin-infused soy milk passes through the human gastrointestinal tract, the oil droplets break down into mixed micelles in which curcumin can remain solubilized, enhancing its gastrointestinal absorption in the small intestine. Various gastrointestinal digestion studies have demonstrated that curcumin in such systems after using the pH-driven method can achieve high bioaccessibility, potentially increasing its oral bioavailability (Gao et al., 2022; Ren et al., 2024; Zhou et al., 2021a, 2021b). However, further in vivo and human studies are still needed to determine whether this increased absorption translates into enhanced biological effects, such as anti-inflammatory and anti-cancer properties.

Conclusions

This study proposed a two-in-one PPD processing strategy for incorporating curcumin from turmeric into soymilk, demonstrating increased processing efficiency and sustainability. The two-in-one efficiency was $94.2 \pm 1.6\%$, with a high extraction efficiency of $96.4 \pm 0.5\%$. Additionally, the use of raw turmeric, rather than purified curcumin, significantly enhanced processing sustainability (e.g., reduced CO_2 -eq emissions), even with a small percentage of curcumin (~ 0.3 mg) included in each gram of curcumin-infused soymilk powder. The success of this approach highlights the importance of using raw materials and minimizing processing steps to develop practical and sustainable food systems. The study further investigated the impact of adding curcumin on the physicochemical properties of soymilk. It was found that curcumin imparted a yellow color to soymilk. However, no significant changes were observed in other properties, including particle size, zeta potential, and DSC profiles, as most curcumin molecules were encapsulated within the lipid phase of soymilk. Curcumin in both curcumin-soymilk and turmeric-soymilk maintained excellent storage stability under a freezing condition. These results

suggested that the two-in-one PPD strategy was effective to formulate curcumin-infused soymilk, which can be used in developing health-promoting PBMAs. Further research is needed to apply this processing strategy to other PBMAs, particularly by leveraging the value of phenolic compounds. Additionally, sensory testing will be essential to determine if curcumin infusion significantly alters the taste and impacts consumer acceptance. Exploring specific health-promoting properties—such as antioxidant capacity, anti-inflammatory effects, and anticancer potential—will also be crucial to highlight the health benefits of curcumin-infused PBMAs, providing valuable insights for health-conscious consumers. This study provides valuable insights for scientists aiming to extend the range of plant-powered novel foods. For the food industry, this research represents an innovative step toward utilizing green technology in producing more sustainable, healthy, and affordable next-generation foods.

References

- Abdo, E. M., O. E. Shaltout., and H. M. M. Mansour. 2023. "Natural Antioxidants From Agro-Wastes Enhanced the Oxidative Stability of Soybean Oil During Deep-Frying." *LWT* Food Science and Technology, 173: 114321. https://doi.org/10.1016/j.lwt.2022.114321.
- Aggarwal, B. B., and B. Sung. (2009). "Pharmacological Basis for the Role of Curcumin in Chronic Diseases: An Age-Old Spice With Modern Targets." *Trends in Pharmacological Sciences* 30, no.2: 85-94. https://doi.org/10.1016/j.tips.2008.11.002.
- Basha, S. J., K. Kaur., P. Kaur., and T. P. Singh. 2024. "Enhancing the Technological, Functional and Storage Quality of Plant-Based Milk With Supplementation of Turmeric Juice."

 Journal of Stored Products Research 109: 102405.**

 https://doi.org/10.1016/j.jspr.2024.102405.**
- Cosme, P., A. B. Rodriguez, J. Espino, and M. Garrido. 2020. "Plant Phenolics: Bioavailability as a Key Determinant of Their Potential Health-Promoting Applications." *Antioxidants* 9, no.12: 1263. https://www.mdpi.com/2076-3921/9/12/1263.
- Csuti, A., B. Zheng, and H. Zhou. 2023. "Post pH-Driven Encapsulation of Polyphenols in Next-Generation Foods: Principles, Formation and Applications." *Critical Reviews in Food Science and Nutrition* 64, no. 33: 12892-12906. https://doi.org/10.1080/10408398.2023.2258214.
- Cuevas-Cianca, S. I., C. Romero-Castillo, J. L. Gálvez-Romero, Z. N. Juárez, Z, & L. R. Hernández. 2023. "Antioxidant and Anti-Inflammatory Compounds from Edible Plants with Anti-Cancer Activity and Their Potential Use as Drugs." *Molecules (Basel, Swithzerland)* 28, no. 3: 1488. https://www.mdpi.com/1420-3049/28/3/1488.

- Dhivya, S., and A. Rajalakshmi. 2018. "A Review on the Preparation Methods of Curcumin Nanoparticles." *Pharma Tutor 6*, no.9: 6-10.
- Downham, A., and P. Collins. 2000. "Colouring Our Foods in the Last and Next Millennium."

 *International Journal of Food Science & Technology 35, no.1: 5-22.

 https://doi.org/10.1046/j.1365-2621.2000.00373.x.
- Du, X., H. Jing, L. Wang. et al. 2022. "pH-Shifting Formation of Goat Milk Casein Nanoparticles From Insoluble Peptide Aggregates and Encapsulation of Curcumin for Enhanced Dispersibility and Bioactivity." *LWT* 154: 112753. https://doi.org/10.1016/j.lwt.2021.112753.
- Elnaggar, Y. S. R., M. A. El-Massik, O. Y. Abdallah, and A. E. R. Ebian. 2010. "Maltodextrin: A Novel Excipient Used in Sugar-Based Orally Disintegrating Tablets and Phase Transition Process." *AAPS Pharmscitech [Electronic Source]* 11, no. 2: 645-651. https://doi.org/10.1208/s12249-010-9423-y.
- Gao, H., C. Cheng, S. Fang, et al. 2022. "Study on Curcumin Encapsulated in Whole Nutritional Food Model Milk: Effect of Fat Content, and Partitioning Situation." *Journal of Functional Foods* 90:104990. https://doi.org/10.1016/j.jff.2022.104990.
- Gökdemir, B., N. Baylan, and S. Çehreli. 2020. Application of a Novel Ionic Liquid as an Alternative Green Solvent for the Extraction of Curcumin from Turmeric with Response Surface Methodology: Determination and Optimization Study." *Analytical Letters* 53, 13: 2111-2121. https://doi.org/10.1080/00032719.2020.1730394.
- Industrial Efficiency & Decarbonization Office (IEDO). 2024. *Life Cycle Assessment and Techno- Economic Analysis Training*. Washington, D.: US. Department of Energy headquarters.

- https://www.energy.gov/eere/iedo/life-cycle-assessment-and-techno-economic-analysis-training
- Jiang, T., R. Ghosh, R, and C. Charcosset. 2021. "Extraction, Purification and Applications of Curcumin from Plant Materials-A Comprehensive Review." *Trends in Food Science & Technology* 112: 419-430. https://doi.org/10.1016/j.foodres.2020.109035.
- Jiang, T., W. Liao, and C. Charcosset. 2020. Recent Advances in Encapsulation of Curcumin in Nanoemulsions: A Review of Encapsulation Technologies, Bioaccessibility and Applications." Food Research International 132: 109035. https://doi.org/10.1016/j.foodres.2020.109035.
- Kharat, M., Z. Du, G. Zhang, and D. J. McClements. 2017.

 "Physical and Chemical Stability of Curcumin in Aqueous Solutions and Emulsions:

 Impact of pH, Temperature, and Molecular Environment." *Journal of Agricultural and Food Chemistry* 65, no.8: 1525-1532. https://doi.org/10.1021/acs.jafc.6b04815.
- Kocaadam, B., and N. Şanlier. 2017. "Curcumin, an Active Component of Turmeric (*Curcuma longa*), and Its Effects on Health." *Critical Reviews in Food Science and Nutrition* 57, no.13: 2889-2895. https://doi.org/10.1080/10408398.2015.1077195.
- Kurniawati, D. A., W. Supartono, and P. Saroyo. 2023.

 The Importance of LCA in the Production of Turmeric Powder and Chilli Powder at PT

 X." BIO Web of Conferences 80, 04007. https://doi.org/10.10151/bioconf/20238004007.
- Liu, Z., J. D. Smart, and A. S. Pannala (2020). "Recent Developments in Formulation Design for Improving Oral Bioavailability of Curcumin: A review." *Journal of Drug Delivery Science* and Technology 60: 102082. https://doi.org/10.1016/j.ddst.2020.102082.

- Manasa, P. S. L., A.D. Kamble, and U. Chilakamarthi. 2023. "Various Extraction Techniques of Curcumin—A Comprehensive Review." *ACS Omega* 8, no.38: 34868-34878. https://doi.org/10.1021/acsomega.3c04205.
- McClements, D. J. 2020. "Development of Next-Generation Nutritionally Fortified Plant-Based Milk Substitutes: Structural Design Principles." *Foods* 9, no.4: 421.
- Pan-On, S., P. Dilokthornsakul, and W. Tiyaboonchai. 2022. "Trends in Advanced Oral Drug Delivery System for Curcumin: A Systematic Review." *Journal of Controlled Release*, 348: 335-345. https://doi.org/10.1016/j.jconrel.2022.05.048.
- Peng, S., L. Zou, W. Zhou, W. Liu, C. Liu, and D. J. McClements. 2019. "Encapsulation of Lipophilic Polyphenols into Nanoliposomes Using pH-Driven Method: Advantages and Disadvantages" *Journal of Agricultural and Food Chemistry* 67, no.26: 7506-7511. https://doi.org/10.1021/acs.jafc.9b01602.
- Peng, Y., M. Ao, B. Dong, et al. 2021. "Anti-Inflammatory Effects of Curcumin in the Inflammatory Diseases: Status, Limitations and Countermeasures." *Drug Design*, *Development and Therapy* 15: 4503-4525. https://doi.org/10.2147/DDDT.S327378
- Rafiee, Z., M. Nejatian, M. Daeihamed, and S. M. Jafari. 2019. "Application of curcumin-loaded nanocarriers for food, drug and cosmetic purposes." *Trends in Food Science & Technology* 88: 445-458. https://doi.org/10.1016/j.tifs.2019.04.017.
- Ren, J., H. Wu, Z. Lu, et al. 2024. "Improved Stability and Anticancer Activity of Curcumin Via pH-Driven Self-Assembly with Soy Protein Isolate." *Process Biochemistry* 137: 217-228. https://doi.org/10.1016/j.procbio.2024.01.008.

- Salehi, B., E. Azzini, P. Zucca, et al. 2020. "Plant-Derived Bioactives and Oxidative Stress-Related Disorders: A Key Trend towards Healthy Aging and Longevity Promotion." *Applied Sciences* 10, no.3: 947. https://www.mdpi.com/2076-3417/10/3/947
- Sanphui, P., N. R. Goud, U. R. Khandavilli, S. Bhanoth, and A. Nangia. 2011. "New Polymorphs of Curcumin." *Chemical Communications* 47, no.17: 5013-5015.
- Sathyabhama, M., L. C. Priya Dharshini, A. Karthikeyan, S. Kalaiselvi, and T. Min. 2022. "The Credible Role of Curcumin in Oxidative Stress-Mediated Mitochondrial Dysfunction in Mammals." *Biomolecules* 12. no.10: 1405. https://www.mdpi.com/2218-273X/12/10/1405
- Shirsath, S. R., S.S. Sable, S.G. Gaikwad, and P.R. Gogate. 2021. "Ultrasound Assisted Curcumin Recovery from Curcuma Aromatica: Understanding the Effect of Fifferent Operating Parameters." *Chemical Engineering and Processing Process Intensification* 169: 108604. https://doi.org/10.1016/j.cep.2021.108604.
- Vasavada, N. 2016. One-Way ANOVA (Analysis of Variance) With Post-Hoc Tukey HSD (Honestly Significant Difference) Test Calculator for Comparing Multiple Treatments.

 https://astatsa.com/OneWay Anova with TukeyHSD
- Yuan, Y., S. Zhang, M. Ma, Y. Xu, and D. Wang. 2022. "Delivery of Curcumin by Shellac Encapsulation: Stability, Bioaccessibility, Freeze-Dried Redispersibility, and Solubilization." *Food Chemistry: X 15*: 100431. https://doi.org/10.1016/j.fochx.2022.100431.
- Zerazion, E., R. Rosa, E. Ferrari, et al. 2016. "Phytochemical Compounds or Their Synthetic Counterparts? A Detailed Comparison of the Quantitative Environmental Assessment for the Synthesis and Extraction of Curcumin." *Green Chemistry* 18, no.6: 1807-1818. https://doi.org/10.1039/C6GC00090H.

- Zheng, B., H. Lin, X. Zhang, and D. J. McClements. 2019. Fabrication of Curcumin-Loaded Dairy Milks Using the pH-Shift Method: Formation, Stability, and Bioaccessibility. *Journal of Agricultural and Food Chemistry* 67, no.44: 12245-12254. https://doi.org/10.1021/acs.jafc.9b04904.
- Zheng, B., and D. J. McClements. 2020. "Formulation of More Efficacious Curcumin Delivery Systems Using Colloid Science: Enhanced Solubility, Stability, and Bioavailability." *Molecules (Basel, Swithzerland)* 25, no. 12: 2791. https://www.mdpi.com/1420-3049/25/12/2791.
- Zheng, B., X. Zhang, H. Lin, and D. J. McClements. 2019. "Loading Natural Emulsions with Nutraceuticals Using the pH-driven Method: Formation & Stability of Curcumin-Loaded Soybean Oil Bodies." *Food & Function* 10, no. 9: 5473-5484. https://doi.org/10.1039/C9FO00752K.
- Zheng, B., Z. Zhang, F. Chen, X. Luo, and D. J. McClements. 2017. "Impact of Delivery System Type on Curcumin Stability: Comparison of Curcumin Degradation in Aqueous Solutions,
 Emulsions, and Hydrogel Beads." Food Hydrocolloids 71: 187-197.
 https://doi.org/10.1016/j.foodhyd.2017.05.022.
- Zheng, B., H. Zhou, and D. J. McClements. 2021a. "Nutraceutical-Fortified Plant-Based Milk Analogs: Bioaccessibility of Curcumin-Loaded Almond, Cashew, Coconut, and Oat Milks." *LWT* 147: 111517. https://doi.org/10.1016/j.lwt.2021.111517.
- Zheng, B., H. Zhou, and D. J. McClements. 2021b. "Nutraceutical-Fortified Plant-Based Milk Analogs: Bioaccessibility of Curcumin-Loaded Almond, Cashew, Coconut, and Oat Milks." *LWT* 147: 111517. https://doi.org/10.1016/j.lwt.2021.111517.

- Zheng, B., X. Zhang, S. Peng, and D. J. McClements. 2019. "Impact of Curcumin Delivery System Format on Bioaccessibility: Nanocrystals, Nanoemulsion Droplets, and Natural Oil Bodies." *Foods & function* 10, no. 8: 4339-4349. https://doi.org/10.1039/C8FO02501J.
- Zheng, B., H. Zhou, and D. J. McClements. 2023. "Co-Encapsulation of Multiple Polyphenols in Plant-Based Milks: Formulation, Gastrointestinal Stability, and Bioaccessibility." *Foods* 12. no. 18: 3432. https://www.mdpi.com/2304-8158/12/18/3432.
- Zhou, H., B. Zheng, and D. J. McClements. 2021a. "Encapsulation of Lipophilic Polyphenols in Plant-Based Nanoemulsions: Impact of Carrier Oil on Lipid Digestion and Curcumin, Resveratrol and Quercetin Bioaccessibility". Food & Function 12. no. 8: 3420-3432. https://doi.org/10.1039/D1FO00275A.
- Zhou, H., B. Zheng, and D. J. McClements. 2021b. "In Vitro Gastrointestinal Stability of Lipophilic Polyphenols is Dependent on their Oil–Water Partitioning in Emulsions: Studies on Curcumin, Resveratrol, and Quercetin." *Journal of Agricultural and Food Chemistry* 69, no. 11: 3340-3350. https://doi.org/10.1021/acs.jafc.0c07578.
- Zhou, H., B. Zheng, and D. J. McClements. 2024. "Utilization of pH-Driven Methods to Fortify Nanoemulsions With Multiple Polyphenols." Food Science and Human Wellness 13. no. 4: 1943-1950. https://doi.org/10.26599/FSHW.2022.9250161.

Supplementary Information

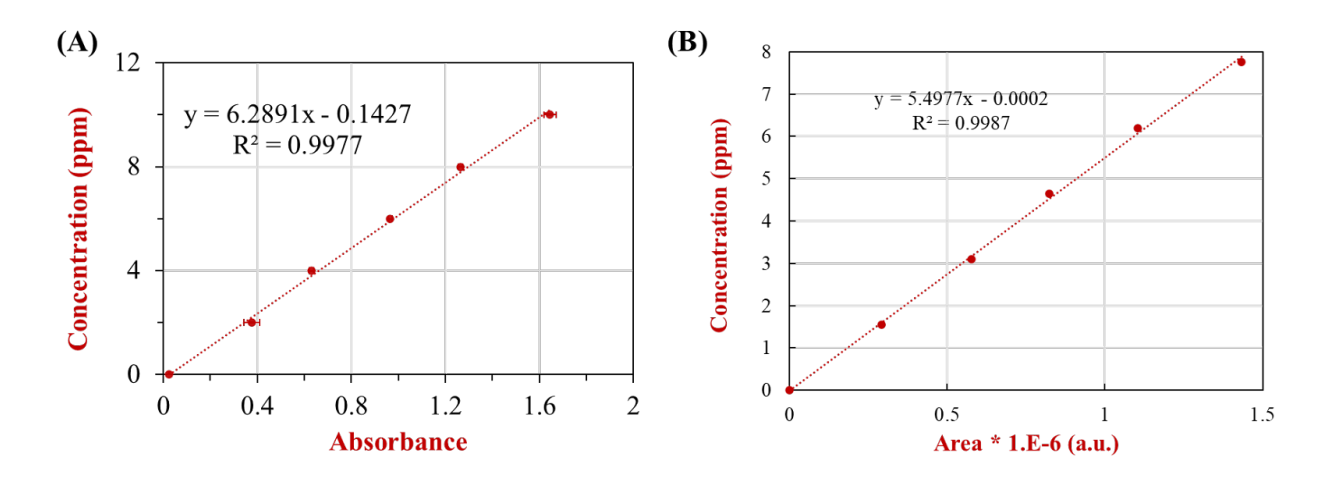


Figure S1. Standard curves for curcumin using the (A) UV-vis spectrophotometer and (B) HPLC. Their linear equations and R^2 values are labeled, respectively.

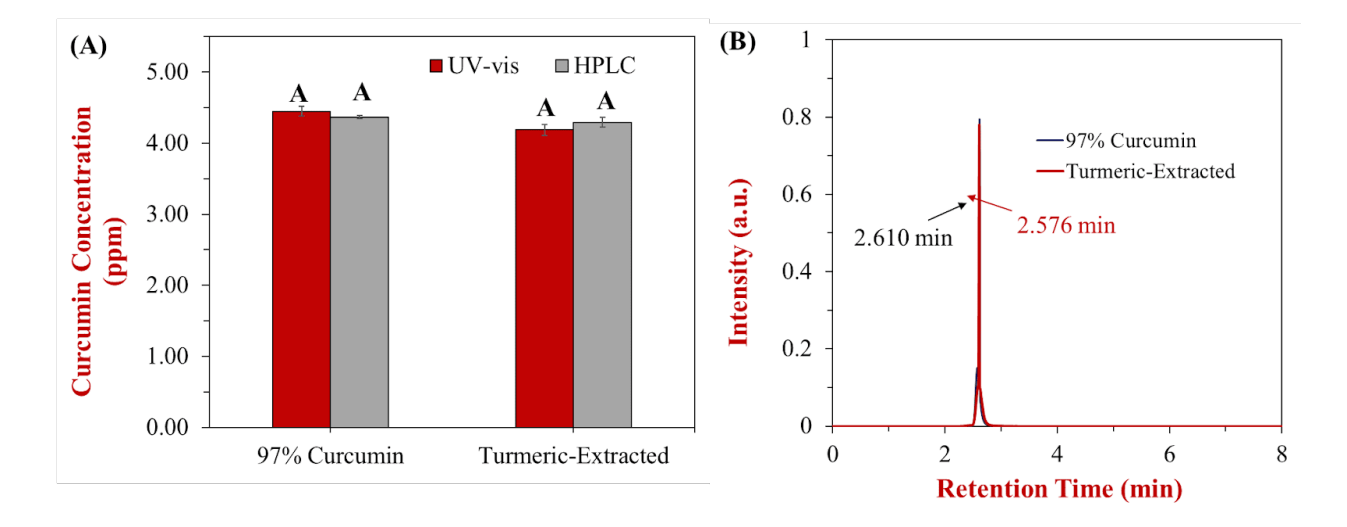


Figure S2. (A) Impact of different measurement methods (HPLC vs. UV-vis spectrophotometer) on the concentration of curcumin in either >97% curcumin or turmeric extract sample. (B) HPLC chromatograms of both >97% curcumin and turmeric samples. The upper letter (A) represents significant differences between samples (p < 0.05). The "97% Curcumin" was considered as a purified curcumin sample, while the "Turmeric-Extracted" sample refers to curcumin extracted from turmeric powder using the PPD method.

Table S1. Nutrition fact of turmeric powder used in this study. The data was calculated based on one serving size (Company, 2024).

Serving size	12 g
Calories	15 calories
Total Fat	3 g
Total Carbohydrate	4 g
Protein	1 g

Table S2. Nutrition facts and ingredients of Silk vanilla soy creamer (Silk, 2024).

Serving Size	1 Tbsp (15ml)
Amount per serving	
Caloríes	30
	% Daily Value
Total Fat: 1.5g	2%
Saturated Fat: 0.5g	3%
Trans Fat: 0g	
Polyunsaturated Fat: 0g	
Monounsaturated Fat: 0.5g	
Cholesterol: Omg	0%
Sodium: Omg	0%
Total Carbohydrate: 4g	1%
Dietary Fiber: 0g	0%
Total Sugars: 3g	
Includes 3g Added Sugars	6%
Protein: 0g	
Vitamin D: Omcg	0%
Calcium: Omg	0%
Iron: 0mg	0%
Potassium: Omg	0%

Table S3. Ingredients of Silk vanilla soy creamer (Silk, 2024).

Main ingredients: Soymilk (Filtered Water and Soybeans), Cane Sugar, Palm Oil, Maltodextrin.

Contains 2% or less of ingredients: Soy Lecithin, Natural Flavor, Tapioca Starch, Locust Bean Gum, and Dipotassium Phosphate.

S1. Data inputs for assessing environment impacts of PPD processing strategy

S1.1. Raw material inputs

Table S4. The inventory of raw material inputs for producing curcumin-soymilk powder.

Curcumin-Soymilk	Total amount	Material inputs
Soymilk	1E5 kg	1E5 kg soymilk
Turmeric	-	-
Curcumin	10 kg	10 kg curcumin
0.1 M KOH solution	1E3 kg	5.6 kg KOH (s)
		994.4 kg water
Citric acid (l), 3 wt%	213 kg	6.4 kg citric acid (s)
		206.6 kg water

Calculations

Soymilk: 1E5 kg.

Curcumin: It is based on the concentration, 0.1 mg/g soymilk, so we will need 10 kg curcumin.

0.1 M KOH solution: It is based on 1 mL 0.1 M KOH can dissolve 10 mg curcumin, and its density is around 1 g/mL, then we need 1E3 kg 0.1 M KOH solution, so we will need 5.6 kg KOH (s) and 994.4 kg water.

Citric acid (1), 3 wt%: The citric acid is used to neutralize the KOH solution, so we can use an acid-based reaction balance to calculate the amount of citric acid (s),

$$3 \text{ KOH (aq)} + \text{H}_3\text{C}_6\text{H}_5\text{O}_7 \text{ (aq)} \rightarrow \text{Na}_3\text{C}_6\text{H}_5\text{O}_7 \text{ (aq)} + 3 \text{ H}_2\text{O}$$

Mass [citric acid (s)] = $0.1E3 \text{ mol} / 3 \times 192.124 \text{ g/mol} \approx 6.4 \text{ kg}$. We assume that the 3 wt% citric acid buffer is used, then we need 206.6 kg water to prepare the citric acid buffer.

Table S5. The inventory of raw material inputs for producing turmeric-soymilk powder.

Turmeric-Soymilk	Total amount	Material inputs
Soymilk	1E5 kg	1E5 kg soymilk
Turmeric	166.7 kg	166.7 kg turmeric
Curcumin	-	-

0.1 M KOH solution	333.4 kg	1.9 kg KOH (s)
Citric acid (l), 3 wt%	70 kg	331. 5 kg water 2.1 kg citric acid (s) 67.9 kg water

Calculations

Soymilk: 1E5 kg.

Turmeric: It is based on 10 kg curcumin we need, and 6 wt% of curcumin is present in the turmeric (Hettiarachchi, Dunuweera, Dunuweera, et al., 2021). We then need 166.7 kg turmeric powder.

0.1 M KOH solution: It is based on an estimation: 20 mL 0.1 M KOH can be used to dissolve 0.5 g turmeric, to fully extract the curcumin. We then need 333.4 kg 0.1 M KOH solution, which requires 1.9 kg KOH (s) and 331.5 kg water.

Citric acid (1), 3 wt%: Using the citric acid is to neutralize the KOH solution, so we can use an acid-based reaction balance to obtain the amount of citric acid (s),

 $3 \text{ KOH } (\text{aq}) + \text{H}_3\text{C}_6\text{H}_5\text{O}_7 \left(\text{aq}\right) \boldsymbol{\rightarrow} \text{Na}_3\text{C}_6\text{H}_5\text{O}_7 \left(\text{aq}\right) + 3 \text{ H}_2\text{O}$

Mass [citric acid (s)] = $0.1 \times 333.4 \text{ mol} / 3 \times 192.124 \text{ g/mol} \approx 2.1 \text{ kg}$. We assume that the 3 wt% citric acid buffers used, then 67.9 kg water will be used to prepare the citric acid buffer.

S1.2. Specific embodied energy, carbon emissions, and cost

Tap water

Data source: x'(MFI) database (NREL, 2024)

Functional unit: 1 kg tap water

Specific embodied energy: 0.002336 MJ/kg = 2.216 Btu/kg

Specific embodied carbon: 0.000188 kg CO₂-eq/kg

Price: 0.00007794 USD/kg

KOH (s)

Data source: MFI database (NREL, 2024)

Functional unit: 1 kg KOH powder

Specific embodied energy: 22.877194 MJ/kg = 21,684.12 Btu/kg

Specific embodied carbon: 1.452922 kg CO₂-eq/kg

Price: 0.93 USD/kg (Mike, 2024)

Soymilk

Data source: Data of producing soymilk was similarly applied based on the statement "Producing one 48 oz. (1.42 L) bottle of unsweetened almond milk uses 14.8 MJ of TPE, consumes 175 kg of freshwater, and generates 0.71 kg of CO₂-eq." (Winans, Macam-Somer, Kendall et al., 2020)

Functional unit: 1 L or kg soymilk

Specific embodied energy: 14. MJ / 1.42 L = 0.00988 MMBtu / L ≈ 9880 Btu/kg

Specific embodied carbon: 0.71 kg / 1.42 L = 0.5 kg CO_2 -eq/L \approx 0.5 kg CO_2 -eq/kg

Price: 1.76 USD/kg

Citric acid (s)

Data source: MFI database (NREL, 2024)

Functional unit: 1 kg citric acid powder

Specific embodied energy: 85.434304 MJ/kg = 81,009.22 Btu/kg

Specific embodied carbon: 5.407139 kg CO₂-eq/kg

Price: 0.12 USD/kg (Alibaba, 2024)

Turmeric powder

Data source: Data was based on the statement, "7,963 MJ are needed to manufacture 1 kilogram

of turmeric powder, with a potential environmental impact of GWP 0.7627 kg CO₂-eq"

(Kurniawati, Supartono, and Saroyo, 2023)

Functional unit: 1 kg turmeric powder

Total primary energy (TPE) use: 7963 MJ/kg = 7.55 MMBtu/kg

Specific embodied carbon: 0.7627 kg CO₂-eq/kg

Price: 3.33 USD/kg (Alibaba, 2024)

Curcumin powder

Data source: Data was collected from Table 3 in the supplemental document of the reference

(Zerazion, Rosa, Ferrari, et al., 2016)

Functional unit: 1 kg curcumin

Specific embodied energy: (2.19E6 + 1.05E5) MJ/kg $\approx 2,175.59$ MMBtu/kg

Specific embodied carbon: 1.04E5 kg CO₂-eq/kg

Price: 6.00 USD/kg (Alibaba, 2024)

Electricity

Data source: MFI database (NREL, 2024)

Source-to-Site Ratio: 2.86

Specific 100-yr GWP: 49.25 kg CO₂-eq/MMBtu

Specific price: 21.04 USD/MMBtu

S1.3. Flow charts for producing both curcumin-soymilk and turmeric-soymilk powders

The mass balance flow charts for producing both curcumin-soymilk and turmeric-soymilk powders are presented in **Figure S3**. The data were collected based on **Tables S3 and S4**. This calculation assumes that the material loss during processing is negligible.

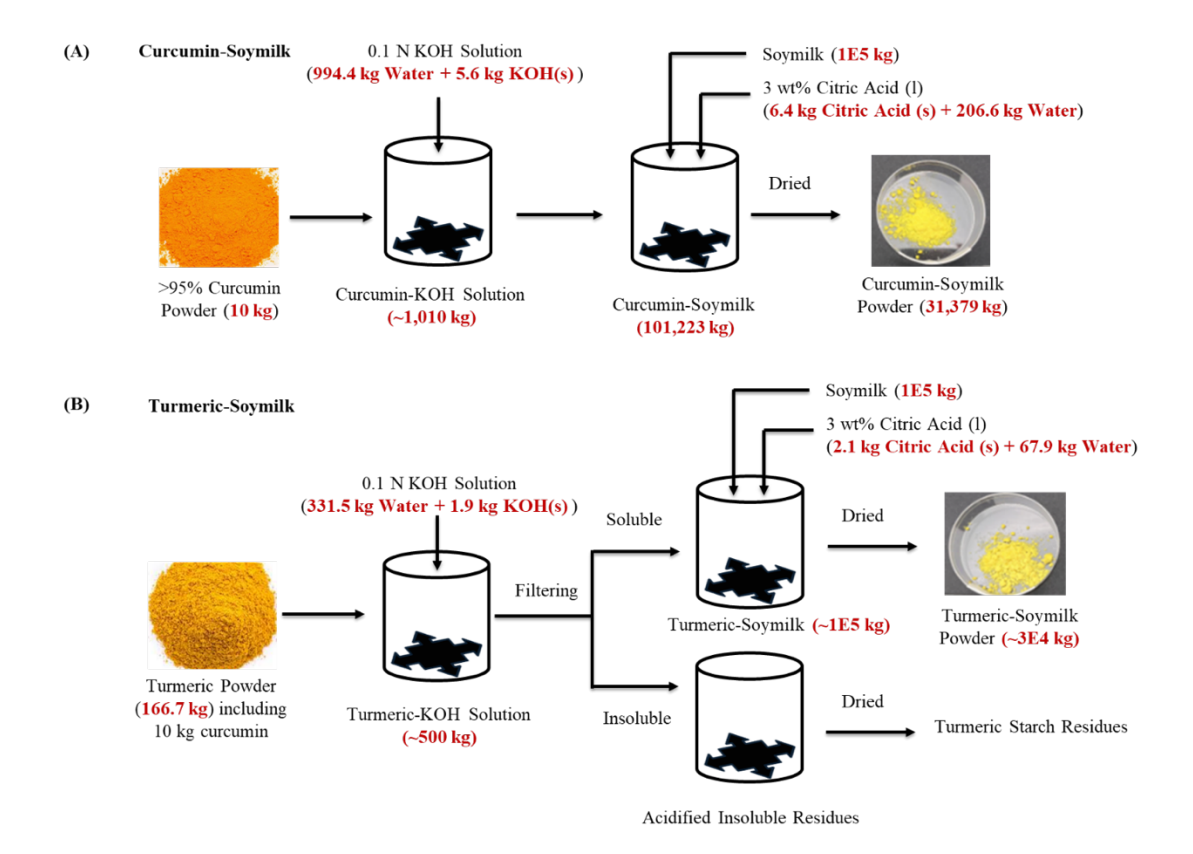


Figure S3. Mass balance flow charts for producing curcumin-soymilk (**A**) and turmeric-soymilk (**B**) powders with 10 kg of curcumin.

S1.4. Manufacturing energy

Table S6. Approximate energy consumption for producing both curcumin-soymilk and turmeric-soymilk powders with approximately 1 kg of curcumin. The base-case for the production rate is 1E4 kg soymilk solution fed to the process during each batch. The following data is estimated by a techno-economic analysis of extraction of curcumin from turmeric (Kunta, 2018).

Energy use (kWh)	Curcumin-Soymilk	Turmeric-Soymilk
Homogenizers	6	6
Centrifugation & Filtration	-	40
Packaging Equipment	4	4
Dryer	1100	1100
Total (kWh)	1110	1150
Total (MMBtu)	3.79	3.92

S1.5. The summary of raw material embodied energy, emissions, and costs

Table S7. A snapshot of raw material inputs to produce the turmeric-soymilk powder with 10 kg curcumin. Calculations can be found in **section S1.1** and **S1.2**.

Material Inputs	Amount of Material (to produce reference volume)	Unit	Specific Embodied Energy (Btu/unit) (for this material)	Specific Embodied Carbon (kg CO2- eq/unit) (for this material)	Specific Cost (\$/unit) (for this material)	Embodied Energy (MMBtu) (per reference volume of product)	Embodied Carbon (kg CO2-eq) (per reference volume of product)	Cost (\$) (per reference volume of product)
Turmeric	166.7	kg	7,550,000	0.8	3.3	1,258.6	127.1	555.1
Water	399.4	kg	2.2	0.0	0.0	0.0	0.1	3.2
KOH Powder	1.9	kg	21,684.1	1.5	0.9	0.0	2.8	1.8
Soymilk	100,000.0	kg	9,880.0	0.5	1.8	988.0	50,000.0	176,000.0
Citric Acid Powder	2.1	kg	81,009.2	5.4	0.1	0.2	11.4	0.3
Total embo	Total embodied energy and cost to input materials:						50,141.4 kg CO2-eq	\$176,560.4

Table S8. A snapshot of raw material inputs to produce the curcumin-soymilk powder with 10 kg curcumin. Calculations can be found in **section S1.1 and S1.2**.

Material Inputs	Amount of Material (to produce reference volume)	Unit	Specific Embodied Energy (Btu/unit) (for this material)	Specific Embodied Carbon (kg CO2- eq/unit) (for this material)	Specific Cost (\$/unit) (for this material)	Embodied Energy (MMBtu) (per reference volume of product)	Embodied Carbon (kg CO2-eq) (per reference volume of product)	Cost (\$) (per reference volume of product)
Curcumin Powder	10	kg	2,175,590,000.0	104,000	6.0	21,755.9	1,040,000.0	60.0
Water	1201.0	kg	2.2	0	0	0.0	0.2	9.6
KOH Powder	5.6	kg	21,684.1	1.5	0.9	0.1	8.1	5.2
Soymilk	100,000	kg	9,880	0.5	1.8	988.0	50,000.0	176,000.0
Citric Acid Powder	6.4	kg	81,009.2	5.4	0.1	0.5	34.6	0.3
Total embo	Total embodied energy and cost to input materials:						1,090,043 kg CO2-eq	\$176,560.1

References

- Alibaba. 2024. Best Citric Acid Anhydrous and Citric Acid Monohydrate bp93 Supplier. https://www.alibaba.com/product-detail/Best-citric-acid-anhydrous-and-citric_60718078134.html?spm=a2700.7724857.0.0.39e31e2bSapKje
- Alibaba. 2024. High Quality Seasonings Spices Turmeric Curcuma Root for Cooking Use

 Available at Affordable Price from India. https://www.alibaba.com/product-detail/_10000011471547.html
- Alibaba. 2024. Hot Selling Powder Turmeric Root Extract Curcumin 95%-98% Extract Powder.

 https://www.alibaba.com/product-detail/Hot-Selling-Powder-Turmeric-Root-Extract1601212924489.html
- Curcumin Extract Curcumin Powder. https://www.alibaba.com/product-detail/hot-selling-powder-turmeric-root-extract_1600583826732.html?spm=a2700.galleryofferlist.p_offer.d_title.2b6115acCbiql5
 <a href="https://www.alibaba.com/product-detail/hot-selling-powder-turmeric-root-extract_1600583826732.html?spm=a2700.galleryofferlist.p_offer.d_title.2b6115acCbiql5
 <a href="https://www.alibaba.com/product-detail/hot-selling-powder-turmeric-root-extract_1600583826732.html?spm=a2700.galleryofferlist.p_offer.d_title.2b6115acCbiql5
- Company, A. T. 2024. *Lead-Free Turmeric Powder*. americanturmeric.com
- Silk. 2024. Vanilla Soy Creamer. https://silk.com/plant-based-products/creamer/vanilla-soy-creamer/#:~:text=Ingredients,Locust%20Bean%20Gum%2C%20Dipotassium%20Phosp hate
- Hettiarachchi, S. S., S. P. Dunuweera, A. N. Dunuweera, et al. 2021. "Synthesis of Curcumin Nanoparticles from Raw Turmeric Rhizome." *ACS Omega* 6, no. 12: 8246-8252. 10.1021/acsomega.0c06314.

- NREL. 2024. *Material Flow Through Industry Data Extractor Tool*. https://www.energy.gov/eere/ammto/material-flow-through-industry-data-extractor-tool
- Mike. 2024. Potassium Hydroxide Price Undex.

 https://businessanalytiq.com/procurementanalytics/index/potassium-hydroxide-price-

 index.
- Winans, K. S., I. Macadam-Somer, A. Kendall, R. Geyer, et al. 2020. "Life Cycle Assessment of California Unsweetened Almond Milk." *The International Journal of Life Cycle Assessment* 25, no. 3: 577-587. 10.1007/s11367-019-01716-5.
- Kurniawati, D. A., W. Supartono, and P. Saroyo. 2023.

 The Importance of LCA in the Production of Turmeric Powder and Chilli Powder at PT

 X." BIO Web of Conferences 80, 04007. https://doi.org/10.10151/bioconf/20238004007.
- Zerazion, E., R. Rosa, E. Ferrari, et al. 2016. "Phytochemical Compounds or Their Synthetic Counterparts? A Detailed Comparison of the Quantitative Environmental Assessment for the Synthesis and Extraction of Curcumin." *Green Chem* 18, no. 6: 1807-1818. 10.1039/C6GC00090H.
- Kunta, N. 2018. "Techno-Economic Analysis of Extraction Curcumin from Turmeric." Oregon State University, ScholarsArchive@OSU.

CHAPTER 3

HEATING AND ACIDIFICATION SIGNIFICANTLY IMPACT PH-SHIFTING TREATMENT: A CASE STUDY ON OAT PROTEIN ISOLATE³

³ Suryamiharja, A., Gong, X., and Zhou, H. To be submitted to *Food Hydrocolloids*.

Abstract

Oat globulin protein is known for its poor solubility at neutral pH due to its compact hexamer structure. Recent studies have demonstrated that combining alkaline treatment with pH shifting can significantly alter protein functionalities, including protein solubility. This study examined specific processing conditions, such as heating temperature and acidification type, requires further investigation using oat protein isolate (OPI) as the protein source. We evaluated the effects of different heating temperatures at pH 12 and compared the impact of acidification with HCl and citric acid on OPI solubility. Our results showed that simple pH shifting (from pH 7 to 12 to 7) did not significantly improve protein solubility while, integrating heat treatment (100°C for 30 min) with citric acid acidification significantly enhanced and maintained OPI solubility at neutral pH, ranging at 70-75%. This finding was supported by additional physicochemical characterizations, including nanoscale particle size at neutral pH, the disappearance of the thermal denaturation peak in differential scanning calorimetry (DSC) chromatograms, the formation of protein peptides ranging from 2–10 kDa in protein electrophoresis, and a reduction in β-sheet content with an increase in random coil structures. Furthermore, citric acid, compared to HCl, in combination with 100°C heating at pH 12, maintained a higher zeta potential, resulting in improved protein solubility stability for up to seven days. These results provide valuable insights into the role of non-enzymatic processing methods in modifying plant protein functionalities, particularly oat protein, and its potential applications in food formulations.

Keywords: Oat protein isolate, pH-shifting treatment, protein solubility, thermal processing, acidification, citric acid

Introduction

Oats (*Avena Sativa*) are one of the most common cereals in the world after maize, rice, wheat, barley, and sorghum (Kumar, et al., 2021; Nieto, et al., 2014). Compared to other cereals, oat protein has the highest amount of protein, as well as higher digestibility and biological values (Mirmoghtadaie, et al., 2009). These nutritional benefits are important for oats utilization in different food applications such as plant-based milk, oatmeal, and granola bars (Suryamiharja, et al., 2024). Oat proteins primarily consist of oat globulin, exhibiting a poor solubility at neutral pH but significantly improves at higher or lower pH levels due to increased electrostatic repulsion and enhanced molecular flexibility from protein unfolding (Loponen, et al., 2007). Oat globulin protein composition is mainly composed of hexamer, which builds up a compact structure that produces a strong protein-protein interaction. Additionally, oat protein amino acid composition is predominantly non-polar amino acids such as leucine, proline, and valine, with lesser amount of polar and charged amino acids (McLauchlan, et al., 2024). This problem leads to a huge challenge to the food industry to produce high protein content oat-based products like oat milk.

Among the non-enzymatic chemical modification methods, pH-shifting treatment has emerged as a simple strategy to extract the proteins from raw materials and alter protein functionalities (Jiang, Chen, & Xiong, 2009; Jiang, Wang, & Xiong, 2018). This process involves adjusting the protein solution to either extreme alkaline or acidic conditions, followed by neutralization, which induces structural rearrangements and improves functional properties (Tang, Ying, & Shi, 2021). The pH-shifting method has been widely applied to plant proteins, demonstrating its ability to enhance protein solubility (Jiang, et al., 2017), modify aggregation behavior (Li, et al., 2020), and improve emulsifying characteristics (Yu, et al., 2021; Zhang, et

al., 2021). A key point is that alkaline or acidic conditions can enhance electrostatic repulsion by increasing surface charges through protein residue ionization (Loponen, et al., 2007). This likely induces changes in protein conformation, intermolecular interactions, and surface properties, ultimately improving dispersibility and processability in food systems.

As pH-shifting or pH-driven treatment has become a common approach for modifying plant proteins, it is often combined with conventional heat treatment (Wang, Jin, & Xiong, 2018). From a structural perspective, heating can induce either reversible or irreversible protein denaturation, depending on the heating parameters and the inherent thermal stability of the plant proteins. This process is crucial for achieving the desired level of protein denaturation, particularly when targeting specific functional properties (Bogahawaththa, et al., 2019). The combination of pH-shifting and heat treatment can induce structural changes in plant proteins, such as protein rearrangement (Wu et al., 2021). This concept also extends to the Post pH-Driven (PPD) method, which has been applied in various plant-based milk applications, such as the extraction and encapsulation of bioactive compounds of curcumin (Suryamiharja et al., 2025). In this context, heating enhances the continuation of the pH-driven modification of the protein solution, influencing structural changes in the protein. The combination of heating and pHshifting method has been utilized in multiple applications, including inducing protein gelation and enhancing plant protein functionalities such as emulsification properties, surface hydrophobicity, water-holding capacity, and protein solubility (Yuntao Wang et al., 2020; Yu Wang et al., 2024).

However, variation in reported parameters make it challenging to apply this method consistently across different proteins. For example, inaccurate heating and pH-driven conditions may cause excessive denaturation, leading to protein aggregation and misorientation (Zhao,

Mine, & Ma, 2004). Achieving balanced control over plant protein modification requires a fundamental understanding of how processing conditions influence protein structure. However, the specific effects of individual processing parameters remain insufficiently explored. While previous studies have primarily focused on overall improvements in protein solubility and functionality following pH shifting and heating, detailed investigations into the influence of heating temperatures and acidification methods are still lacking. For instance, heating at different temperatures during alkaline treatment may induce distinct structural modifications, impacting protein aggregation, solubility, and surface properties. Additionally, the choice of acid for neutralization—such as strong acids (e.g., HCl) versus organic acids (e.g., citric acid) can lead to variations in protein behavior due to differences in ionic strength and interactions with protein molecules. Despite the potential of these factors to modulate protein properties, systematic research on their combined effects within the pH-shifting process remains limited. A deeper understanding of how these processing conditions interact to influence protein structure and solubility is essential for optimizing plant protein applications in food formulations.

This study examined the effects of heating temperature and acidification methods on the pH-shifting treatment of oat protein isolate (OPI), using it as a model plant protein. We hypothesized that combining heating with pH shifting under optimal conditions would enhance oat protein solubility at neutral pH by inducing structural modifications that promote better dispersion. We evaluated different heating temperatures at pH 12 and compared acidification with HCl and citric acid to assess their impact on OPI solubility. To gain mechanistic insights, we conducted physicochemical characterizations, including particle size analysis, microscopy, Differential Scanning Calorimetry (DSC), Sodium Dodecyl Sulfate-Polyacrylamide Gel Electrophoresis (SDS-PAGE), and Fourier-transform infrared (FTIR) spectroscopy. These

analyses allowed us to examine how heating and acidification influence protein aggregation, surface charge, and structural modifications, ultimately affecting solubility. Our findings provide valuable insights into optimizing plant protein processing for food applications.

Materials and Methods

Materials

Quaker Oats (Old Fashioned, 32650104084) was purchased from Walmart in Griffin,
GA. Chemicals from Sigma-Aldrich (St. Louis, MO, USA) included fluorescein isothiocyanate
(FITC, CAS No: 27072-43-3, purity >97.5%, analytical grade), citric acid (C₀HՖO¬, CAS No: 7792-9, purity ≥99.5%), and sodium hydroxide (NaOH, CAS No: 1310-73-2, purity ≥97%).

Chemicals from Fisher Scientific (Hampton, NH, USA) included 1.0 N hydrochloric acid
solution (HCl, CAS No: 7647-01-0, certified ACS reagent), sodium phosphate monobasic
anhydrous (NaH₂PO₄, CAS No: 7558-80-7), sodium phosphate dibasic anhydrous (Na₂HPO₄,
CAS No: 7558-79-4), methanol (MeOH, CAS No: 67-56-1, HPLC grade), acetic acid glacial
(CH₃COOH, CAS No: 64-19-7, ACS certified), and hexane (C₀H₁₄, CAS No: 92112-69-1, ACS
certified). The Pierce™ Modified Lowry Protein Assay Kit, including Modified Lowry protein
assay reagent (480 mL), 2 N Folin-Ciocalteu phenol reagent (50 mL), and albumin standard
ampules (2 mg/mL, 10 × 1 mL), was purchased from Thermo Scientific (Waltham, MA, USA).

All experiments were conducted using double-distilled water purified with a Millipore Milli-Q
7000.

Preparation of oat protein isolate

Oat flour was prepared by grinding Quaker Oats in a coffee grinder (SG-10 Electric Spice-and-Nut Grinder, Mini, Ontario, Canada) for 1 min and sieving through a fine mesh

strainer (0.841–0.250 mm). OPI was extracted following a modified protocol (Yung Ma, 1983). Oat flour was first defatted using hexanes in a 1:4 (w/v) ratio for 1 h, followed by suction filtration to separate the oil. The defatting process was repeated twice, and the defatted oat flour was left under a fume hood overnight to allow hexane volatilization. The defatted oat flour was then mixed with double-distilled water (1:10 g/v), and the pH was adjusted to 10.0 using 1 M NaOH. The slurry was stirred at room temperature (21°C) for 1 hour and then centrifuged at $4,000 \times \text{rpm}$ for 15 min. The supernatant pH was lowered to 5.0 using 1 M HCl, followed by another centrifugation at $4,000 \times \text{rpm}$ for 15 min. The resulting precipitate was washed twice with deionized water, neutralized to pH 7 using 1 M NaOH, freeze-dried, and stored in a desiccator at room temperature (23°C).

Proximate analysis

Moisture content analysis was performed according to the Association of Official Analytical Chemists (AOAC) official method (Thiex, 2019). Briefly, the sample weight was recorded before and after heating in a vacuum oven at 60°C overnight, and the moisture content was determined based on the weight difference. Total crude protein content was measured using the Dumas method (Roland, Aguilera-Toro, Nielsen, Poulsen, & Larsen, 2023). OPI was analyzed using the N-Cube Elementar (Ronkonkoma, NY, USA), with a nitrogen conversion factor of 5.84 to measure the oat protein. Aspartic acid was used as the blank for calibration. Ash content was determined by following AOAC official method (Thiex, Novotny, & Crawford, 2019). Approximately 2 g of the sample was weighed into a crucible and heated overnight in a muffle furnace at 600°C. The weight difference before and after heating was used to calculate the percentage of ash in OPI. Crude fat content was measured using the Soxhlet extraction method (Alemayehu, et al., 2021). Approximately 1 g of the sample was placed in a cellulose thimble,

which was then inserted into a Soxhlet apparatus connected to a round-bottom flask. The extraction was conducted overnight, and the solvent was subsequently removed using a rotary evaporator. The weight difference before and after extraction was used to calculate the percentage of crude fat in OPI. The percentage of carbohydrates was determined by subtracting the sum of % moisture, % crude protein, % ash, and % crude fat from 100%.

pH-shifting and heating treatment of OPI

The OPI powder was dissolved in a 10 mM phosphate buffer at pH values ranging from 7 to 12, with a 1% (w/v) protein concentration and stirred overnight using a magnetic stir bar at 800 rpm at room temperature. Acidification was performed using either 3% citric acid or 0.1 M HCl, with a 10-min hydration period for each pH reduction (pH 12 OPI solution to pH 11 OPI solution (10 min) to pH 10 OPI solution (10 min) until the target pH). Heating was applied using a water bath with gentle shaking at 50 rpm, at either 25°C, 50°C or 100°C for 30 min. The solution was immediately cooled in an ice bath until it reached room temperature, which was monitored using a thermometer. The agitation was applied during an acidification process and its speed was maintained at a high rate (1000-1100 rpm) to ensure rapid pH changes and prevent local pH variations that could cause protein aggregation.

Determination of protein solubility

Protein concentration was determined using the Lowry method using a PierceTM

Modified Lowry Protein Assay Kit (Thermofischer Scientific, Waltham, MA). The OPI solution was centrifuged at 5,000 rpm for 10 min prior to measurement. The assay was conducted at 750 nm by combining 0.2 mL of the oat protein sample, 1 mL of modified Lowry reagent, and 0.1 mL of 1 N Folin-Ciocalteu reagent. The oat protein sample was first diluted and allowed to sit for 15 min, followed by the addition of 1 mL of modified Lowry reagent, with a 10-min

incubation. Then, 0.1 mL of 1 N Folin-Ciocalteu reagent was added, and the mixture was incubated for 30 min. During the procedure, the samples were vortexed for approximately 15 s and kept in a dark drawer with test tube caps on. The pH 12 OPI solution was used to generate the standard curve, which was verified by the DUMAS method to measure the % protein with a conversion factor of 5.84. The standard curve equation obtained was y = 2.5475x + 0.0685, with an R^2 value of 0.9965, where x-axis represents absorbance (nm), and y-axis represents the protein concentration (mg/mL). The % protein solubility was determined as follows:

% Protein Solubility =
$$\frac{\text{Amount of protein in the OPI protein solution }(g)}{\text{Amount of protein in the OPI powder }(g)} \times 100.$$

Particle size and zeta potential

The particle size was measured using Zetasizer pro (Malvern Panalytical, Westborough, MA) in the form of the intensity-weighted mean diameter (Z-average particle size). Samples for a solubility test were centrifuged at 10,000 rpm for 15 min prior to measurement to obtain the particle size of soluble proteins. The OPI solution at pH 7-12 was diluted using different phosphate buffers (pH 7-12) that match its pH to achieve a final protein concentration (0.1 mg/mL) (Li & Xiong, 2021b). The OPI solution was loaded into DTS0012 (Disposable 10×10 plastic cell) and the parameters were set as follows: protein refractive index of 1.45, water as the dispersant, 25 °C, and 30 s equilibrium time. For zeta potential (ζ) measurement, the same OPI solution from particle analysis was loaded into DTS1070 cell, and the measurement was also run using the same instrument with the same condition as the particle size analysis. Each measurement was run to obtain the Z-average particle size (nm), average Polydispersity Index (PDI), and zeta potential (mV).

Protein electrophoresis (SDS-PAGE)

The SDS-PAGE was run by following a previous method (Sánchez-Velázquez, et al., 2021). Briefly, it used Mini-Protean 3 Gel Electrophoresis (Bio-Rad) and 4–20% Mini-PROTEAN® TGX Stain-FreeTM Protein Gels (64639831, Bio-Rad Laboratories, Inc., CA, USA). Precision Plus ProteinTM standard (10-250 kDa, Bio-Rad Laboratories Inc., CA, USA) was used as the molecular marker. OPI solution at pH 12 (heated and unheated), OPI solution at pH 7 acidified using citric acid or HCl (after pH 12 OPI solution was heated at 100 °C, or not), and OPI solution at pH 7 (dissolved in phosphate buffer pH 7, heated and unheated) were dissolved in running buffer (200 mM Tris-HCl, pH 6.8, 40% glycerol, 2% SDS, 0.04% Coomassie Blue G-250) along with \geq 98% pure 2-mercaptoethanol (14.2 M) at 5 % (w/v). The sample was placed into the water bath at 100 °C for 5 min and centrifuged for 15 min at 10,000 rpm prior to load into the gel (10 µL, 20 µg protein/ well). The gel was run at 150 V for 30 min. The gel was stained using Coomassie Blue R250 Dye, followed up by the fixation with 10% acetic acid and 50% MeOH (v/v) and three times washes of 10% acetic acid. The picture of the gel was then taken using an iPhone 13 camera.

Differential scanning calorimetry

Differential Scanning Calorimetry (DSC 204 F1 Phoenix, NETZSCH Instruments North America LLC, Burlington, MA) was used to determine the denaturation temperature of various OPI solutions. The tested samples included OPI solutions at pH 12 (heated and unheated), OPI solutions acidified to pH 7 using citric acid or HCl after heating the pH 12 solution to 100°C, and OPI solutions at pH 7 (dissolved in phosphate buffer, heated and unheated). All solutions were prepared at a 10% (w/v) protein concentration, freeze-dried, and approximately 10 mg of each sample was loaded into a sealed crucible. The temperature program was set from 50°C to 170°C

at a heating rate of 10°C/min, with a nitrogen flow rate of 30 mL/min. Samples were analyzed under a nitrogen atmosphere, and the data were extracted using Proteus® thermal analysis software.

Fourier transform infrared spectroscopy

The same OPI powder used in DSC analysis was analyzed using Nicolet 6700 FTIR Spectrometer (Thermo Fischer Scientific Inc., Waltham, MA) following the method described in a previous study (Liu, et al., 2009). The sample was run under ambient condition and 4 cm⁻¹ resolution. The OPI powder was placed on the Attenuated Total Reflectance (ATR) crystal and pressed using the ATR probe accessory. The original FTIR spectrum deconvolution was performed in Origin Pro 2021 using gaussian multiple peaks function from region 1600 cm⁻¹ to 1700 cm⁻¹, which represents the amide 1 peak. The peaks were selected by following a previous study, including 1630-1638 cm⁻¹, 1682-1690 cm⁻¹, 1640-1648 cm⁻¹ 1650-1659 cm⁻¹, and 1660-1670 cm⁻¹, which represent β-sheets, antiparallel β-sheets, random coils, α-helixes, and β-turns respectively (Ma, Rout, & Mock, 2001; Murayama & Tomida, 2004; Ngarize, Herman, Adams, & Howell, 2004).

Stability of protein solubility

The stability of protein solubility test was performed on acidified OPI solutions from pH 12 OPI solution (unheated, heated at 50 °C, and heated at 100 °C) to pH 7 using either HCl or citric acid. The OPI solutions for particle size and ζ measurements were stored in 10 mL test tubes, while centrifuged samples used to measure % protein solubility were stored in 1.5 mL centrifuge tubes at 4 °C. The stability of each sample was evaluated on day 0, 1, 3, and 7. The % protein solubility remaining in the solution was measured by centrifuging the sample at 5,000 rpm for 10 min, which was only done on day 0. The particle size, polydispersity index (PDI), and

zeta potential of the OPI solutions were measured without centrifugation. Photos were taken before and after heating, as well as post-acidification, on days 0, 1, 3, and 7.

Microstructure

The microstructure of the sample was measured using A Nikon Eclipse Ti2 widefield fluorescence microscope (Nikon, Tokyo, Japan). To obtain microscopy photos, 200 µL of the 1% (w/v) OPI solutions were mixed with 0.1% (w/v) Fluorescein Isothiocyanate (FTIC) dissolved with 95% proof ethanol. The samples were then vortexed for 5 seconds immediately, and 10 µL of the sample was placed on the pre-clean microscope slides covered with the cover glass. The protein was visualized at 550 nm and the observation was conducted at 40X objective lens. The photos were captured and analyzed using NIS-Elements software from Nikon.

Statistical analysis

All measurements were performed in triplicate, and the mean and standard error (represented by error bars) were calculated. Statistical significance was determined using one-way ANOVA followed by a post hoc Tukey HSD test ($p \le 0.05$) in Statistical Package for the Social Sciences (SPSS) Statistics 27, IBM.

Results and Discussion

Physicochemical properties of oat protein isolate

The proximate composition of OPI was determined to quantify the macronutrient distribution, revealing protein as the predominant component, accounting for $67.6 \pm 1.0\%$ of the total content (**Figure 3.1A**). The remaining fractions included carbohydrates ($21.0 \pm 1.1\%$), moisture ($8.6 \pm 0.5\%$), fat ($1.2 \pm 0.0\%$), and ash ($1.4 \pm 0.1\%$), indicating a relatively low lipid and mineral contents. DSC was further used to assess its thermal properties. The thermogram

(Figure 3.1B) exhibited a sharp endothermic peak at 113.9 °C, corresponding to the denaturation temperature of OPI. This transition reflects the unfolding of protein structures upon heating, which is consistent with previous observations at approximately 110 °C (Brückner-Gühmann, Kratzsch, Sozer, & Drusch, 2021). Notably, this thermal denaturation temperature is relatively high compared to other widely used plant proteins, such as pea protein (76.5–93°C) and soybean protein (79–87°C) (Mession, Sok, Assifaoui, & Saurel, 2013). The higher denaturation temperature of OPI suggests enhanced thermal stability, which could be beneficial in high-temperature food processing applications. The well-defined peak observed in the DSC thermogram also indicates that the extracted OPI retains a structured conformation after processing. These findings confirm that the native structure of OPI was successfully persevered after protein extraction from oat flour, which is well-suited for further investigations into the effects of different processing conditions on OPI solubility.

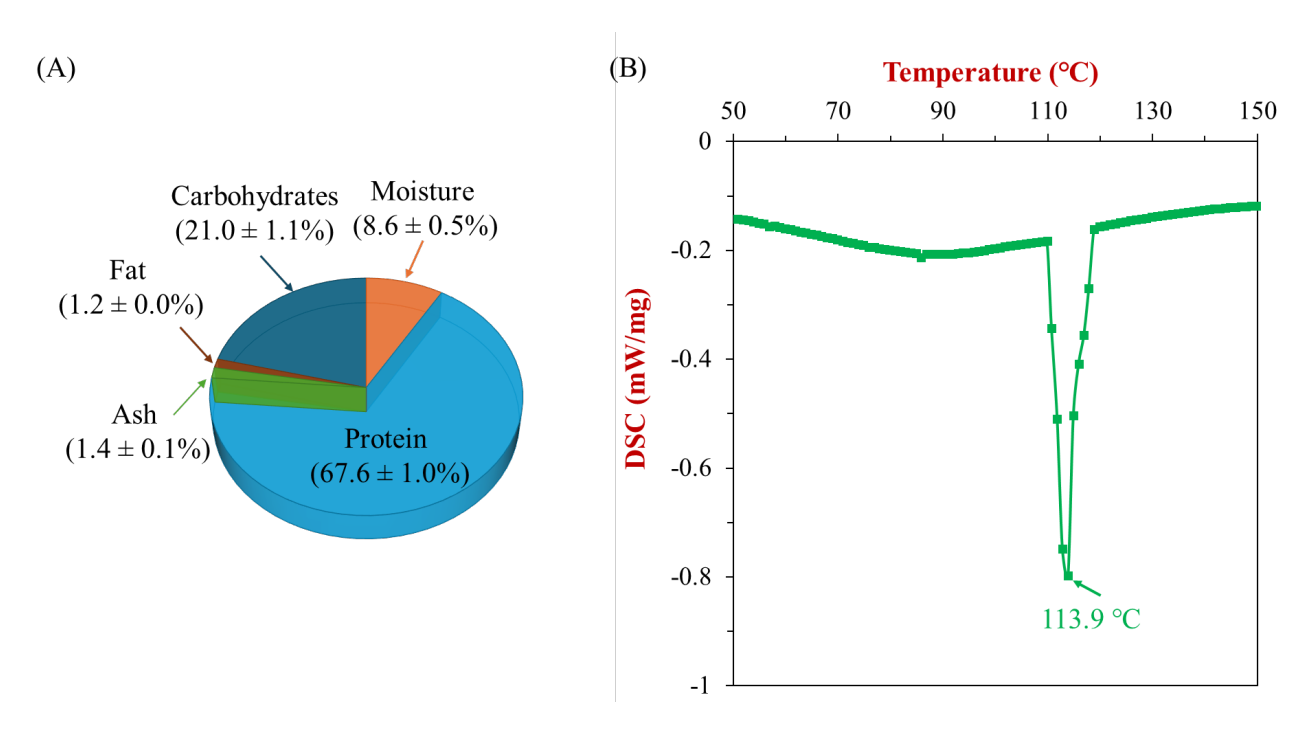


Figure 3.1. (A) Proximate composition of oat protein isolate, highlighting the protein content $(67.6 \pm 1.0\%)$ as the major component. (B) Differential scanning calorimetry thermogram of OPI, showing a denaturation peak at 113.9 °C.

Impact of different processing conditions on the OPI solubility

Experimental design

To investigate the effects of pH-shifting and heating treatments on OPI solubility, a more controlled experimental design was implemented, incorporating alkaline treatment, heat application, and acidification. As illustrated in Figure 3.2, the process began with an initial pH adjustment to 12, followed by different heating conditions (25°C, 50°C, and 100°C) to assess the impact of thermal treatment on protein structure. The treated protein solutions were acidified using either 3% citric acid or 0.1 M hydrochloric acid (HCl) to assess the impact of different acidification methods on protein solubility and aggregation behavior. Citric acid was chosen due to its widespread use in the food industry, while HCl is commonly used in experimental research. This stepwise treatment approach was designed to examine how varying temperatures during alkaline treatment affect protein conformation, aggregation, and solubility. The selection of 50°C and 100°C for heating conditions was based on their relevance to food processing applications such as pasteurization, while 25°C served as a control condition without heat treatment (Le, Hermansen, & Vuong, 2025). The final acidification step using citric acid or HCl was included to determine whether the type of acid influences oat protein refolding, charge distribution, or aggregation. These two acids were chosen based on the consideration that HCl is the most commonly used acid in the acidification process, while citric acid is the one most commonly used in the food industry. By systematically varying these processing conditions, this study aims to provide deeper insights into the physicochemical changes occurring due to heating and

acidification in pH-shifting treatment, thereby optimizing processing strategies for plant protein applications.

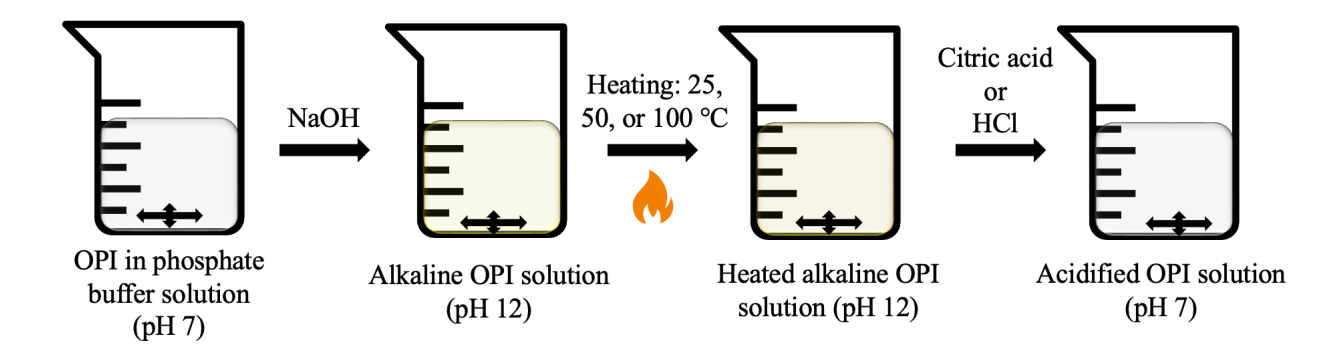


Figure 3.2. Schematic representation of the pH-shifting and heating treatment process for oat protein isolate. The process includes an initial pH adjustment to 12, heating at different temperatures (50 °C, and 100 °C) versus no-heat (25 °C), and subsequent acidification using either 3% citric acid or 0.1 M HCl. It highlights the structural changes induced by varying heating conditions and acid types during the treatment.

Impacts of different heating temperatures at pH 12

To assess the impact of heating temperature at pH 12 on OPI solubility, protein samples were subjected to different thermal treatments before acidification. Protein solubility was evaluated across a range of pH values, and the results demonstrated that heating plays a critical role in maintaining protein solubility upon acidification (**Figure 3.3**). First, the OPI solubility was increased progressively as the pH was raised from 7 to 12, reaching its peak at pH 12. However, upon acidification back to neutral, the no-heat condition (25°C) exhibited a sharp decline in solubility, whereas the 50°C and 100°C heat-treated samples still maintained significantly higher solubility levels at 70-75%. This indicates that heating at alkaline pH could promote structural changes that prevent excessive protein aggregation upon acidification. The fluorescence microscopy image (inset) also supports this observation, showing large protein

aggregates formed in the no-heat condition, which were less prevalent in the heated samples. These findings suggest that thermal treatment at pH 12 facilitates protein structural modifications, preventing the formation of large insoluble aggregates during subsequent acidification. As a result, protein solubility is only slightly reduced despite changes in environmental ionic conditions (Tang, Roos, & Miao, 2023). The improved solubility observed in the 100°C-treated sample implies that higher temperatures may further enhance these structural changes, potentially by increasing protein flexibility or disrupting intermolecular interactions.

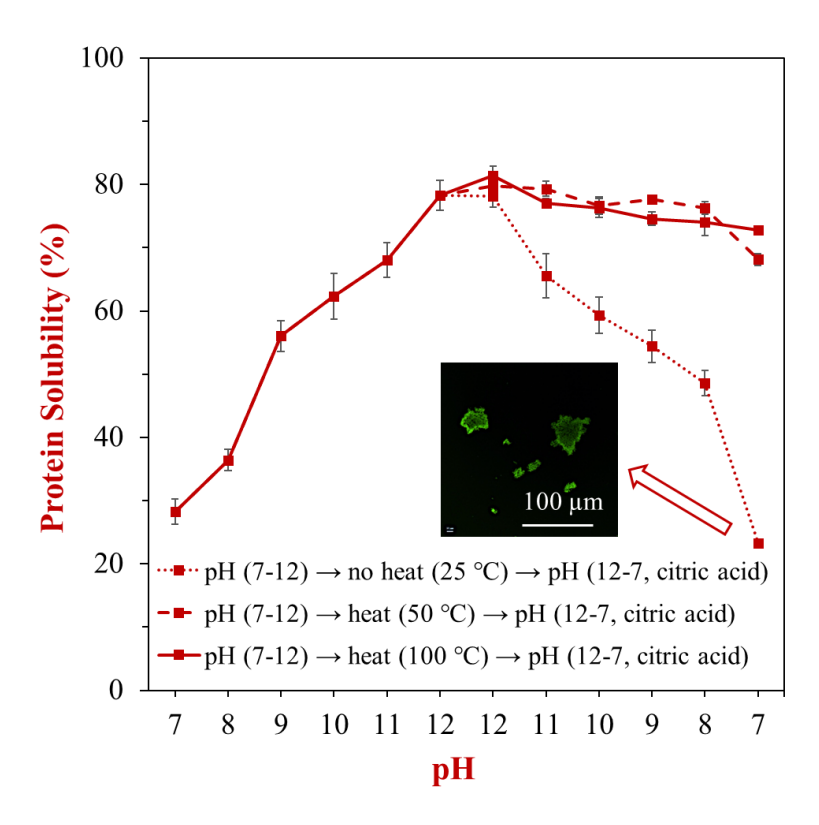


Figure 3.3 Protein solubility (%) of oat protein isolate at varying pH levels and heating conditions. The treatments include (1) no heating (25 °C), (2) heating at 50 °C, and (3) heating at 100 °C, followed by pH adjustment using 3% citric acid. The inset fluorescence image shows protein aggregates formed under the no-heat condition with citric acid, as indicated by the arrow. The scale bar is 100 μm.

To further evaluate the stability of soluble OPI after different heat treatments at pH 12, samples were stored for up to 7 days, and their stability of protein solubility was analyzed. As shown in Figure 3.4A, the remaining soluble protein content varied significantly among the different heating conditions (S1: 25 °C, S2: 50 °C, S3: 100 °C) over time. On day 0, all samples were set to 100% remaining protein solubility for the comparisons. After 1 day of storage, the S1 (25 °C) sample showed a sharp decline in solubility, with only approximately 30% of the protein remaining soluble by day 7. In contrast, S2 (50 °C) and S3 (100 °C) retained more than 90% of their soluble proteins throughout the 7-day storage period, suggesting that heating at alkaline pH helps stabilize protein solubility over time. Visual observations of sedimentation behavior also verified these solubility trends (Figure 3.4B). The S1 sample (25 °C) exhibited significant sedimentation, forming a visible precipitation layer with a height of 1.1 cm after 1 day of storage. In contrast, S2 (50 °C) and S3 (100 °C) demonstrated no visible sedimentation after being stored up to 7 days. These findings indicate that heating at 50 °C and 100 °C reduces protein aggregation and precipitation in the solution. Overall, these results highlight the importance of thermal treatment at alkaline pH in maintaining the long-term stability of OPI. Heating at 50 °C and 100 °C showed promising results in preventing protein precipitation. This insight can be applied to ensure consistent protein solubility in food formulations.

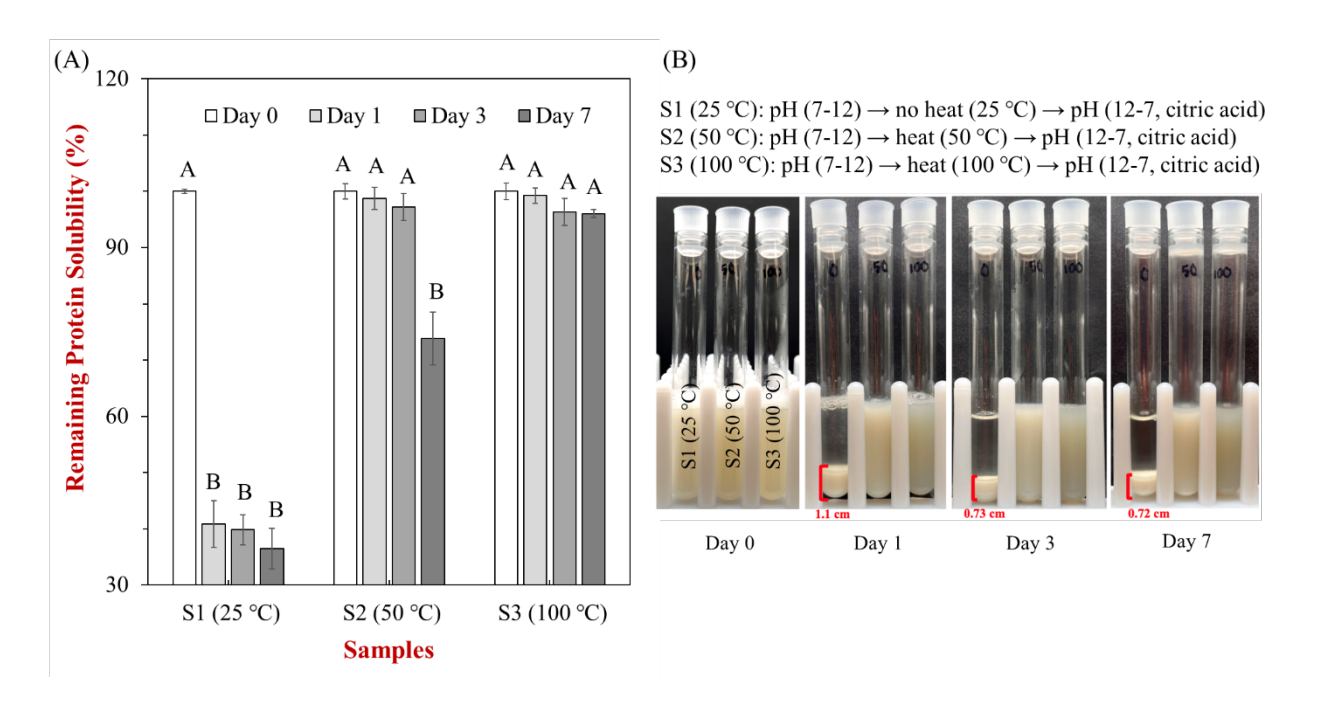


Figure 3.4. (A) Remaining soluble proteins (%) of oat protein isolate under different heating conditions (S1: 25 °C, S2: 50 °C, S3: 100 °C) over storage periods of 0, 1, 3, and 7 days. (B) Visual observations of samples (S1, S2, S3) showing sedimentation behavior over time, with sediment heights indicated in red (Letter shows significance at $p \le 0.05$ among different days in each sample).

Impacts of different types of acid for acidification

We also evaluated the effect of acid type on protein solubility. Besides citric acid, OPI was also subjected to acidification using HCl after undergoing heat treatments at pH 12. The solubility trends across varying pH levels and heating conditions are presented in **Figure 3.5**, demonstrating how thermal processing influences OPI solubility upon HCl acidification. Similar to previous observations with citric acid, the protein solubility increased along with the increase of the pH, reaching its peak at pH 12, followed by a decline upon acidification back to neutral (pH 7). As expected, the extent of protein solubility loss varied among different heat treatments,

supporting that heating also plays a crucial role in preventing aggregation upon HCl acidification.

No-heat condition (25 °C) exhibited the most significant solubility loss, showing a steep decline as pH was reduced from 12 to neutral among the three treatments. The inset fluorescence microscopy image (Figure 3.5) confirms the formation of large insoluble protein aggregates under this condition. In contrast, samples heated at 50 °C and 100 °C retained higher solubility, suggesting that heat treatment at an alkaline pH promotes protein unfolding, thereby improving protein solubility in the solution and making oat protein more resistant to precipitation.

Compared to citric acid-treated samples (Figure 3.3), the HCl-treated samples exhibited a more pronounced drop in solubility upon acidification, suggesting that HCl-induced charge neutralization can induce more protein aggregation. In summary, the benefits of heating at pH 12 remain evident, reinforcing the role of thermal treatment in modulating protein interactions and enhancing solubility retention during acidification. Additionally, these results highlight the importance of acid selection in pH-shifting treatments, as acid type influenced protein aggregation and solubility recovery.

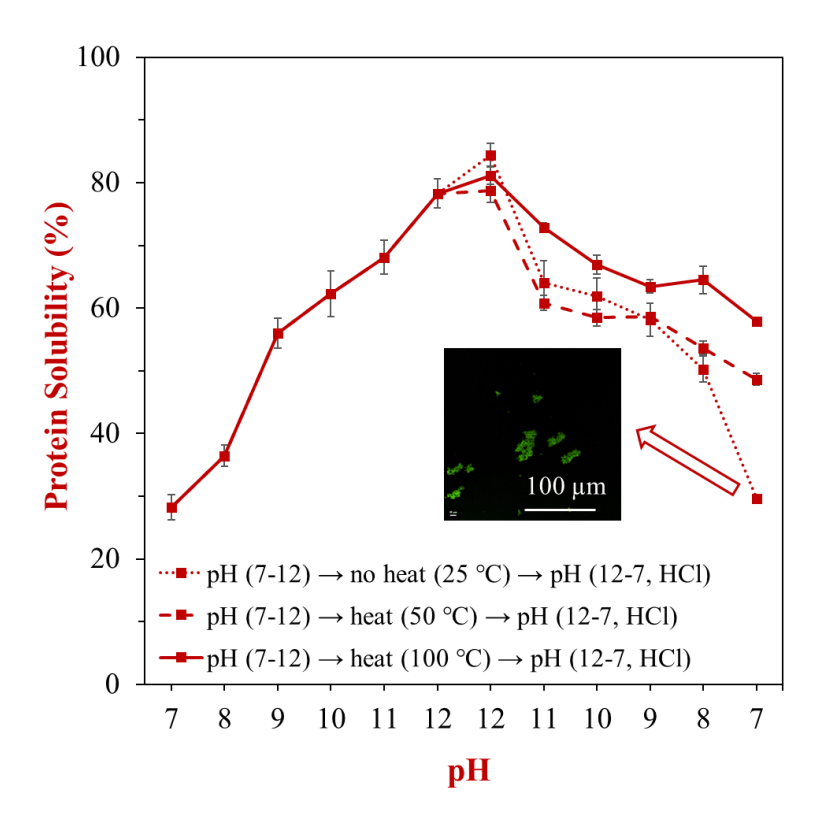


Figure 3.5. Protein solubility (%) of oat protein isolates at varying pH levels and heating conditions, with acidification using 0.1 M HCl. Treatments include (1) no heating (25 °C), (2) heating at 50 °C, and (3) heating at 100 °C. The inset fluorescence image shows protein aggregates formed under the no-heat condition with HCl acidification, as indicated by the arrow. The scale bar is 100 μm.

Understanding the mechanism: how heating at pH 12 enhances OPI solubility

Formation of OPI-based nanoparticles

The particle size and appearance analysis were conducted to elucidate the mechanism behind the enhanced OPI solubility after heating at pH 12. The visual images in **Figure 3.6A** show OPI dispersions at pH 12 and pH 7 under different heating conditions (25 °C, 50 °C, and 100 °C) followed by acidification using citric acid. At pH 12, all samples appeared homogeneous and well-dispersed, indicating almost maximum solubilization under alkaline conditions.

However, after adjusting the pH back to neutral (pH 7), noticeable differences were observed in precipitation and turbidity. A noticeable color change from dark yellow at pH 12 to white at pH 7 was observed, likely due to the presence of phenolic acids (Ha et al., 2025). The no-heat sample (25°C) exhibited significant aggregation after acidification, as evidenced by increased solution turbidity and visible precipitation after centrifugation. In contrast, the heated samples (50°C and 100°C) retained turbidity, indicating improved solubility in the solution. This suggests that thermal treatment enhance protein solubility upon acidification. To further understand the impact of heating on protein structural behavior, the particle size distributions of soluble proteins after different heating treatments were analyzed (**Figure 3.6B**). The results revealed a slight shift in particle size depending on the heating condition. The no-heat sample (25 °C) exhibited the largest protein particles, while the samples heated at 50 °C and 100 °C displayed even smaller particles after acidification. Notably, the 100 °C-heated samples contained a fraction of very small particles, measuring just a few tens of nanometers which may come from small soluble aggregates (Wouters & Nicolai, 2024).

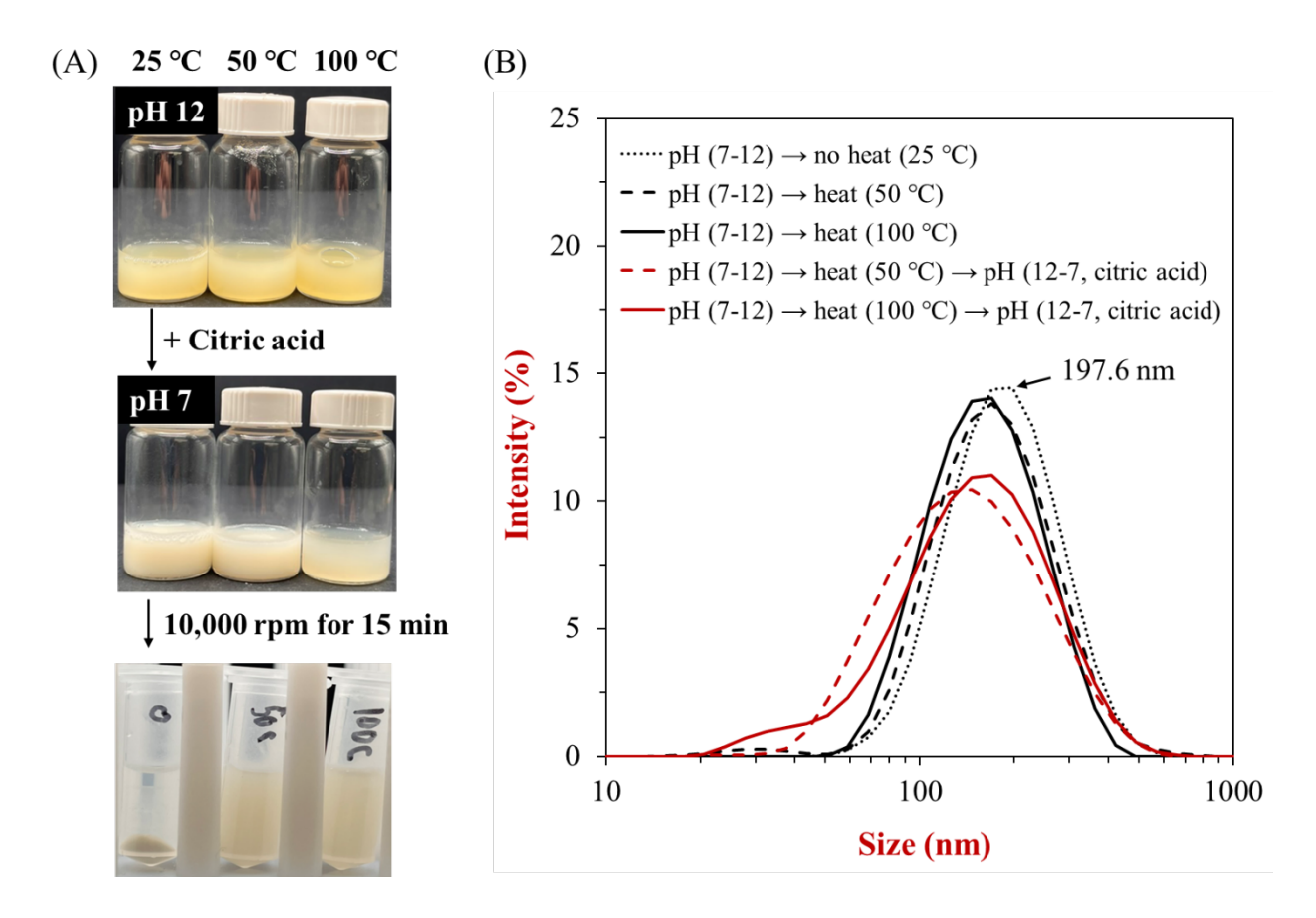


Figure 3.6. (A) Visual observations of oat protein isolate samples at pH 12 and pH 7 after treatments with no heat (25 °C), heating at 50 °C, and heating at 100 °C, followed by acidification using citric acid. (B) Particle size distribution of the treated samples, measured after centrifugation at 10,000 rpm for 15 min, highlighting the impact of heating and pH adjustment.

Improved electrostatic repulsion interactions due to reduced zeta potential

The zeta potential measurements were also conducted to assess changes in surface charge and electrostatic interactions across different pH levels. The results, shown in **Figure 3.7**, revealed the impact of heating temperature and acidification method (citric acid vs. HCl) on the zeta potential of OPI. Generally, all samples exhibited negative zeta potential values, indicating that oat protein carries an overall negative surface charge in the tested pH range because of the presence of negatively charged residues on the surface (McLauchlan, et al., 2024). However, the

values are less negative than previous reports, which could be due to the different salt concentrations, because the ionic environment can affect the zeta potential of proteins in the solution (Ercili-Cura, et al., 2015; Li & Xiong, 2021a). As we can see, the extent of surface charge varied with heating treatment and acid type, suggesting that thermal processing at pH 12 modifies the surface chemistry of protein nanoparticles. As observed in Figure 3.7A, when citric acid was used for acidification, the no-heat sample (25°C) displayed the least charge recovery upon acidification, showing a significant shift towards lower surface potential at neutral pH condition. In contrast, samples heated at 50°C and 100°C maintained more negative zeta potential values, suggesting that heat treatment at alkaline pH improves electrostatic repulsion interactions upon acidification, thereby improving protein stability. A similar trend was observed in Figure 3.7B, where samples acidified with HCl exhibited a more negative zeta potential with higher heating temperatures. Notably, the 100°C-treated sample displayed the most negative surface charge at neutral pH, supporting that thermal processing can lead a minimal protein aggregation upon acidification, regardless of the acid types (Cruz-Solis, Ibarra-Herrera, Rocha-Pizaña, & Luna-Vital, 2023).

These results indicate that heating at pH 12 reduces the amount of protein surface charge retention, leading to stronger electrostatic repulsion and an improved protein solubility even after acidification. The reduced negative charge upon neutralization was expected due to the neutralization of some types of protein residues, like tyrosine. This effect was more pronounced in citric acid-treated samples, likely due to stronger ionic interactions of citric acid and protein compared to HCl. One possible explanation is that citric acid may interact with protein nanoparticles by forming complexes or coating their surface, thereby enhancing stability and solubility (Jayachandran, Parvin, Alam, Chanda, & MM, 2022; Li, et al., 2018; Reddy, Li, &

Yang, 2009; Xu, Shen, Xu, & Yang, 2015). These findings highlight the crucial role of electrostatic repulsion interactions in stabilizing OPI during pH shifting, reinforcing the benefits of thermal treatment at alkaline pH and emphasizing the importance of acid type in enhancing solubility.

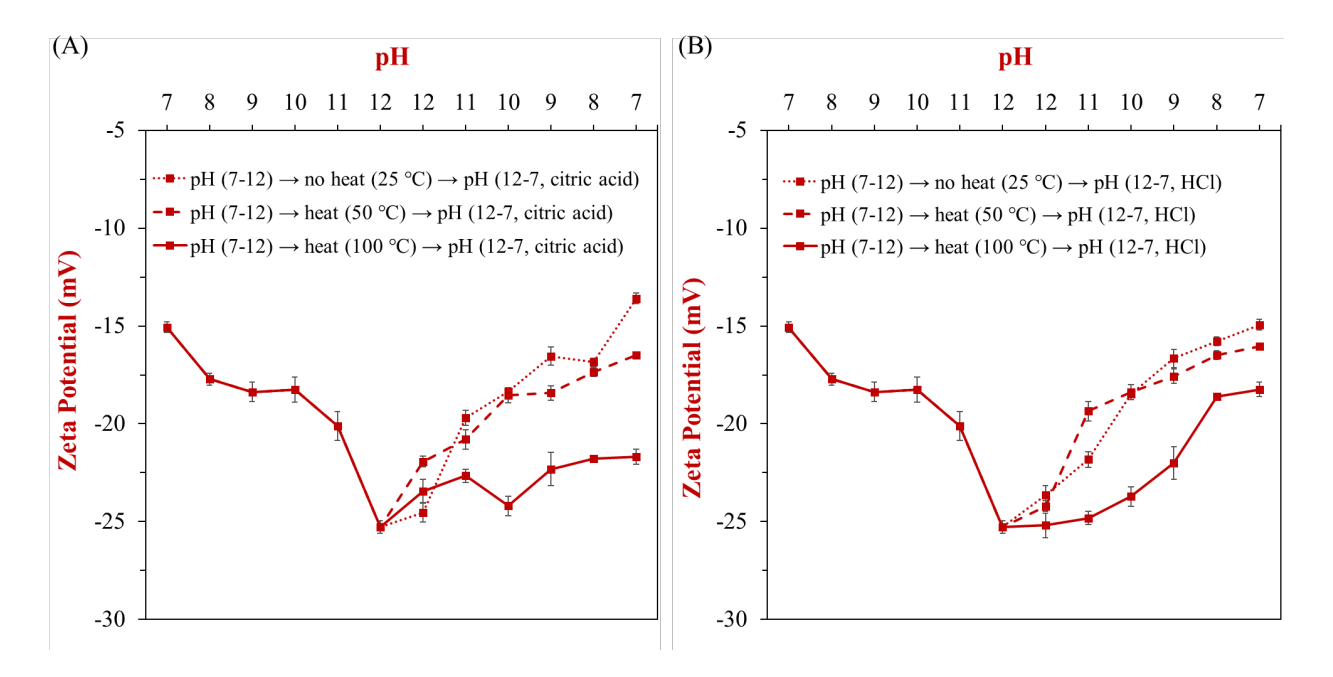


Figure 3.7. Zeta potential (mV) of oat protein isolate across varying pH levels and heat treatments. (A) Samples acidified with 3% citric acid after no heating (25 °C), heating at 50 °C, or heating at 100 °C. (B) Samples acidified with 0.1M HCl after no heating (25 °C), heating at 50 °C, or heating at 100 °C.

Surface charges and particle sizes are stable within a week

We also assessed the stability of protein solubility up to 7 days according to their particle size and zeta potential. The particle size (Z-average) and zeta potential were monitored over a 7-day storage period for samples treated at 50 °C (S2) and 100 °C (S3) at pH 12. As shown in **Figure 3.8A**, the Z-average particle size remained relatively stable over time for both heated samples. The S2 (50 °C) sample exhibited the particle sizes within a range (~170-200 nm) with a

slight fluctuation in day 1. Surprisingly, the particle size of S2 sample was first increased on day 0 and then was decreased after that. In contrast, the S3 ($100\,^{\circ}$ C) sample had a smaller particle size (\sim 140-170 nm) across all storage days. Although the particle size was decreased as wellas the day increased, they are not significantly different from one and another (p < 0.05).

Figure 3.8B shows the zeta potential values over the same 7-day storage period. The S2 (50°C) sample exhibited a less negative surface charge (~ -16 to -18 mV) throughout storage, whereas the sample S3 (100°C) initially had a more negative zeta potential (~ -20 to -22 mV), which slightly decreased to ~-20 mV after day 1. This suggests that higher-temperature treatment leads to more negative zeta potential, preventing particle size variations that could contribute to protein aggregation. The relatively stable surface charge and particle size of S3 (100°C) confirm that heat treatment at pH 12 can prevent the oat protein aggregation and maintain relatively stable protein stability. These findings support the previous sections on zeta potential, protein solubility, and particle size, indicating that appropriate thermal treatment combined with citric acid acidification not only enhances immediate solubility but also contributes to long-term stability.

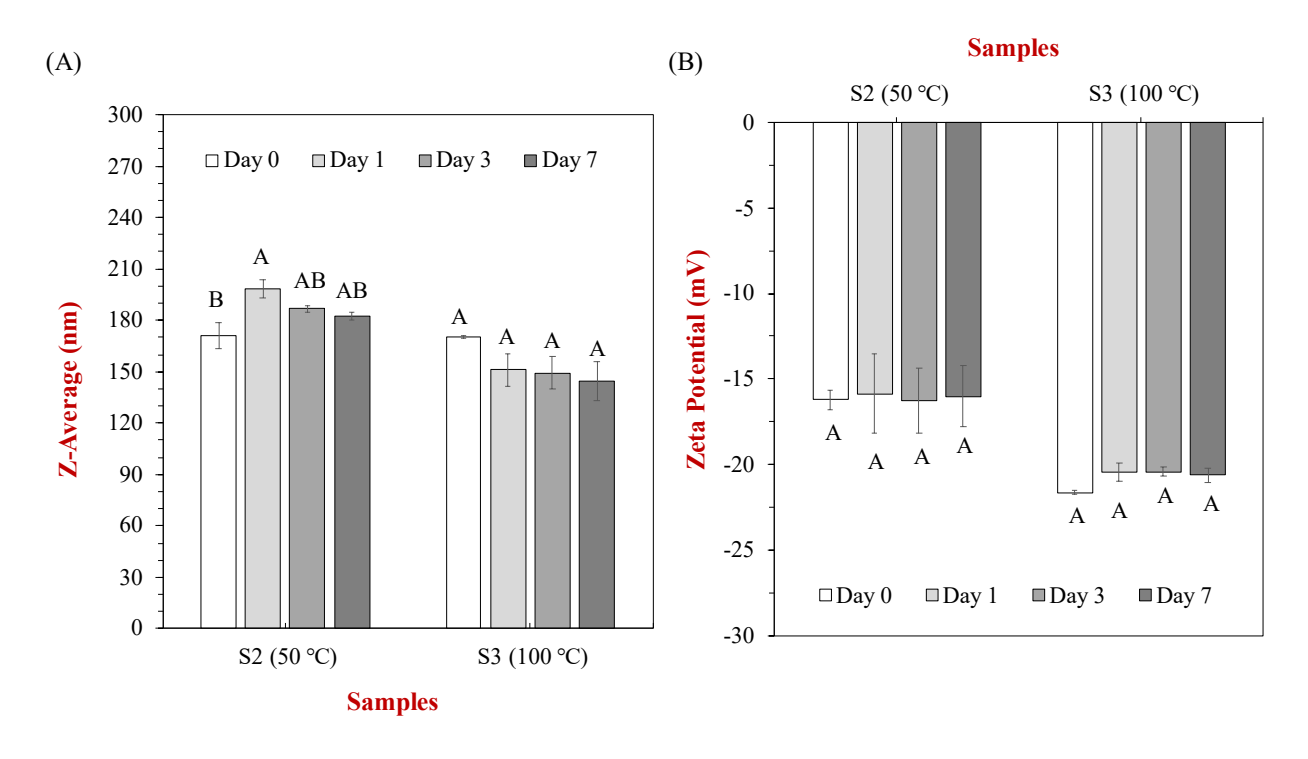


Figure 3.8. (A) Z-average particle size (nm) of oat protein isolate samples (S2: 50 °C, S3: 100 °C) over storage periods of 0, 1, 3, and 7 days. (B) Zeta potential (mV) of the same samples over the same storage periods, illustrating the effects of heating and storage on particle size and surface charge stability. The samples (S2 and S3) are defined in **Figure 3.4B** (The letters, A, B, C, show the significance at $p \le 0.05$ among different days within each sample).

Structural changes of OPI in solution

To investigate the structural modifications induced by heating at pH 12, SDS-PAGE analysis was conducted to examine the molecular weight distribution upon different treatments. The results, presented in **Figure 3.9**, highlight the effects of different heating temperatures and acid types, alongside samples heated at pH 7 as a control. Overall, all OPI solutions showed clear bands at 20-25 kDa and 30-35 kDa which correspond to α -subunits of oat globulin protein and β -subunits of oat globulin protein respectively (Ercili-Cura, et al., 2015). There is also a few bands in between α -subunits and β -subunits which could be due to the presence of prolamin protein

fraction (Robert, Nozzolillo, & Altosaar, 1985). Upon exposure to pH 12, notable changes in protein bands were observed, particularly after heating. At 25°C (without heat treatment), the protein bands of both α- and β-subunits remained visible but appeared slightly smeared, suggesting partial structural unfolding. In contrast, heating at 100°C caused a significant reduction in distinct protein bands, with a noticeable smear and diminished intensity in the predominant bands. This resulted in the appearance of bands in the lower molecular weight region (2–10 kDa, highlighted by the red box), indicating hydrolysis due to the combined effects of alkaline conditions and heat. These findings suggest that heating at pH 12 promotes the formation of protein peptides, aligning with the previously observed nanoscale particle sizes. Moreover, these peptides remained stable upon acidification to pH 7, contributing to enhanced OPI solubility. This structural transformation explains the improved solubility and stability of heat-treated OPI, reinforcing the role of thermal processing under alkaline conditions in optimizing protein functionality.

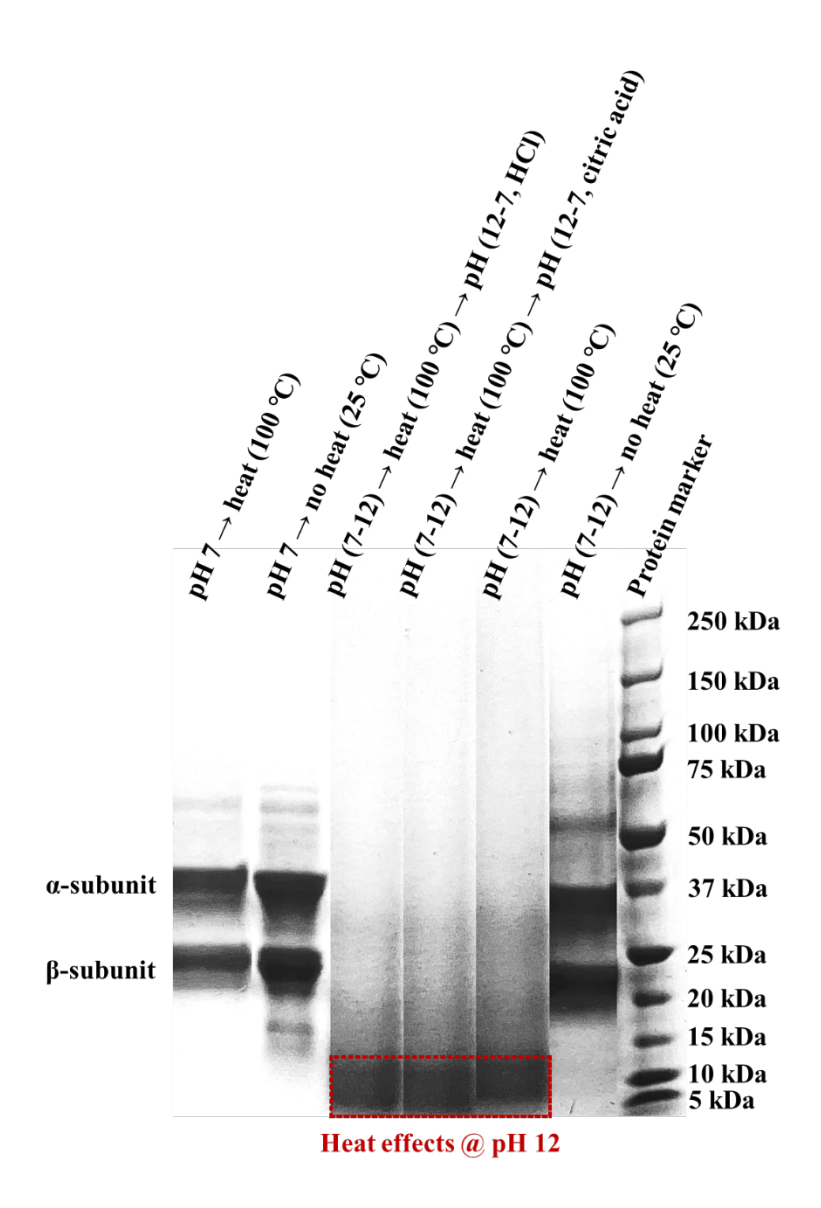


Figure 3.9. SDS-PAGE analysis of OPI under different pH and heating conditions. Samples include treatments at pH 7 and pH 12 with no heat (25 °C), heating at 50 °C, and heating at 100 °C, alongside a protein ladder for molecular weight reference. The red box highlights the heat-induced changes at pH 12, indicating production of protein peptides.

Thermal denaturation temperatures were determined using DSC to analyze peak variations across different treatments. As shown in **Figure 3.10**, the thermograms reveal significant differences in denaturation temperature and enthalpy changes, highlighting how pH and heat treatment influence protein stability and structural transitions. For samples kept at pH 7,

the unheated (25°C) sample exhibited a denaturation peak at 113.4 °C, whereas the 100°C-heated sample at pH 7 showed a slight decrease of denaturation temperature to 108.6°C, indicating partial protein unfolding due to a heat exposure. Once the pH was shifted to 12, there was a significant reduction of ΔH and ΔT_{1/2} values. Additionally, when heating was applied at this alkaline pH, the peak was barely seen anymore, indicating the OPI has undergone a significant conformational change such as irreversible denaturation (Ma and Harwalkar, 1985). As expected, the pH-shifting treatment (7 to 12 to 7) with heating showed no DSC peaks when samples were heated to 100°C at pH 12, followed by acidification with HCl or citric acid. This disappearance of the thermal denaturation peak suggests that heating at pH 12 induced an irreversible structural change in OPI. Interestingly, even after acidification, the absence of thermal denaturation peaks persisted, indicating that certain structural attributes acquired at pH 12 were retained. This finding supports the hypothesis that pH-induced structural modifications, enhanced by heat, can significantly alter protein conformation, ultimately improving solubility.

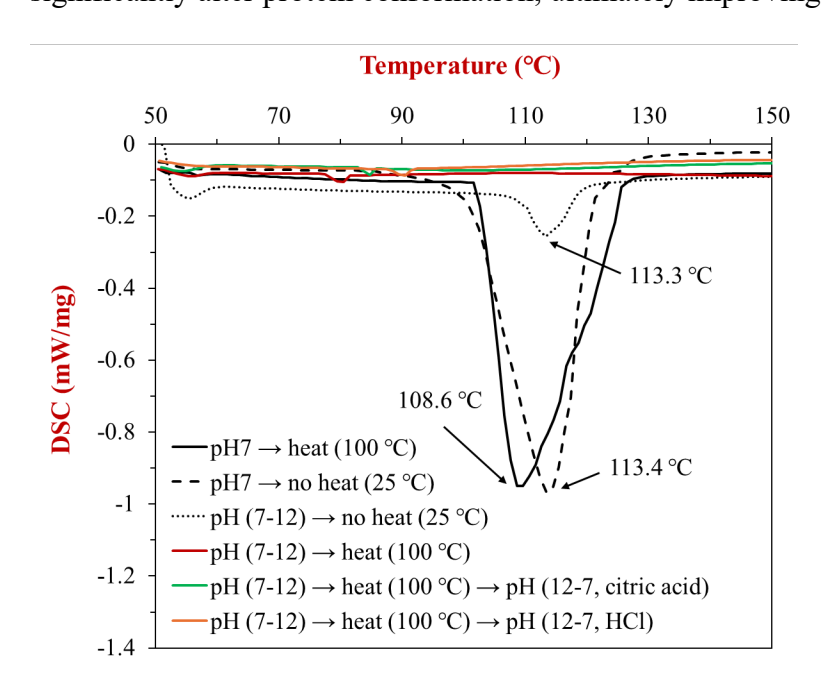


Figure 3.10. DSC thermograms of oat protein isolate under different pH and heating conditions. Treatments include samples at pH 7 (heated at 100 °C or unheated at 25 °C) and samples subjected to pH-shifting (7 to 12 to 7) with no heat (25 °C) or heating at 100 °C, followed by acidification using either HCl or citric acid. Denaturation temperatures are labeled as 108.6 °C, 113.3 °C, and 113.4 °C for the samples with peaks.

We further ran an experiment using FTIR spectroscopy to analyze the secondary structure content of OPI. The data presented in Figure 3.11 illustrate the relative proportions of β -sheet, α helix, β-turns, and random coil structures across different treatments, including OPI powder, pHshifted samples with and without heating, and samples subjected to acidification using 3% citric acid or 0.1 M HCl. These structural changes offer valuable insights into how pH-shifting and thermal treatment impact protein secondary structure, ultimately influencing protein solubility and stability. Compared to OPI powder, which had a high β -sheet content, all pH 12-treated samples showed a notable decrease in ordered β -sheets and an increase in random coil content, suggesting that pH shifting leads to protein unfolding and structural rearrangement. This phenomenon can be attributed to the increased surface charges that increased electrostatic repulsion and greater flexibility of oat protein compared to that at neutral pH (Tang, et al., 2023). Compared to OPI powder, the β -sheet content at pH 12 under no-heat conditions (25°C) showed an insignificant decrease (p > 0.05). However, structural transformation became more pronounced when heating at 100 °C was applied, leading to a significant reduction in β -sheet content (p \leq 0.05), indicating further protein unfolding. Besides β -sheet, there was an increase of random coil content upon the pH shift to 12 and after heating at pH 12. This is because the reduction in β -sheet content is often accompanied by the corresponding increase in random coil, suggests an unfolding of compact protein structures. As a result, the protein adopts more

disordered and flexible conformations, represented by the random coil. This trend is consistent with findings from a previous study on kiln roasting parameters (140 °C for 45 min), which closely resemble the heating conditions used in our study (He, Wang, & Hu, 2021).

Upon acidification, samples treated at 100 °C followed by citric acid or HCl acidification showed only a small recovery of β -sheet structures, though the content remained significantly lower than that of native OPI powder, suggesting some degree of refolding or reorganization upon returning to neutral pH. These two acidified samples exhibited β -turn values approximately similar to those of heated pH 12 OPI solutions, indicating that structural reorientation may have redistributed β -sheet content into β -turns. This transition could result in a more flexible structure, thereby improving solubility. Additionally, the increased random coil proportion in the acidified sample with HCl suggests that the higher degree of acidification or denaturation may be due to HCl's strong acidic nature, while citric acid may interact more with oat protein constituents, potentially forming hydrogen bonds. These findings indicate that heating at pH 12 promotes structural flexibility by disrupting ordered secondary structures, which may facilitate better solubility by preventing rigid aggregation. Moreover, the differences between citric acid and HCl treatments suggest that the choice of acid influences refolding behavior, with citric acid-treated samples showing a slightly higher recovery of β -sheet structures. This structural transition further supports the hypothesis that heat treatment at pH 12 alters protein conformation and intermolecular interaction.

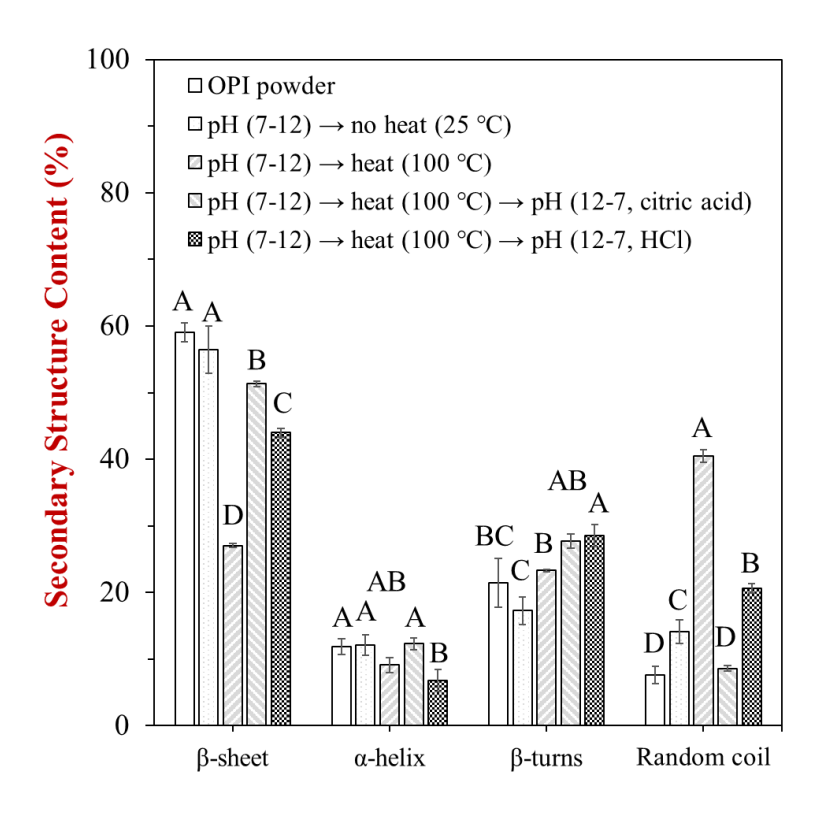


Figure 3.11. Secondary structure content (%) of OPI under various pH and heating treatments, as determined by FTIR spectroscopy. The samples include OPI powder and OPI treated at pH 7 \rightarrow 12 with no heat (25 °C), heating at 100 °C, or after subsequent acidification to pH 7 using citric acid or HCl. The contributions of β -sheet, α -helix, β -turns, and random coil structures highlight the effects of pH-shifting, heating, and acidification on protein secondary structure (The letters, A, B, C, show the significance at p \leq 0.05 between samples for a specific secondary structure).

Conclusion

We investigated the effects of heating temperature at pH 12 and acidification types on the solubility and structural properties of OPI, using a combination of pH shifting, thermal treatment, and acidification. Our findings demonstrate that a simple pH shift from 12 to 7 does not significantly enhance OPI solubility, whereas integrating heat treatment (100 °C for 30 min) with

citric acid acidification leads to a substantial improvement in solubility at neutral pH that can be retained up to 7 days. Through a series of physicochemical characterizations, including particle size analysis, microscopy, DSC, SDS-PAGE, and FTIR spectroscopy, we further investigated the mechanism on how heating enhances protein solubility proven by nanoscale particle size, disappearance of thermal denaturation peaks, formation of peptides at 2-10 kDa, and reduced amount of β -sheet increased number of random coils. Heating at pH 12 promotes the formation of protein nanoparticles, improves electrostatic repulsion interactions due to the increased zeta potentials, and hydrolyzes the protein structure forming smaller soluble peptide, thereby preventing excessive aggregation upon acidification. Furthermore, the use of citric acid, compared to HCl, further increases surface charge repulsions, and thus improves protein solubility. These findings provide valuable insights into how non-enzymatic processing methods can be optimized to improve plant protein functionalities, offering a simple and effective strategy to enhance the solubility of oat protein for food applications.

References

- Alemayehu, G. F., Forsido, S. F., Tola, Y. B., Teshager, M. A., Assegie, A. A., & Amare, E. (2021). Proximate, mineral and anti-nutrient compositions of oat grains (Avena sativa) cultivated in Ethiopia: implications for nutrition and mineral bioavailability. *Heliyon*, 7, 8. https://doi.org/10.1016/j.heliyon.2021.e07722
- Bogahawaththa, D., Chau, N. H. B., Trivedi, J., Dissanayake, M., & Vasiljevic, T. (2019). Impact of controlled shearing on solubility and heat stability of pea protein isolate dispersed in solutions with adjusted ionic strength. *Food Research International*, 125, 108522. https://doi.org/10.1016/j.foodres.2019.108522
- Brückner-Gühmann, M., Kratzsch, A., Sozer, N., & Drusch, S. (2021). Oat protein as plant-derived gelling agent: Properties and potential of modification. *Future Foods*, *4*, 100053. https://doi.org/10.1016/j.fufo.2021.100053
- Cruz-Solis, I., Ibarra-Herrera, C. C., Rocha-Pizaña, M. d. R., & Luna-Vital, D. (2023). Alkaline sxtraction—isoelectric precipitation of plant proteins. *Green Protein Processing Technologies from Plants: Novel Extraction and Purification Methods for Product Development* (pp. 1-29). Cham: Springer International Publishing.
- Ercili-Cura, D., Miyamoto, A., Paananen, A., Yoshii, H., Poutanen, K., & Partanen, R. (2015).

 Adsorption of oat proteins to air—water interface in relation to their colloidal state. *Food Hydrocolloids*, 44, 183-190. https://doi.org/10.1016/j.foodhyd.2014.09.017
- Ha, S. M. L., de Bruijn, W. J. C., Vreeke, G. J. C., Bruins, M. E., Nieuwland, M., van der Goot,A. J., & Keppler, J. K. (2025). Protein extraction from oat: isoelectric precipitation and

- water-based extraction. *Future Foods*, *11*, 100591. https://doi.org/10.1016/j.fufo.2025.100591
- He, T., Wang, J., & Hu, X. (2021). Effect of heat treatment on the structure and digestion properties of oat globulin. *Cereal Chemistry*, 98, 740-748. https://doi.org/10.1002/cche.10417
- Jayachandran, B., Parvin, T. N., Alam, M. M., Chanda, K., & MM, B. (2022). Insights on chemical crosslinking strategies for proteins. *Molecules*, 27, 8124. https://doi.org/10.3390/molecules27238124
- Jiang, J., Chen, J., & Xiong, Y. L. (2009). Structural and emulsifying properties of soy protein isolate subjected to acid and alkaline pH-shifting processes. *Journal of Agricultural and Food Chemistry*, 57, 7576-7583. 1 https://doi.org/10.1021/jf901585n
- Jiang, J., Wang, Q., & Xiong, Y. L. (2018). A pH shift approach to the improvement of interfacial properties of plant seed proteins. *Current Opinion in Food Science*, 19, 50-56. https://doi.org/10.1016/j.cofs.2018.01.002
- Jiang, S., Ding, J., Andrade, J., Rababah, T. M., Almajwal, A., Abulmeaty, M. M., & Feng, H. (2017). Modifying the physicochemical properties of pea protein by pH-shifting and ultrasound combined treatments. *Ultrasonics Sonochemistry*, 38, 835-842. https://doi.org/10.1016/j.ultsonch.2017.03.046
- Kumar, L., Sehrawat, R., & Kong, Y. (2021). Oat proteins: A perspective on functional properties. *LWT Food Science and Technology*, 152, 112307. https://doi.org/10.1016/j.lwt.2021.112307

- Le, M. S., Hermansen, C., & Vuong, Q. V. (2025). Oat milk by-product: a review of nutrition, processing and applications of oat pulp. *Food Reviews International*, 1-38. https://doi.org/10.1080/87559129.2025.2450263
- Li, J., Wu, M., Wang, Y., Li, K., Du, J., & Bai, Y. (2020). Effect of pH-shifting treatment on structural and heat induced gel properties of peanut protein isolate. *Food Chemistry*, 325, 126921. https://doi.org/10.1080/87559129.2025.2450263
- Li, R., & Xiong, Y. L. (2021a). Sensitivity of oat protein solubility to changing ionic strength and pH. *Journal of Food Science*, 86, 78-85. 10.1111/1750-3841.15544
- Li, R., & Xiong, Y. L. (2021b). Ultrasound-induced structural modification and thermal properties of oat protein. *LWT*, *149*, 111861. https://doi.org/10.1016/j.lwt.2021.111861
- Li, T., Wang, C., Li, T., Ma, L., Sun, D., Hou, J., & Jiang, Z. (2018). Surface hydrophobicity and functional properties of citric acid cross-linked whey protein isolate: the impact of pH and concentration of citric acid. *Molecules*, 23(9), 2383. https://doi.org/10.3390/molecules23092383
- Liu, G., Li, J., Shi, K., Wang, S., Chen, J., Liu, Y., & Huang, Q. (2009). Composition, secondary structure, and self-assembly of oat protein isolate. *Journal of Agricultural and Food Chemistry*, 57, 4552-4558. 10.1021/jf900135e
- Loponen, J., Laine, P., Sontag-Strohm, T., & Salovaara, H. (2007). Behaviour of oat globulins in lactic acid fermentation of oat bran. *European Food Research and Technology*, 225, 105-110. 10.1007/s00217-006-0387-9
- Ma, C.-Y., & Harwalkar, V.R. (1985). Studies of thermal denaturation of oat globulin by differential scanning calorimetry. *Journal of Food Science*, *53*, 531-534. https://doi.org/10.1111/j.1365-2621.1988.tb07749.x

- Ma, C.-Y., Rout, M. K., & Mock, W.-Y. (2001). Study of oat globulin conformation by fourier transform infrared spectroscopy. *Journal of Agricultural and Food Chemistry*, 49, 3328-3334. 10.1021/jf010053f
- McLauchlan, J., Tyler, A. I. I., Chakrabarti, B., Orfila, C., & Sarkar, A. (2024). Oat protein: review of structure-function synergies with other plant proteins. *Food Hydrocolloids*, *154*, 110139. https://doi.org/10.1016/j.foodhyd.2024.110139
- Mession, J.-L., Sok, N., Assifaoui, A., & Saurel, R. (2013). Thermal denaturation of pea globulins (Pisum sativum L.)—molecular interactions leading to heat-induced protein aggregation. *Journal of Agricultural and Food Chemistry*, 61, 1196-1204. 10.1021/jf303739n
- Mirmoghtadaie, L., Kadivar, M., & Shahedi, M. (2009). Effects of succinylation and deamidation on functional properties of oat protein isolate. *Food Chemistry*, 114, 127-131. https://doi.org/10.106/j.foodchem.2008.09.025
- Murayama, K., & Tomida, M. (2004). Heat-induced secondary structure and conformation Change of bovine serum albumin investigated by fourier transform infrared spectroscopy. *Biochemistry*, 43, 11526-11532. 10.1021/bi0489154
- Nieto, T.V.N., Wang, Y.X., Ozimek, L., and Chen, L. (2014). Effect of partial hydrolysis on structure and gelling properties of oat globulin proteins. *Food Research International*, *55*, 418-425. https://doi.org/10.1016/j.foodres.2013.11.038
- Ngarize, S., Herman, H., Adams, A., & Howell, N. (2004). Comparison of changes in the secondary structure of unheated, heated, and high-pressure-treated β-lactoglobulin and ovalbumin proteins using fourier transform raman spectroscopy and self-deconvolution.

 Journal of Agricultural and Food Chemistry, 52, 6470-6477. 10.021/jf030649y

- Reddy, N., Li, Y., & Yang, Y. (2009). Alkali-catalyzed low temperature wet crosslinking of plant proteins using carboxylic acids. *Biotechnology Progress*, 25, 139-146. 10.1002/btpr.86
- Robert, L. S., Nozzolillo, C., & Altosaar, I. (1985). Characterization of oat (avena sativa L.) residual proteins. *Cereal Chem, 62*, 276-279.
- Roland, I. S., Aguilera-Toro, M., Nielsen, S. D.-H., Poulsen, N. A., & Larsen, L. B. (2023). Processing-induced markers in proteins of commercial plant-based drinks in relation to compositional aspects. *Foods*, *12*, 3282. 10.3390/foods12173282
- Sánchez-Velázquez, O. A., Cuevas-Rodríguez, E. O., Mondor, M., Ribéreau, S., Arcand, Y., Mackie, A., & Hernández-Álvarez, A. J. (2021). Impact of in vitro gastrointestinal digestion on peptide profile and bioactivity of cooked and non-cooked oat protein concentrates. *Current Research in Food Science*, 4, 93-104. https://doi.org/10.1016/j.crfs.2021.02.003
- Suryamiharja, A., Gong, X., Akoh, C.C., & Zhou, H. (2025). Enhancing the efficiency and sustainability of producing curcumin-infused plant-based milk alternatives with a two-in-one post pH-driven processing strategy. *Food Frontiers*, *6*, 716-726. https://doi.org/10.1002/fft2.534
- Suryamiharja, A., Gong, X., & Zhou, H. (2024). Towards more sustainable, nutritious, and affordable plant-based milk alternatives: A critical review. *Sustainable Food Protein, 2*, 250-267. https://doi.org/10.1002/sfp2.1040
- Tang, Q., Roos, Y. H., & Miao, S. (2023). Plant protein versus dairy proteins: a pH-dependency investigation on their structure and functional properties. *Foods*, *12*, 368. https://doi.org/10.3390/foods12020368

- Tang, Z.-X., Ying, R.-F., & Shi, L.-E. (2021). Physicochemical and functional characteristics of proteins treated by a pH-shift process: a review. *International Journal of Food Science and Technology*, *56*, 515-529. https://doi.org/10.1111/ijfs.14758
- Thiex, N. (2019). Evaluation of analytical methods for the determination of moisture, crude protein, crude fat, and crude fiber in distillers dried grains with solubles. *Journal of AOAC INTERNATIONAL*, 92, 61-73. https://doi.org/10.1093/jaoac/92.1.61
- Thiex, N., Novotny, L., & Crawford, A. (2019). Determination of ash in animal feed: AOAC Official Method 942.05 Revisited. *Journal of AOAC Intetnational*, 95, 1392-1397. https://doi.org/10.5740/jaoacint.12-129
- Wang, Q., Jin, Y., & Xiong, Y. L. (2018). Heating-aided pH shifting modifies hemp seed protein structure, cross-linking, and emulsifying properties. *Journal of Agricultural and Food Chemistry*, 66, 10827-10834. 10.1021/acs.jafc.8b03901
- Wang, Y., Yang, F., Wu, M., Li, J., Bai, Y., Xu, W., & Qiu, S. (2020). Synergistic effect of pH shifting and mild heating in improving heat induced gel properties of peanut protein isolate.

 LWT Food Science and Technology, 131, 109812.

 https://doi.org/10.1016/j.lwt.2020.109812
- Wang, Y., Yuan, J., Zhang, Y., Chen, X., Wang, J., Chen, B., Li, K., & Bai, Y. (2024).
 Unraveling the effect of combined heat and high-pressure homogenization treatment on the improvement of chickpea protein solubility from the perspectives of colloidal state change and structural characteristic modification. *Food Chemistry*, 442, 138470.
 https://doi.org/10.1016/j.foodchem.2024.138470

- Wouters, A. G. B., & Nicolai, T. (2024). Self-assembly of oat proteins into various colloidal states as function of the NaCl concentration and pH. *Food Hydrocolloids*, *149*, 109603. https://doi.org/10.1016/j.foodhyd.2023.109603
- Wu, X., Wang, X., Zhang, J., Shen, J., Li, Y., Jin, M., & Wu, W. (2021). Effect of alkaline pH-shifting combined with heat treatment on the structural and functional properties of rice bran protein. *Shipin Kexue / Food Science*, 42, 23–30. 10.7506/spkx1002-6630-20191223-273
- Xu, H., Shen, L., Xu, L., & Yang, Y. (2015). Low-temperature crosslinking of proteins using non-toxic citric acid in neutral aqueous medium: mechanism and kinetic study. *Industrial Crops and Products*, 74, 234-240. https://doi.org/10.1016/j.indcrop.2015.05.010
- Yu, Y., Guan, Y., Wen, H., Zhang, Y., Liu, J., & Zhang, T. (2021). Mild heating assisted alkaline pH shifting modify the egg white protein: The mechanism and the enhancement of emulsifying properties. *LWT*, *151*, 112094. https://doi.org/10.1016/j.lwt.2021.112094
- Yung Ma, C. (1983). Preparation, composition and functional properties of oat protein isolates.

 Canadian Institute of Food Science and Technology Journal, 16, 201-205.

 https://doi.org/10.1016/S0315-5463(83)72208-X
- Zhang, W., Liu, C., Zhao, J., Ma, T., He, Z., Huang, M., & Wang, Y. (2021). Modification of structure and functionalities of ginkgo seed proteins by pH-shifting treatment. *Food Chemistry*, 358, 129862. https://doi.org/10.1016/j.foodchem.2021.129862
- Zhao, Y., Mine, Y., & Ma, C.-Y. (2004). Study of thermal aggregation of oat globulin by laser light scattering. *Journal of Agricultural and Food Chemistry*, 52, 3089-3096. 10.1021/jf030735

Future Directions

Future directions for this approach encompass a wide range of applications across different food systems. In the context of curcumin extraction and encapsulation from turmeric in soymilk, further investigation into the interactions between curcumin and oil molecules or other compounds, such as polysaccharides, would be valuable. Understanding these interactions could provide insights into curcumin's behavior in various food matrices, ultimately expanding its application as a natural colorant in different food products. Additionally, classifying the molecular phase of curcumin in different encapsulation matrices is crucial. While we successfully improved curcumin stability for up to 30 days in powder form, it remains unclear whether curcumin undergoes conformational changes, leading to byproducts such as ferulic acid, vanillin, and feruloyl methane. Scaling up this process would allow us to validate our Life Cycle Assessment (LCA) and Techno-Economic Analysis (TEA) calculations, ensuring their industrial relevance. Furthermore, since curcumin-fortified soymilk exhibits a yellow color, assessing consumer preferences and their willingness to purchase such a product for its health benefits would be an important consideration.

Regarding oat protein isolate study, further investigation is needed to determine its application in oat milk production. Assessing whether this method can be scaled up for larger manufacturing processes to produce high-protein oat milk efficiently is essential. Based on our preliminary data, we believe that this method can be applied before centrifugation and after enzymatic treatment to break down complex starches. This approach may improve protein yield in oat milk while reducing byproduct waste (oat okara). Additionally, the optimal enzyme

concentration for breaking down complex starches still requires further investigation to maximize protein retention.

From a processing perspective, oat milk undergoes two major heating treatments: gelatinization (enzymatic deactivation) and sterilization. Since our study suggests that a combination of heating and pH shifting improves oat protein solubility, a key question is whether or not sterilization could be performed earlier or immediately after pH treatment, so that it also functions as a heat treatment. Additionally, indirect heat generated during processes such as homogenization may influence oat protein solubility and functionality. Future studies should investigate the impact of each heating step on oat protein solubility to better understand how thermal processing influences its functional properties. From an energy standpoint, additional heat treatments could increase overall energy consumption and production costs. Therefore, if this method is finalized, Life Cycle Assessment (LCA) and Techno-Economic Analysis (TEA) should be re-evaluated to assess the feasibility and cost-effectiveness of producing high-protein oat milk using this approach compared to existing method.

Lastly, sensory evaluation will be necessary to assess the impact of this treatment on plant-based milk's sensory properties. The pH treatment could lead to salt formation, potentially altering flavor and influencing consumer preferences. Additionally, as observed in Chapter 3, pH treatment affects oat milk's color due to the presence of phenolic acids, even when acidification has been performed. Further research is needed to determine whether this color change affects consumer acceptance, as consumers may prefer a color closer to that of bovine milk. Understanding these changes will be essential for optimizing the final product for commercial success. Overall, further studies on the scalability and molecular interactions of the post pH-

driven method are needed to fully understand its applicability across different food matrices, particularly in plant-based milk.

Concluding Statement

This study explored the application of the post pH-driven method in plant-based milk development, focusing on the extraction and encapsulation of curcumin from turmeric in soymilk, as well as the enhanced solubility of oat protein through combined heat treatment. We demonstrated the method's effectiveness in extracting the bioactive compound curcumin from turmeric, achieving high extraction efficiency (96.4 \pm 0.5%) and two-in-one efficiency (94.2 \pm 1.6%). Additionally, the post pH-driven method was applied to oat protein extraction, where its combination with heat treatment at 100°C significantly improved oat protein solubility. The study also highlighted the role of citric acid in acidification, which helps maintain electrostatic repulsion, thereby enhancing protein solubility as a solution for non-enzymatic treatment approach. These findings highlight the versatility of the post pH-driven method in developing functional, health-promoting plant-based milk. Future research should explore its scalability and further applications in plant-based food systems.